8 The Discrete Fourier Transform

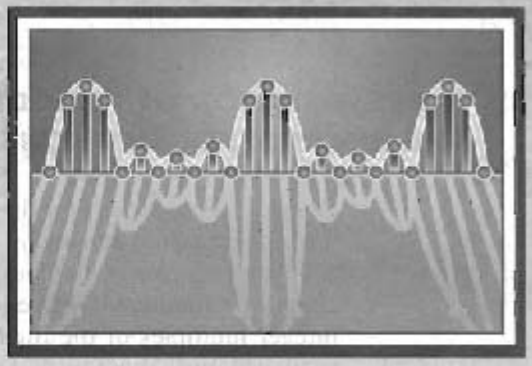

8.0 INTRODUCTION

In Chapters 2 and 3, we discussed the representation of sequences and LTI systems in terms of the discrete-time Fourier and z-transforms, respectively. For finite-duration sequences, there is an alternative discrete-time Fourier representation, referred to as the *discrete Fourier transform* (DFT). The DFT is itself a sequence rather than a function of a continuous variable, and it corresponds to samples, equally spaced in frequency, of the DTFT of the signal. In addition to its theoretical importance as a Fourier representation of sequences, the DFT plays a central role in the implementation of a variety of digital signal-processing algorithms. This is because efficient algorithms exist for the computation of the DFT. These algorithms will be discussed in detail in Chapter 9. The application of the DFT to spectrum analysis will be described in Chapter 10.

Although several points of view can be taken toward the derivation and interpretation of the DFT representation of a finite-duration sequence, we have chosen to base our presentation on the relationship between periodic sequences and finite-length sequences. We begin by considering the Fourier series representation of periodic sequences. Although this representation is important in its own right, we are most often interested in the application of Fourier series results to the representation of finite-length sequences. We accomplish this by constructing a periodic sequence for which each period is identical to the finite-length sequence. The Fourier series representation of the periodic sequence then corresponds to the DFT of the finite-length sequence. Thus, our approach is to define the Fourier series representation for periodic sequences and to study the properties of such representations. Then, we repeat essentially the same derivations, assuming that the sequence to be represented is a finite-length sequence.

This approach to the DFT emphasizes the fundamental inherent periodicity of the DFT representation and ensures that this periodicity is not overlooked in applications of the DFT.

8.1 REPRESENTATION OF PERIODIC SEQUENCES: THE DISCRETE FOURIER SERIES

Consider a sequence $\tilde{x}[n]$ that is periodic[1] with period N, so that $\tilde{x}[n] = \tilde{x}[n + rN]$ for any integer values of n and r. As with continuous-time periodic signals, such a sequence can be represented by a Fourier series corresponding to a sum of harmonically related complex exponential sequences, i.e., complex exponentials with frequencies that are integer multiples of the fundamental frequency $(2\pi/N)$ associated with the periodic sequence $\tilde{x}[n]$. These periodic complex exponentials are of the form

$$e_k[n] = e^{j(2\pi/N)kn} = e_k[n + rN], \tag{8.1}$$

where k is any integer, and the Fourier series representation then has the form[2]

$$\tilde{x}[n] = \frac{1}{N}\sum_{k} \tilde{X}[k]e^{j(2\pi/N)kn}. \tag{8.2}$$

The Fourier series representation of a continuous-time periodic signal generally requires infinitely many harmonically related complex exponentials, whereas the Fourier series for any discrete-time signal with period N requires only N harmonically related complex exponentials. To see this, note that the harmonically related complex exponentials $e_k[n]$ in Eq. (8.1) are identical for values of k separated by N; i.e., $e_0[n] = e_N[n]$, $e_1[n] = e_{N+1}[n]$, and, in general,

$$e_{k+\ell N}[n] = e^{j(2\pi/N)(k+\ell N)n} = e^{j(2\pi/N)kn}e^{j2\pi\ell n} = e^{j(2\pi/N)kn} = e_k[n], \tag{8.3}$$

where ℓ is any integer. Consequently, the set of N periodic complex exponentials $e_0[n]$, $e_1[n]$, ..., $e_{N-1}[n]$ defines all the distinct periodic complex exponentials with frequencies that are integer multiples of $(2\pi/N)$. Thus, the Fourier series representation of a periodic sequence $\tilde{x}[n]$ need contain only N of these complex exponentials. For notational convenience, we choose k in the range of 0 to $N - 1$; hence, Eq. (8.2) has the form

$$\tilde{x}[n] = \frac{1}{N}\sum_{k=0}^{N-1} \tilde{X}[k]e^{j(2\pi/N)kn}. \tag{8.4}$$

However, choosing k to range over any full period of $\tilde{X}[k]$ would be equally valid.

To obtain the sequence of Fourier series coefficients $\tilde{X}[k]$ from the periodic sequence $\tilde{x}[n]$, we exploit the orthogonality of the set of complex exponential sequences.

[1] Henceforth, we will use the tilde (~) to denote periodic sequences whenever it is important to clearly distinguish between periodic and aperiodic sequences.

[2] The multiplicative constant $1/N$ is included in Eq. (8.2) for convenience. It could also be absorbed into the definition of $\tilde{X}[k]$.

After multiplying both sides of Eq. (8.4) by $e^{-j(2\pi/N)rn}$ and summing from $n = 0$ to $n = N - 1$, we obtain

$$\sum_{n=0}^{N-1} \tilde{x}[n]e^{-j(2\pi/N)rn} = \sum_{n=0}^{N-1} \frac{1}{N} \sum_{k=0}^{N-1} \tilde{X}[k]e^{j(2\pi/N)(k-r)n}. \tag{8.5}$$

After interchanging the order of summation on the right-hand side, Eq. (8.5) becomes

$$\sum_{n=0}^{N-1} \tilde{x}[n]e^{-j(2\pi/N)rn} = \sum_{k=0}^{N-1} \tilde{X}[k] \left[\frac{1}{N} \sum_{n=0}^{N-1} e^{j(2\pi/N)(k-r)n} \right]. \tag{8.6}$$

The following identity expresses the orthogonality of the complex exponentials:

$$\frac{1}{N} \sum_{n=0}^{N-1} e^{j(2\pi/N)(k-r)n} = \begin{cases} 1, & k - r = mN, \quad m \text{ an integer}, \\ 0, & \text{otherwise}. \end{cases} \tag{8.7}$$

This identity can easily be proved (see Problem 8.54), and when it is applied to the summation in brackets in Eq. (8.6), the result is

$$\sum_{n=0}^{N-1} \tilde{x}[n]e^{-j(2\pi/N)rn} = \tilde{X}[r]. \tag{8.8}$$

Thus, the Fourier series coefficients $\tilde{X}[k]$ in Eq. (8.4) are obtained from $\tilde{x}[n]$ by the relation

$$\tilde{X}[k] = \sum_{n=0}^{N-1} \tilde{x}[n]e^{-j(2\pi/N)kn}. \tag{8.9}$$

Note that the sequence $\tilde{X}[k]$ defined in Eq. (8.9) is also periodic with period N if Eq. (8.9) is evaluated outside the range $0 \le k \le N - 1$; i.e., $\tilde{X}[0] = \tilde{X}[N]$, $\tilde{X}[1] = \tilde{X}[N + 1]$, and, more generally,

$$\begin{aligned} \tilde{X}[k + N] &= \sum_{n=0}^{N-1} \tilde{x}[n]e^{-j(2\pi/N)(k+N)n} \\ &= \left(\sum_{n=0}^{N-1} \tilde{x}[n]e^{-j(2\pi/N)kn} \right) e^{-j2\pi n} = \tilde{X}[k], \end{aligned}$$

for any integer k.

The Fourier series coefficients can be interpreted to be a sequence of finite length, given by Eq. (8.9) for $k = 0, \ldots, (N - 1)$, and zero otherwise, or as a periodic sequence defined for all k by Eq. (8.9). Clearly, both of these interpretations are acceptable, since in Eq. (8.4) we use only the values of $\tilde{X}[k]$ for $0 \le k \le (N - 1)$. An advantage to interpreting the Fourier series coefficients $\tilde{X}[k]$ as a periodic sequence is that there is then a duality between the time and frequency domains for the Fourier series representation of periodic sequences. Equations (8.9) and (8.4) together are an analysis–synthesis pair and will be referred to as the *discrete Fourier series* (DFS) representation of a periodic sequence.

For convenience in notation, these equations are often written in terms of the complex quantity

$$W_N = e^{-j(2\pi/N)}, \tag{8.10}$$

With this notation, the DFS analysis–synthesis pair is expressed as follows:

$$\text{Analysis equation:} \quad \tilde{X}[k] = \sum_{n=0}^{N-1} \tilde{x}[n] W_N^{kn}. \tag{8.11}$$

$$\text{Synthesis equation:} \quad \tilde{x}[n] = \frac{1}{N} \sum_{k=0}^{N-1} \tilde{X}[k] W_N^{-kn}. \tag{8.12}$$

In both of these equations, $\tilde{X}[k]$ and $\tilde{x}[n]$ are periodic sequences. We will sometimes find it convenient to use the notation

$$\tilde{x}[n] \overset{DFS}{\longleftrightarrow} \tilde{X}[k] \tag{8.13}$$

to signify the relationships of Eqs. (8.11) and (8.12). The following examples illustrate the use of those equations.

Example 8.1 DFS of a Periodic Impulse Train

We consider the periodic impulse train

$$\tilde{x}[n] = \sum_{r=-\infty}^{\infty} \delta[n - rN] = \begin{cases} 1, & n = rN, \quad r \text{ any integer,} \\ 0, & \text{otherwise.} \end{cases} \tag{8.14}$$

Since $\tilde{x}[n] = \delta[n]$ for $0 \le n \le N-1$, the DFS coefficients are found, using Eq. (8.11), to be

$$\tilde{X}[k] = \sum_{n=0}^{N-1} \delta[n] W_N^{kn} = W_N^0 = 1. \tag{8.15}$$

In this case, $\tilde{X}[k] = 1$ for all k. Thus, substituting Eq. (8.15) into Eq. (8.12) leads to the representation

$$\tilde{x}[n] = \sum_{r=-\infty}^{\infty} \delta[n - rN] = \frac{1}{N} \sum_{k=0}^{N-1} W_N^{-kn} = \frac{1}{N} \sum_{k=0}^{N-1} e^{j(2\pi/N)kn}. \tag{8.16}$$

Example 8.1 produced a useful representation of a periodic impulse train in terms of a sum of complex exponentials, wherein all the complex exponentials have the same magnitude and phase and add to unity at integer multiples of N and to zero for all other integers. If we look closely at Eqs. (8.11) and (8.12), we see that the two equations are very similar, differing only in a constant multiplier and the sign of the exponents. This duality between the periodic sequence $\tilde{x}[n]$ and its DFS coefficients $\tilde{X}[k]$ is illustrated in the following example.

Example 8.2 Duality in the DFS

In this example, the DFS coefficients are a periodic impulse train:

$$\tilde{Y}[k] = \sum_{r=-\infty}^{\infty} N\delta[k - rN].$$

Substituting $\tilde{Y}[k]$ into Eq. (8.12) gives

$$\tilde{y}[n] = \frac{1}{N}\sum_{k=0}^{N-1} N\delta[k]W_N^{-kn} = W_N^{-0} = 1.$$

In this case, $\tilde{y}[n] = 1$ for all n. Comparing this result with the results for $\tilde{x}[n]$ and $\tilde{X}[k]$ of Example 8.1, we see that $\tilde{Y}[k] = N\tilde{x}[k]$ and $\tilde{y}[n] = \tilde{X}[n]$. In Section 8.2.3, we will show that this example is a special case of a more general duality property.

If the sequence $\tilde{x}[n]$ is equal to unity over only part of one period, we can also obtain a closed-form expression for the DFS coefficients. This is illustrated by the following example.

Example 8.3 The DFS of a Periodic Rectangular Pulse Train

For this example, $\tilde{x}[n]$ is the sequence shown in Figure 8.1, whose period is $N = 10$. From Eq. (8.11),

$$\tilde{X}[k] = \sum_{n=0}^{4} W_{10}^{kn} = \sum_{n=0}^{4} e^{-j(2\pi/10)kn}. \tag{8.17}$$

This finite sum has the closed form

$$\tilde{X}[k] = \frac{1 - W_{10}^{5k}}{1 - W_{10}^{k}} = e^{-j(4\pi k/10)}\frac{\sin(\pi k/2)}{\sin(\pi k/10)}. \tag{8.18}$$

The magnitude and phase of the periodic sequence $\tilde{X}[k]$ are shown in Figure 8.2.

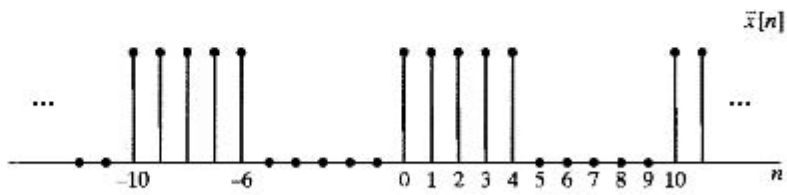

Figure 8.1 Periodic sequence with period $N = 10$ for which the Fourier series representation is to be computed.

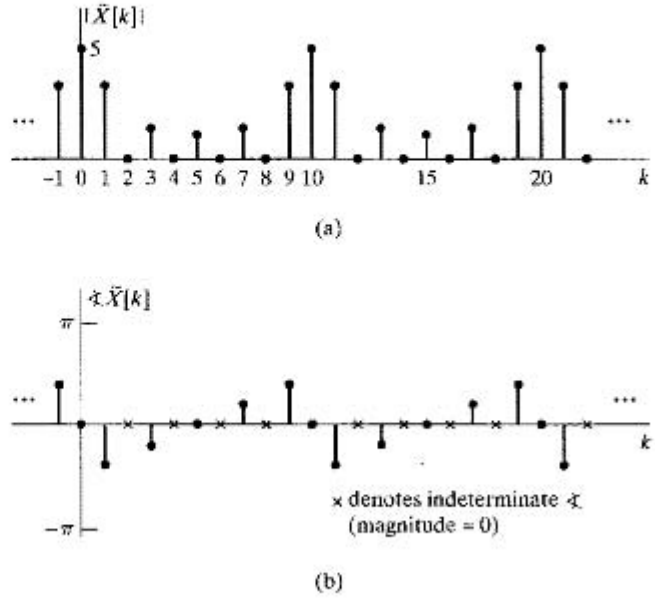

Figure 8.2 Magnitude and phase of the Fourier series coefficients of the sequence of Figure 8.1.

We have shown that any periodic sequence can be represented as a sum of complex exponential sequences. The key results are summarized in Eqs. (8.11) and (8.12). As we will see, these relationships are the basis for the DFT, which focuses on finite-length sequences. Before discussing the DFT, however, we will consider some of the basic properties of the DFS representation of periodic sequences in Section 8.2, and then, in Section 8.3, we will show how we can use the DFS representation to obtain a DTFT representation of periodic signals.

8.2 PROPERTIES OF THE DFS

Just as with Fourier series and Fourier and Laplace transforms for continuous-time signals, and with discrete-time Fourier and z-transforms for nonperiodic sequences, certain properties of the DFS are of fundamental importance to its successful use in signal-processing problems. In this section, we summarize these important properties. It is not surprising that many of the basic properties are analogous to properties of the z-transform and DTFT. However, we will be careful to point out where the periodicity of both $\tilde{x}[n]$ and $\tilde{X}[k]$ results in some important distinctions. Furthermore, an exact duality exists between the time and frequency domains in the DFS representation that does not exist in the DTFT and z-transform representation of sequences.

8.2.1 Linearity

Consider two periodic sequences $\tilde{x}_1[n]$ and $\tilde{x}_2[n]$, both with period N, such that

$$\tilde{x}_1[n] \overset{DFS}{\longleftrightarrow} \tilde{X}_1[k], \tag{8.19a}$$

and

$$\tilde{x}_2[n] \overset{DFS}{\longleftrightarrow} \tilde{X}_2[k]. \tag{8.19b}$$

Then

$$a\tilde{x}_1[n] + b\tilde{x}_2[n] \overset{DFS}{\longleftrightarrow} a\tilde{X}_1[k] + b\tilde{X}_2[k]. \tag{8.20}$$

This linearity property follows immediately from the form of Eqs. (8.11) and (8.12).

8.2.2 Shift of a Sequence

If a periodic sequence $\tilde{x}[n]$ has Fourier coefficients $\tilde{X}[k]$, then $\tilde{x}[n-m]$ is a shifted version of $\tilde{x}[n]$, and

$$\tilde{x}[n-m] \overset{DFS}{\longleftrightarrow} W_N^{km}\tilde{X}[k]. \tag{8.21}$$

The proof of this property is considered in Problem 8.55. Note that any shift that is greater than or equal to the period (i.e., $m \geq N$) cannot be distinguished in the time domain from a shorter shift m_1 such that $m = m_1 + m_2N$, where m_1 and m_2 are integers and $0 \leq m_1 \leq N-1$. (Another way of stating this is that $m_1 = m$ modulo N or, equivalently, m_1 is the remainder when m is divided by N.) It is easily shown that with this representation of m, $W_N^{km} = W_N^{km_1}$; i.e., as it must be, the ambiguity of the shift in the time domain is also manifest in the frequency-domain representation.

Because the sequence of Fourier series coefficients of a periodic sequence is a periodic sequence, a similar result applies to a shift in the Fourier coefficients by an integer ℓ. Specifically,

$$W_N^{-n\ell}\tilde{x}[n] \overset{DFS}{\longleftrightarrow} \tilde{X}[k-\ell]. \tag{8.22}$$

Note the difference in the sign of the exponents in Eqs. (8.21) and (8.22).

8.2.3 Duality

Because of the strong similarity between the Fourier analysis and synthesis equations in continuous time, there is a duality between the time domain and frequency domain. However, for the DTFT of aperiodic signals, no similar duality exists, since aperiodic signals and their Fourier transforms are very different kinds of functions: Aperiodic discrete-time signals are, of course, aperiodic sequences, whereas their DTFTs are always periodic functions of a continuous frequency variable.

From Eqs. (8.11) and (8.12), we see that the DFS analysis and synthesis equations differ only in a factor of $1/N$ and in the sign of the exponent of W_N. Furthermore, a periodic sequence and its DFS coefficients are the same kinds of functions; they are both

periodic sequences. Specifically, taking account of the factor $1/N$ and the difference in sign in the exponent between Eqs. (8.11) and (8.12), it follows from Eq. (8.12) that

$$N\tilde{x}[-n] = \sum_{k=0}^{N-1} \tilde{X}[k]W_N^{kn} \tag{8.23}$$

or, interchanging the roles of n and k in Eq. (8.23),

$$N\tilde{x}[-k] = \sum_{n=0}^{N-1} \tilde{X}[n]W_N^{nk}. \tag{8.24}$$

We see that Eq. (8.24) is similar to Eq. (8.11). In other words, the sequence of DFS coefficients of the periodic sequence $\tilde{X}[n]$ is $N\tilde{x}[-k]$, i.e., the original periodic sequence in reverse order and multiplied by N. This duality property is summarized as follows: If

$$\tilde{x}[n] \overset{\mathcal{DFS}}{\longleftrightarrow} \tilde{X}[k], \tag{8.25a}$$

then

$$\tilde{X}[n] \overset{\mathcal{DFS}}{\longleftrightarrow} N\tilde{x}[-k]. \tag{8.25b}$$

8.2.4 Symmetry Properties

As we discussed in Section 2.8, the Fourier transform of an aperiodic sequence has a number of useful symmetry properties. The same basic properties also hold for the DFS representation of a periodic sequence. The derivation of these properties, which is similar in style to the derivations in Chapter 2, is left as an exercise. (See Problem 8.56.) The resulting properties are summarized for reference as properties 9–17 in Table 8.1 in Section 8.2.6.

8.2.5 Periodic Convolution

Let $\tilde{x}_1[n]$ and $\tilde{x}_2[n]$ be two periodic sequences, each with period N and with DFS coefficients denoted by $\tilde{X}_1[k]$ and $\tilde{X}_2[k]$, respectively. If we form the product

$$\tilde{X}_3[k] = \tilde{X}_1[k]\tilde{X}_2[k], \tag{8.26}$$

then the periodic sequence $\tilde{x}_3[n]$ with Fourier series coefficients $\tilde{X}_3[k]$ is

$$\tilde{x}_3[n] = \sum_{m=0}^{N-1} \tilde{x}_1[m]\tilde{x}_2[n-m]. \tag{8.27}$$

This result is not surprising, since our previous experience with transforms suggests that multiplication of frequency-domain functions corresponds to convolution of time-domain functions and Eq. (8.27) looks very much like a convolution sum. Equation (8.27) involves the summation of values of the product of $\tilde{x}_1[m]$ with $\tilde{x}_2[n-m]$, which is a time-reversed and time-shifted version of $\tilde{x}_2[m]$, just as in aperiodic discrete convolution. However, the sequences in Eq. (8.27) are all periodic with period N, and the summation is over only one period. A convolution in the form of Eq. (8.27) is referred

to as a *periodic convolution*. Just as with aperiodic convolution, periodic convolution is commutative; i.e.,

$$\tilde{x}_3[n] = \sum_{m=0}^{N-1} \tilde{x}_2[m]\tilde{x}_1[n-m]. \tag{8.28}$$

To demonstrate that $\tilde{X}_3[k]$, given by Eq. (8.26), is the sequence of Fourier coefficients corresponding to $\tilde{x}_3[n]$ given by Eq. (8.27), let us first apply Eq. (8.11), the DFS analysis equation, to Eq. (8.27) to obtain

$$\tilde{X}_3[k] = \sum_{n=0}^{N-1} \left(\sum_{m=0}^{N-1} \tilde{x}_1[m]\tilde{x}_2[n-m] \right) W_N^{kn}, \tag{8.29}$$

which, after we interchange the order of summation, becomes

$$\tilde{X}_3[k] = \sum_{m=0}^{N-1} \tilde{x}_1[m] \left(\sum_{n=0}^{N-1} \tilde{x}_2[n-m] W_N^{kn} \right). \tag{8.30}$$

The inner sum on the index n is the DFS for the shifted sequence $\tilde{x}_2[n-m]$. Therefore, from the shifting property of Section 8.2.2, we obtain

$$\sum_{n=0}^{N-1} \tilde{x}_2[n-m] W_N^{kn} = W_N^{km} \tilde{X}_2[k],$$

which can be substituted into Eq. (8.30) to yield

$$\tilde{X}_3[k] = \sum_{m=0}^{N-1} \tilde{x}_1[m] W_N^{km} \tilde{X}_2[k] = \left(\sum_{m=0}^{N-1} \tilde{x}_1[m] W_N^{km} \right) \tilde{X}_2[k] = \tilde{X}_1[k]\tilde{X}_2[k]. \tag{8.31}$$

In summary,

$$\sum_{m=0}^{N-1} \tilde{x}_1[m]\tilde{x}_2[n-m] \overset{DFS}{\longleftrightarrow} \tilde{X}_1[k]\tilde{X}_2[k]. \tag{8.32}$$

The periodic convolution of periodic sequences thus corresponds to multiplication of the corresponding periodic sequences of Fourier series coefficients.

Since periodic convolutions are somewhat different from aperiodic convolutions, it is worthwhile to consider the mechanics of evaluating Eq. (8.27). First, note that Eq. (8.27) calls for the product of sequences $\tilde{x}_1[m]$ and $\tilde{x}_2[n-m] = \tilde{x}_2[-(m-n)]$ viewed as functions of m with n fixed. This is the same as for an aperiodic convolution, but with the following two major differences:

1. The sum is over the finite interval $0 \le m \le N-1$.
2. The values of $\tilde{x}_2[n-m]$ in the interval $0 \le m \le N-1$ repeat periodically for m outside of that interval.

These details are illustrated by the following example.

Example 8.4 Periodic Convolution

An illustration of the procedure for forming the periodic convolution of two periodic sequences corresponding to Eq. (8.27) is given in Figure 8.3, wherein we have illustrated the sequences $\tilde{x}_2[m]$, $\tilde{x}_1[m]$, $\tilde{x}_2[-m]$, $\tilde{x}_2[1-m] = \tilde{x}_2[-(m-1)]$, and $\tilde{x}_2[2-m] = \tilde{x}_2[-(m-2)]$. To evaluate $\tilde{x}_3[n]$ in Eq. (8.27) for $n = 2$, for example, we multiply $\tilde{x}_1[m]$ by $\tilde{x}_2[2-m]$ and then sum the product terms $\tilde{x}_1[m]\tilde{x}_2[2-m]$ for $0 \le m \le N-1$, obtaining $\tilde{x}_3[2]$. As n changes, the sequence $\tilde{x}_2[n-m]$ shifts appropriately, and Eq. (8.27) is evaluated for each value of $0 \le n \le N-1$. Note that as the sequence $\tilde{x}_2[n-m]$ shifts to the right or left, values that leave the interval between the dotted lines at one end reappear at the other end because of the periodicity. Because of the periodicity of $\tilde{x}_3[n]$, there is no need to continue to evaluate Eq. (8.27) outside the interval $0 \le n \le N-1$.

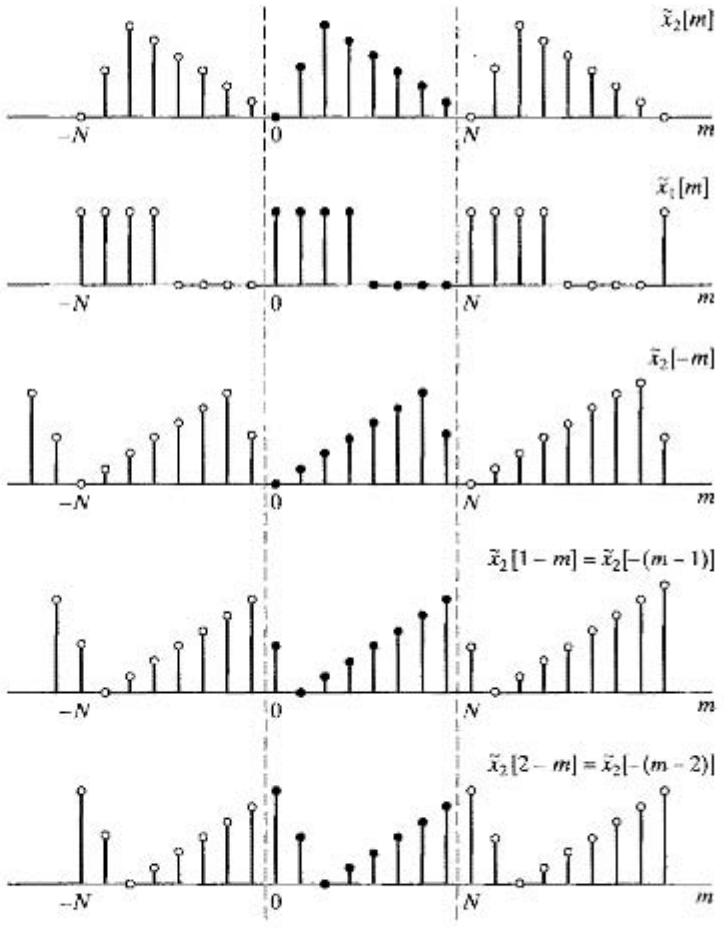

Figure 8.3 Procedure for forming the periodic convolution of two periodic sequences.

The duality theorem in Section 8.2.3 suggests that if the roles of time and frequency are interchanged, we will obtain a result almost identical to the previous result. That is, the periodic sequence

$$\tilde{x}_3[n] = \tilde{x}_1[n]\tilde{x}_2[n], \tag{8.33}$$

where $\tilde{x}_1[n]$ and $\tilde{x}_2[n]$ are periodic sequences, each with period N, has the DFS coefficients given by

$$\tilde{X}_3[k] = \frac{1}{N}\sum_{\ell=0}^{N-1} \tilde{X}_1[\ell]\tilde{X}_2[k-\ell], \tag{8.34}$$

corresponding to $1/N$ times the periodic convolution of $\tilde{X}_1[k]$ and $\tilde{X}_2[k]$. This result can also be verified by substituting $\tilde{X}_3[k]$, given by Eq. (8.34), into the Fourier series relation of Eq. (8.12) to obtain $\tilde{x}_3[n]$.

8.2.6 Summary of Properties of the DFS Representation of Periodic Sequences

The properties of the DFS representation discussed in this section are summarized in Table 8.1.

8.3 THE FOURIER TRANSFORM OF PERIODIC SIGNALS

As discussed in Section 2.7, uniform convergence of the Fourier transform of a sequence requires that the sequence be absolutely summable, and mean-square convergence requires that the sequence be square summable. Periodic sequences satisfy neither condition. However, as we discussed briefly in Section 2.7, sequences that can be expressed as a sum of complex exponentials can be considered to have a Fourier transform representation in the form of Eq. (2.147), i.e., as a train of impulses. Similarly, it is often useful to incorporate the DFS representation of periodic signals within the framework of the discrete-time Fourier transform. This can be done by interpreting the discrete-time Fourier transform of a periodic signal to be an impulse train in the frequency domain with the impulse values proportional to the DFS coefficients for the sequence. Specifically, if $\tilde{x}[n]$ is periodic with period N and the corresponding DFS coefficients are $\tilde{X}[k]$, then the Fourier transform of $\tilde{x}[n]$ is defined to be the impulse train

$$\tilde{X}(e^{j\omega}) = \sum_{k=-\infty}^{\infty} \frac{2\pi}{N}\tilde{X}[k]\delta\left(\omega - \frac{2\pi k}{N}\right). \tag{8.35}$$

Note that $\tilde{X}(e^{j\omega})$ has the necessary periodicity with period 2π since $\tilde{X}[k]$ is periodic with period N, and the impulses are spaced at integer multiples of $2\pi/N$, where N is an

TABLE 8.1 SUMMARY OF PROPERTIES OF THE DFS

Periodic Sequence (Period N)	DFS Coefficients (Period N)
1. $\tilde{x}[n]$	$\tilde{X}[k]$ periodic with period N
2. $\tilde{x}_1[n], \tilde{x}_2[n]$	$\tilde{X}_1[k], \tilde{X}_2[k]$ periodic with period N
3. $a\tilde{x}_1[n] + b\tilde{x}_2[n]$	$a\tilde{X}_1[k] + b\tilde{X}_2[k]$
4. $\tilde{X}[n]$	$N\tilde{x}[-k]$
5. $\tilde{x}[n-m]$	$W_N^{km}\tilde{X}[k]$
6. $W_N^{-\ell n}\tilde{x}[n]$	$\tilde{X}[k-\ell]$
7. $\sum_{m=0}^{N-1}\tilde{x}_1[m]\tilde{x}_2[n-m]$ (periodic convolution)	$\tilde{X}_1[k]\tilde{X}_2[k]$
8. $\tilde{x}_1[n]\tilde{x}_2[n]$	$\frac{1}{N}\sum_{\ell=0}^{N-1}\tilde{X}_1[\ell]\tilde{X}_2[k-\ell]$ (periodic convolution)
9. $\tilde{x}^*[n]$	$\tilde{X}^*[-k]$
10. $\tilde{x}^*[-n]$	$\tilde{X}^*[k]$
11. $\mathcal{R}e\{\tilde{x}[n]\}$	$\tilde{X}_e[k] = \frac{1}{2}(\tilde{X}[k] + \tilde{X}^*[-k])$
12. $j\mathcal{I}m\{\tilde{x}[n]\}$	$\tilde{X}_o[k] = \frac{1}{2}(\tilde{X}[k] - \tilde{X}^*[-k])$
13. $\tilde{x}_e[n] = \frac{1}{2}(\tilde{x}[n] + \tilde{x}^*[-n])$	$\mathcal{R}e\{\tilde{X}[k]\}$
14. $\tilde{x}_o[n] = \frac{1}{2}(\tilde{x}[n] - \tilde{x}^*[-n])$	$j\mathcal{I}m\{\tilde{X}[k]\}$
Properties 15–17 apply only when $x[n]$ is real.	
15. Symmetry properties for $\tilde{x}[n]$ real.	$\begin{cases}\tilde{X}[k] = \tilde{X}^*[-k] \\ \mathcal{R}e\{\tilde{X}[k]\} = \mathcal{R}e\{\tilde{X}[-k]\} \\ \mathcal{I}m\{\tilde{X}[k]\} = -\mathcal{I}m\{\tilde{X}[-k]\} \\ \lvert\tilde{X}[k]\rvert = \lvert\tilde{X}[-k]\rvert \\ \angle\tilde{X}[k] = -\angle\tilde{X}[-k]\end{cases}$
16. $\tilde{x}_e[n] = \frac{1}{2}(\tilde{x}[n] + \tilde{x}[-n])$	$\mathcal{R}e\{\tilde{X}[k]\}$
17. $\tilde{x}_0[n] = \frac{1}{2}(\tilde{x}[n] - \tilde{x}[-n])$	$j\mathcal{I}m\{\tilde{X}[k]\}$

integer. To show that $\tilde{X}(e^{j\omega})$ as defined in Eq. (8.35) is a Fourier transform representation of the periodic sequence $\tilde{x}[n]$, we substitute Eq. (8.35) into the inverse Fourier transform Eq. (2.130); i.e.,

$$\frac{1}{2\pi}\int_{0-\epsilon}^{2\pi-\epsilon}\tilde{X}(e^{j\omega})e^{j\omega n}d\omega = \frac{1}{2\pi}\int_{0-\epsilon}^{2\pi-\epsilon}\sum_{k=-\infty}^{\infty}\frac{2\pi}{N}\tilde{X}[k]\delta\left(\omega-\frac{2\pi k}{N}\right)e^{j\omega n}d\omega, \qquad (8.36)$$

where ϵ satisfies the inequality $0 < \epsilon < (2\pi/N)$. Recall that in evaluating the inverse Fourier transform, we can integrate over any interval of length 2π, since the integrand $\tilde{X}(e^{j\omega})e^{j\omega n}$ is periodic with period 2π. In Eq. (8.36) the integration limits are denoted $0-\epsilon$ and $2\pi-\epsilon$, which means that the integration is from just before $\omega = 0$ to just before $\omega = 2\pi$. These limits are convenient, because they include the impulse at $\omega = 0$ and

exclude the impulse at $\omega = 2\pi$.[3] Interchanging the order of integration and summation leads to

$$\begin{aligned}\frac{1}{2\pi}\int_{0-\epsilon}^{2\pi-\epsilon}\tilde{X}(e^{j\omega})e^{j\omega n}d\omega &= \frac{1}{N}\sum_{k=-\infty}^{\infty}\tilde{X}[k]\int_{0-\epsilon}^{2\pi-\epsilon}\delta\left(\omega-\frac{2\pi k}{N}\right)e^{j\omega n}d\omega \\ &= \frac{1}{N}\sum_{k=0}^{N-1}\tilde{X}[k]e^{j(2\pi/N)kn}.\end{aligned} \tag{8.37}$$

The final form of Eq. (8.37) results because only the impulses corresponding to $k = 0, 1, \ldots, (N-1)$ are included in the interval between $\omega = 0 - \epsilon$ and $\omega = 2\pi - \epsilon$.

Comparing Eq. (8.37) and Eq. (8.12), we see that the final right-hand side of Eq. (8.37) is exactly equal to the Fourier series representation for $\tilde{x}[n]$, as specified by Eq. (8.12). Consequently, the inverse Fourier transform of the impulse train in Eq. (8.35) is the periodic signal $\tilde{x}[n]$, as desired.

Although the Fourier transform of a periodic sequence does not converge in the normal sense, the introduction of impulses permits us to include periodic sequences formally within the framework of Fourier transform analysis. This approach was also used in Chapter 2 to obtain a Fourier transform representation of other nonsummable sequences, such as the two-sided constant sequence (Example 2.19) or the complex exponential sequence (Example 2.20). Although the DFS representation is adequate for most purposes, the Fourier transform representation of Eq. (8.35) sometimes leads to simpler or more compact expressions and simplified analysis.

Example 8.5 The Fourier Transform of a Periodic Discrete-Time Impulse Train

Consider the periodic discrete-time impulse train

$$\tilde{p}[n] = \sum_{r=-\infty}^{\infty}\delta[n - rN], \tag{8.38}$$

which is the same as the periodic sequence $\tilde{x}[n]$ considered in Example 8.1. From the results of that example, it follows that

$$\tilde{P}[k] = 1, \qquad \text{for all } k. \tag{8.39}$$

Therefore, the DTFT of $\tilde{p}[n]$ is

$$\tilde{P}(e^{j\omega}) = \sum_{k=-\infty}^{\infty}\frac{2\pi}{N}\delta\left(\omega-\frac{2\pi k}{N}\right). \tag{8.40}$$

The result of Example 8.5 is the basis for a useful interpretation of the relation between a periodic signal and a finite-length signal. Consider a finite-length signal $x[n]$ such that $x[n] = 0$ except in the interval $0 \le n \le N-1$, and consider the convolution

[3] The limits 0 to 2π would present a problem since the impulses at both 0 and 2π would require special handling.

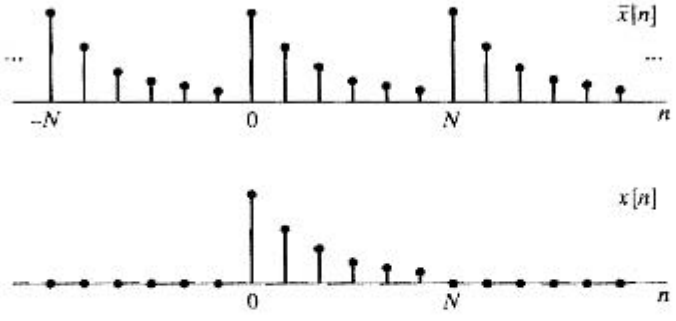

Figure 8.4 Periodic sequence $\tilde{x}[n]$ formed by repeating a finite-length sequence, $x[n]$, periodically. Alternatively, $x[n] = \tilde{x}[n]$ over one period and is zero otherwise.

of $x[n]$ with the periodic impulse train $\tilde{p}[n]$ of Example 8.5:

$$\tilde{x}[n] = x[n] * \tilde{p}[n] = x[n] * \sum_{r=-\infty}^{\infty} \delta[n - rN] = \sum_{r=-\infty}^{\infty} x[n - rN]. \tag{8.41}$$

Equation (8.41) states that $\tilde{x}[n]$ consists of a set of periodically repeated copies of the finite-length sequence $x[n]$. Figure 8.4 illustrates how a periodic sequence $\tilde{x}[n]$ can be formed from a finite-length sequence $x[n]$ through Eq. (8.41). The Fourier transform of $x[n]$ is $X(e^{j\omega})$, and the Fourier transform of $\tilde{x}[n]$ is

$$\begin{aligned}\tilde{X}(e^{j\omega}) &= X(e^{j\omega})\tilde{P}(e^{j\omega}) \\ &= X(e^{j\omega}) \sum_{k=-\infty}^{\infty} \frac{2\pi}{N} \delta\left(\omega - \frac{2\pi k}{N}\right) \\ &= \sum_{k=-\infty}^{\infty} \frac{2\pi}{N} X(e^{j(2\pi/N)k}) \delta\left(\omega - \frac{2\pi k}{N}\right).\end{aligned} \tag{8.42}$$

Comparing Eq. (8.42) with Eq. (8.35), we conclude that

$$\tilde{X}[k] = X(e^{j(2\pi/N)k}) = X(e^{j\omega})\Big|_{\omega=(2\pi/N)k}. \tag{8.43}$$

In other words, the periodic sequence $\tilde{X}[k]$ of DFS coefficients in Eq. (8.11) has an discrete-time interpretation as equally spaced samples of the DTFT of the finite-length sequence obtained by extracting one period of $\tilde{x}[n]$; i.e.,

$$x[n] = \begin{cases} \tilde{x}[n], & 0 \le n \le N-1, \\ 0, & \text{otherwise.} \end{cases} \tag{8.44}$$

This is also consistent with Figure 8.4, where it is clear that $x[n]$ can be obtained from $\tilde{x}[n]$ using Eq. (8.44). We can verify Eq. (8.43) in yet another way. Since $x[n] = \tilde{x}[n]$ for $0 \le n \le N-1$ and $x[n] = 0$ otherwise,

$$X(e^{j\omega}) = \sum_{n=0}^{N-1} x[n]e^{-j\omega n} = \sum_{n=0}^{N-1} \tilde{x}[n]e^{-j\omega n}. \tag{8.45}$$

Comparing Eq. (8.45) and Eq. (8.11), we see again that

$$\tilde{X}[k] = X(e^{j\omega})|_{\omega=2\pi k/N}. \tag{8.46}$$

This corresponds to sampling the Fourier transform at N equally spaced frequencies between $\omega = 0$ and $\omega = 2\pi$ with a frequency spacing of $2\pi/N$.

Example 8.6 Relationship Between the Fourier Series Coefficients and the Fourier Transform of One Period

We again consider the sequence $\tilde{x}[n]$ of Example 8.3, which is shown in Figure 8.1. One period of $\tilde{x}[n]$ for the sequence in Figure 8.1 is

$$x[n] = \begin{cases} 1, & 0 \le n \le 4, \\ 0, & \text{otherwise.} \end{cases} \tag{8.47}$$

The Fourier transform of one period of $\tilde{x}[n]$ is given by

$$X(e^{j\omega}) = \sum_{n=0}^{4} e^{-j\omega n} = e^{-j2\omega} \frac{\sin(5\omega/2)}{\sin(\omega/2)}. \tag{8.48}$$

Equation (8.46) can be shown to be satisfied for this example by substituting $\omega = 2\pi k/10$ into Eq. (8.48), giving

$$\tilde{X}[k] = e^{-j(4\pi k/10)} \frac{\sin(\pi k/2)}{\sin(\pi k/10)},$$

which is identical to the result in Eq. (8.18). The magnitude and phase of $X(e^{j\omega})$ are sketched in Figure 8.5. Note that the phase is discontinuous at the frequencies where $X(e^{j\omega}) = 0$. That the sequences in Figures 8.2(a) and (b) correspond to samples of Figures 8.5(a) and (b), respectively, is demonstrated in Figure 8.6, where Figures 8.2 and 8.5 have been superimposed.

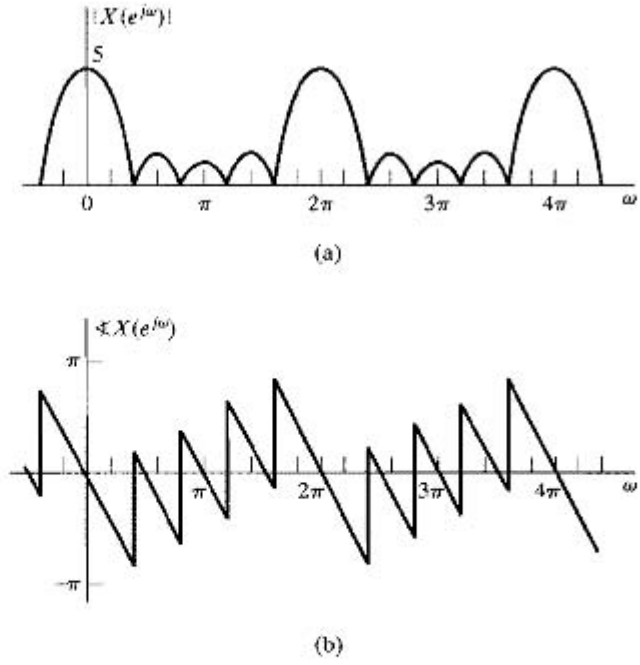

Figure 8.5 Magnitude and phase of the Fourier transform of one period of the sequence in Figure 8.1.

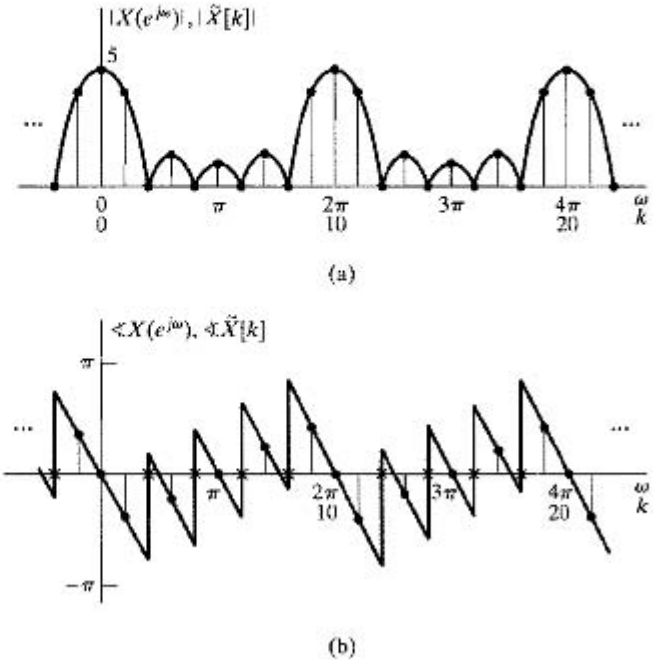

Figure 8.6 Overlay of Figures 8.2 and 8.5 illustrating the DFS coefficients of a periodic sequence as samples of the Fourier transform of one period.

8.4 SAMPLING THE FOURIER TRANSFORM

In this section, we discuss with more generality the relationship between an aperiodic sequence with Fourier transform $X(e^{j\omega})$ and the periodic sequence for which the DFS coefficients correspond to samples of $X(e^{j\omega})$ equally spaced in frequency. We will find this relationship to be particularly important when we discuss the discrete Fourier transform and its properties later in the chapter.

Consider an aperiodic sequence $x[n]$ with Fourier transform $X(e^{j\omega})$, and assume that a sequence $\tilde{X}[k]$ is obtained by sampling $X(e^{j\omega})$ at frequencies $\omega_k = 2\pi k/N$; i.e.,

$$\tilde{X}[k] = X(e^{j\omega})|_{\omega=(2\pi/N)k} = X(e^{j(2\pi/N)k}). \tag{8.49}$$

Since the Fourier transform is periodic in ω with period 2π, the resulting sequence is periodic in k with period N. Also, since the Fourier transform is equal to the z-transform evaluated on the unit circle, it follows that $\tilde{X}[k]$ can also be obtained by sampling $X(z)$ at N equally spaced points on the unit circle. Thus,

$$\tilde{X}[k] = X(z)|_{z=e^{j(2\pi/N)k}} = X(e^{j(2\pi/N)k}). \tag{8.50}$$

These sampling points are depicted in Figure 8.7 for $N = 8$. The figure makes it clear that the sequence of samples is periodic, since the N points are equally spaced starting with zero angle. Therefore, the same sequence repeats as k varies outside the range $0 \le k \le N-1$ since we simply continue around the unit circle visiting the same set of N points.

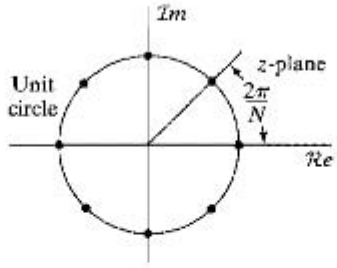

Figure 8.7 Points on the unit circle at which $X(z)$ is sampled to obtain the periodic sequence $\tilde{X}[k]$ $(N = 8)$.

Note that the sequence of samples $\tilde{X}[k]$, being periodic with period N, could be the sequence of DFS coefficients of a sequence $\tilde{x}[n]$. To obtain that sequence, we can simply substitute $\tilde{X}[k]$ obtained by sampling into Eq. (8.12):

$$\tilde{x}[n] = \frac{1}{N}\sum_{k=0}^{N-1} \tilde{X}[k] W_N^{-kn}. \tag{8.51}$$

Since we have made no assumption about $x[n]$ other than that the Fourier transform exists, we can use infinite limits to indicate that the sum is

$$X(e^{j\omega}) = \sum_{m=-\infty}^{\infty} x[m] e^{-j\omega m} \tag{8.52}$$

is over all nonzero values of $x[m]$.

Substituting Eq. (8.52) into Eq. (8.49) and then substituting the resulting expression for $\tilde{X}[k]$ into Eq. (8.51) gives

$$\tilde{x}[n] = \frac{1}{N}\sum_{k=0}^{N-1}\left[\sum_{m=-\infty}^{\infty} x[m] e^{-j(2\pi/N)km}\right] W_N^{-kn}, \tag{8.53}$$

which, after we interchange the order of summation, becomes

$$\tilde{x}[n] = \sum_{m=-\infty}^{\infty} x[m]\left[\frac{1}{N}\sum_{k=0}^{N-1} W_N^{-k(n-m)}\right] = \sum_{m=-\infty}^{\infty} x[m]\tilde{p}[n-m]. \tag{8.54}$$

The term in brackets in Eq. (8.54) can be seen from either Eq. (8.7) or Eq. (8.16) to be the Fourier series representation of the periodic impulse train of Examples 8.1 and 8.2. Specifically,

$$\tilde{p}[n-m] = \frac{1}{N}\sum_{k=0}^{N-1} W_N^{-k(n-m)} = \sum_{r=-\infty}^{\infty} \delta[n-m-rN] \tag{8.55}$$

and therefore,

$$\tilde{x}[n] = x[n] * \sum_{r=-\infty}^{\infty} \delta[n-rN] = \sum_{r=-\infty}^{\infty} x[n-rN], \tag{8.56}$$

where $*$ denotes aperiodic convolution. That is, $\tilde{x}[n]$ is the periodic sequence that results from the aperiodic convolution of $x[n]$ with a periodic unit-impulse train. Thus, the

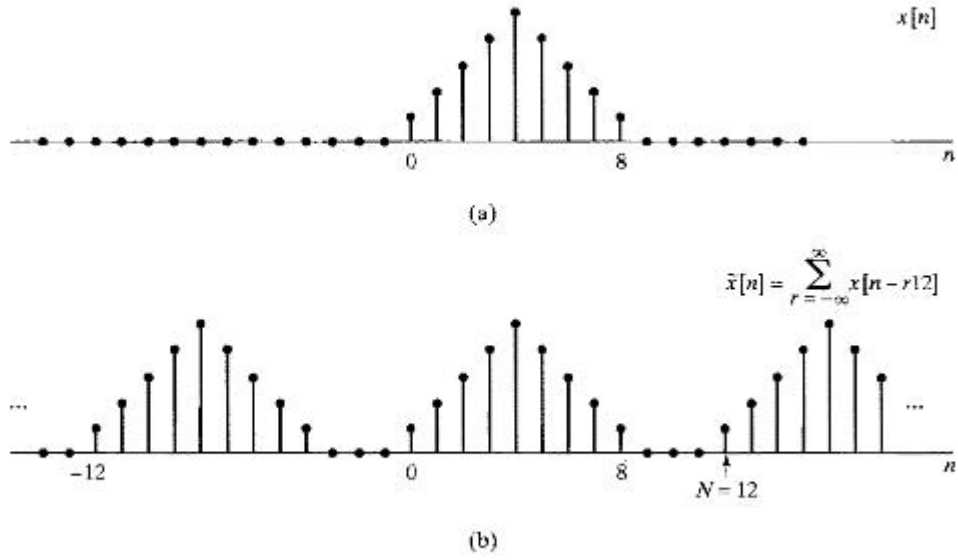

Figure 8.8 (a) Finite-length sequence $x[n]$. (b) Periodic sequence $\tilde{x}[n]$ corresponding to sampling the Fourier transform of $x[n]$ with $N = 12$.

periodic sequence $\tilde{x}[n]$, corresponding to $\tilde{X}[k]$ obtained by sampling $X(e^{j\omega})$, is formed from $x[n]$ by adding together an infinite number of shifted replicas of $x[n]$. The shifts are all the positive and negative integer multiples of N, the period of the sequence $\tilde{X}[k]$. This is illustrated in Figure 8.8, where the sequence $x[n]$ is of length 9 and the value of N in Eq. (8.56) is $N = 12$. Consequently, the delayed replications of $x[n]$ do not overlap, and one period of the periodic sequence $\tilde{x}[n]$ is recognizable as $x[n]$. This is consistent with the discussion in Section 8.3 and Example 8.6, wherein we showed that the Fourier series coefficients for a periodic sequence are samples of the Fourier transform of one period. In Figure 8.9 the same sequence $x[n]$ is used, but the value of N is now $N = 7$. In this case, the replicas of $x[n]$ overlap and one period of $\tilde{x}[n]$ is no longer identical to $x[n]$. In both cases, however, Eq. (8.49) still holds; i.e., in both cases, the DFS coefficients of $\tilde{x}[n]$ are samples of the Fourier transform of $x[n]$ spaced

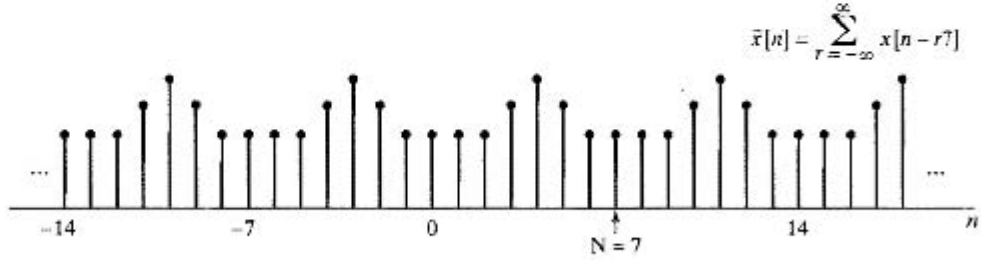

Figure 8.9 Periodic sequence $\tilde{x}[n]$ corresponding to sampling the Fourier transform of $x[n]$ in Figure 8.8(a) with $N = 7$.

in frequency at integer multiples of $2\pi/N$. This discussion should be reminiscent of our discussion of sampling in Chapter 4. The difference is that here we are sampling in the frequency domain rather than in the time domain. However, the general outlines of the mathematical representations are very similar.

For the example in Figure 8.8, the original sequence $x[n]$ can be recovered from $\tilde{x}[n]$ by extracting one period. Equivalently, the Fourier transform $X(e^{j\omega})$ can be recovered from the samples spaced in frequency by $2\pi/12$. In contrast, in Figure 8.9, $x[n]$ cannot be recovered by extracting one period of $\tilde{x}[n]$, and, equivalently, $X(e^{j\omega})$ cannot be recovered from its samples if the sample spacing is only $2\pi/7$. In effect, for the case illustrated in Figure 8.8, the Fourier transform of $x[n]$ has been sampled at a sufficiently small spacing (in frequency) to be able to recover it from these samples, whereas Figure 8.9 represents a case for which the Fourier transform has been undersampled. The relationship between $x[n]$ and one period of $\tilde{x}[n]$ in the undersampled case can be thought of as a form of aliasing in the time domain, essentially identical to the frequency-domain aliasing (discussed in Chapter 4) that results from undersampling in the time domain. Obviously, time-domain aliasing can be avoided only if $x[n]$ has finite length, just as frequency-domain aliasing can be avoided only for signals that have bandlimited Fourier transforms.

This discussion highlights several important concepts that will play a central role in the remainder of the chapter. We have seen that samples of the Fourier transform of an aperiodic sequence $x[n]$ can be thought of as DFS coefficients of a periodic sequence $\tilde{x}[n]$ obtained through summing periodic replicas of $x[n]$. If $x[n]$ is finite length and we take a sufficient number of equally spaced samples of its Fourier transform (specifically, a number greater than or equal to the length of $x[n]$), then the Fourier transform is recoverable from these samples, and, equivalently, $x[n]$ is recoverable from the corresponding periodic sequence $\tilde{x}[n]$. Specifically, if $x[n] = 0$ outside the interval $n = 0$, $n = N - 1$, then

$$x[n] = \begin{cases} \tilde{x}[n], & 0 \le n \le N-1, \\ 0, & \text{otherwise.} \end{cases} \tag{8.57}$$

If the interval of support of $x[n]$ is different than 0, $N - 1$ then Eq. (8.57) would be appropriately modified.

A direct relationship between $X(e^{j\omega})$ and its samples $\tilde{X}[k]$, i.e., an interpolation formula for $X(e^{j\omega})$, can be derived (see Problem 8.57). However, the essence of our previous discussion is that to represent or to recover $x[n]$, it is not necessary to know $X(e^{j\omega})$ at all frequencies if $x[n]$ has finite length. Given a finite-length sequence $x[n]$, we can form a periodic sequence using Eq. (8.56), which in turn can be represented by a DFS. Alternatively, given the sequence of Fourier coefficients $\tilde{X}[k]$, we can find $\tilde{x}[n]$ and then use Eq. (8.57) to obtain $x[n]$. When the Fourier series is used in this way to represent finite-length sequences, it is called the discrete Fourier transform or DFT. In developing, discussing, and applying the DFT, it is always important to remember that the representation through samples of the Fourier transform is in effect a representation of the finite-duration sequence by a periodic sequence, one period of which is the finite-duration sequence that we wish to represent.

8.5 FOURIER REPRESENTATION OF FINITE-DURATION SEQUENCES: THE DFT

In this section, we formalize the point of view suggested at the end of the previous section. We begin by considering a finite-length sequence $x[n]$ of length N samples such that $x[n] = 0$ outside the range $0 \leq n \leq N-1$. In many instances, we will want to assume that a sequence has length N, even if its length is $M \leq N$. In such cases, we simply recognize that the last $(N-M)$ samples are zero. To each finite-length sequence of length N, we can always associate a periodic sequence

$$\tilde{x}[n] = \sum_{r=-\infty}^{\infty} x[n - rN]. \tag{8.58a}$$

The finite-length sequence $x[n]$ can be recovered from $\tilde{x}[n]$ through Eq. (8.57), i.e.,

$$x[n] = \begin{cases} \tilde{x}[n], & 0 \leq n \leq N-1, \\ 0, & \text{otherwise.} \end{cases} \tag{8.58b}$$

Recall from Section 8.4 that the DFS coefficients of $\tilde{x}[n]$ are samples (spaced in frequency by $2\pi/N$) of the Fourier transform of $x[n]$. Since $x[n]$ is assumed to have finite length N, there is no overlap between the terms $x[n - rN]$ for different values of r. Thus, Eq. (8.58a) can alternatively be written as

$$\tilde{x}[n] = x[(n \text{ modulo } N)]. \tag{8.59}$$

For convenience, we will use the notation $((n))_N$ to denote (n modulo N); with this notation, Eq. (8.59) is expressed as

$$\tilde{x}[n] = x[((n))_N]. \tag{8.60}$$

Note that Eq. (8.60) is equivalent to Eq. (8.58a) only when $x[n]$ has length less than or equal to N. The finite-duration sequence $x[n]$ is obtained from $\tilde{x}[n]$ by extracting one period, as in Eq. (8.58b).

One informal and useful way of visualizing Eq. (8.59) is to think of wrapping a plot of the finite-duration sequence $x[n]$ around a cylinder with a circumference equal to the length of the sequence. As we repeatedly traverse the circumference of the cylinder, we see the finite-length sequence periodically repeated. With this interpretation, representation of the finite-length sequence by a periodic sequence corresponds to wrapping the sequence around the cylinder; recovering the finite-length sequence from the periodic sequence using Eq. (8.58b) can be visualized as unwrapping the cylinder and laying it flat so that the sequence is displayed on a linear time axis rather than a circular (modulo N) time axis.

As defined in Section 8.1, the sequence of DFS coefficients $\tilde{X}[k]$ of the periodic sequence $\tilde{x}[n]$ is itself a periodic sequence with period N. To maintain a duality between the time and frequency domains, we will choose the Fourier coefficients that we associate with a finite-duration sequence to be a finite-duration sequence corresponding to one period of $\tilde{X}[k]$. This finite-duration sequence, $X[k]$, will be referred to as the DFT. Thus, the DFT, $X[k]$, is related to the DFS coefficients, $\tilde{X}[k]$, by

$$X[k] = \begin{cases} \tilde{X}[k], & 0 \le k \le N-1, \\ 0, & \text{otherwise}, \end{cases} \tag{8.61}$$

and

$$\tilde{X}[k] = X[(k \text{ modulo } N)] = X[((k))_N]. \tag{8.62}$$

From Section 8.1, $\tilde{X}[k]$ and $\tilde{x}[n]$ are related by

$$\tilde{X}[k] = \sum_{n=0}^{N-1} \tilde{x}[n] W_N^{kn}, \tag{8.63}$$

$$\tilde{x}[n] = \frac{1}{N} \sum_{k=0}^{N-1} \tilde{X}[k] W_N^{-kn}. \tag{8.64}$$

where $W_N = e^{-j(2\pi/N)}$.

Since the summations in Eqs. (8.63) and (8.64) involve only the interval between zero and $(N-1)$, it follows from Eqs. (8.58b) to (8.64) that

$$X[k] = \begin{cases} \sum_{n=0}^{N-1} x[n] W_N^{kn}, & 0 \le k \le N-1, \\ 0, & \text{otherwise}, \end{cases} \tag{8.65}$$

$$x[n] = \begin{cases} \frac{1}{N} \sum_{k=0}^{N-1} X[k] W_N^{-kn}, & 0 \le n \le N-1, \\ 0, & \text{otherwise}. \end{cases} \tag{8.66}$$

Generally, the DFT analysis and synthesis equations are written as follows:

$$\text{Analysis equation:} \quad X[k] = \sum_{n=0}^{N-1} x[n] W_N^{kn}, \qquad 0 \le k \le N-1, \tag{8.67}$$

$$\text{Synthesis equation:} \quad x[n] = \frac{1}{N} \sum_{k=0}^{N-1} X[k] W_N^{-kn}, \qquad 0 \le n \le N-1. \tag{8.68}$$

That is, the fact that $X[k] = 0$ for k outside the interval $0 \le k \le N-1$ and that $x[n] = 0$ for n outside the interval $0 \le n \le N-1$ is implied, but not always stated explicitly. The relationship between $x[n]$ and $X[k]$ implied by Eqs. (8.67) and (8.68) will sometimes be denoted as

$$x[n] \overset{DFT}{\longleftrightarrow} X[k]. \tag{8.69}$$

In recasting Eqs. (8.11) and (8.12) in the form of Eqs. (8.67) and (8.68) for finite-duration sequences, we have not eliminated the inherent periodicity. As with the DFS, the DFT $X[k]$ is equal to samples of the periodic Fourier transform $X(e^{j\omega})$, and if Eq. (8.68) is evaluated for values of n outside the interval $0 \le n \le N-1$, the result will not be zero, but rather a periodic extension of $x[n]$. The inherent periodicity is always present. Sometimes, it causes us difficulty, and sometimes we can exploit it, but to totally ignore it is to invite trouble. In defining the DFT representation, we are simply recognizing that we are interested in values of $x[n]$ only in the interval $0 \le n \le N-1$, because $x[n]$ is really zero outside that interval, and we are interested in values of $X[k]$ only in the interval $0 \le k \le N-1$ because these are the only values needed in Eq. (8.68) to reconstruct $x[n]$.

Example 8.7 The DFT of a Rectangular Pulse

To illustrate the DFT of a finite-duration sequence, consider $x[n]$ shown in Figure 8.10(a). In determining the DFT, we can consider $x[n]$ as a finite-duration sequence with any length greater than or equal to $N = 5$. Considered as a sequence of length $N = 5$, the periodic sequence $\tilde{x}[n]$ whose DFS corresponds to the DFT of $x[n]$ is shown in Figure 8.10(b). Since the sequence in Figure 8.10(b) is constant over the interval $0 \le n \le 4$, it follows that

$$\begin{aligned} \tilde{X}[k] &= \sum_{n=0}^{4} e^{-j(2\pi k/5)n} = \frac{1 - e^{-j2\pi k}}{1 - e^{-j(2\pi k/5)}} \\ &= \begin{cases} 5, & k = 0, \pm 5, \pm 10, \ldots, \\ 0, & \text{otherwise;} \end{cases} \end{aligned} \tag{8.70}$$

i.e., the only nonzero DFS coefficients $\tilde{X}[k]$ are at $k = 0$ and integer multiples of $k = 5$ (all of which represent the same complex exponential frequency). The DFS coefficients are shown in Figure 8.10(c). Also shown is the magnitude of the DTFT, $|X(e^{j\omega})|$. Clearly, $\tilde{X}[k]$ is a sequence of samples of $X(e^{j\omega})$ at frequencies $\omega_k = 2\pi k/5$. According to Eq. (8.61), the five-point DFT of $x[n]$ corresponds to the finite-length sequence obtained by extracting one period of $\tilde{X}[k]$. Consequently, the five-point DFT of $x[n]$ is shown in Figure 8.10(d).

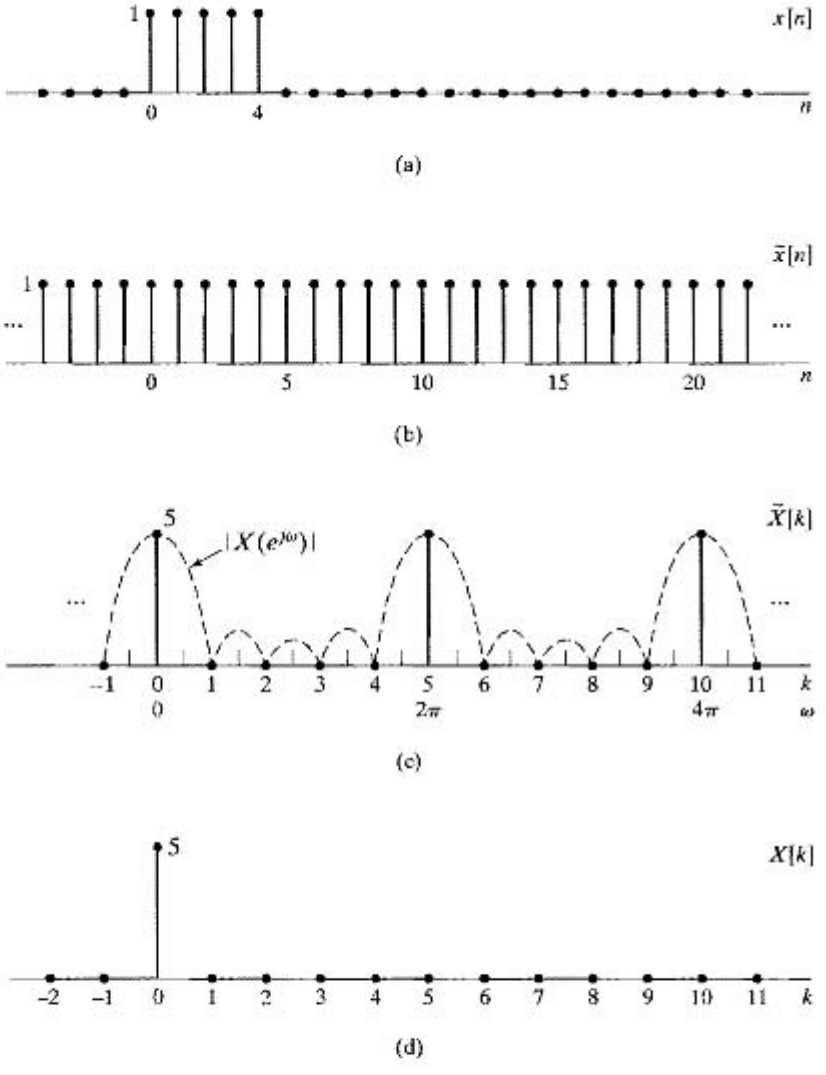

Figure 8.10 Illustration of the DFT. (a) Finite-length sequence $x[n]$. (b) Periodic sequence $\tilde{x}[n]$ formed from $x[n]$ with period $N = 5$. (c) Fourier series coefficients $\tilde{X}[k]$ for $\tilde{x}[n]$. To emphasize that the Fourier series coefficients are samples of the Fourier transform, $|X(e^{j\omega})|$ is also shown. (d) DFT of $x[n]$.

If, instead, we consider $x[n]$ to be of length $N = 10$, then the underlying periodic sequence is that shown in Figure 8.11(b), which is the periodic sequence considered in Example 8.3. Therefore, $\tilde{X}[k]$ is as shown in Figures 8.2 and 8.6, and the 10-point DFT $X[k]$ shown in Figures 8.11(c) and 8.11(d) is one period of $\tilde{X}[k]$.

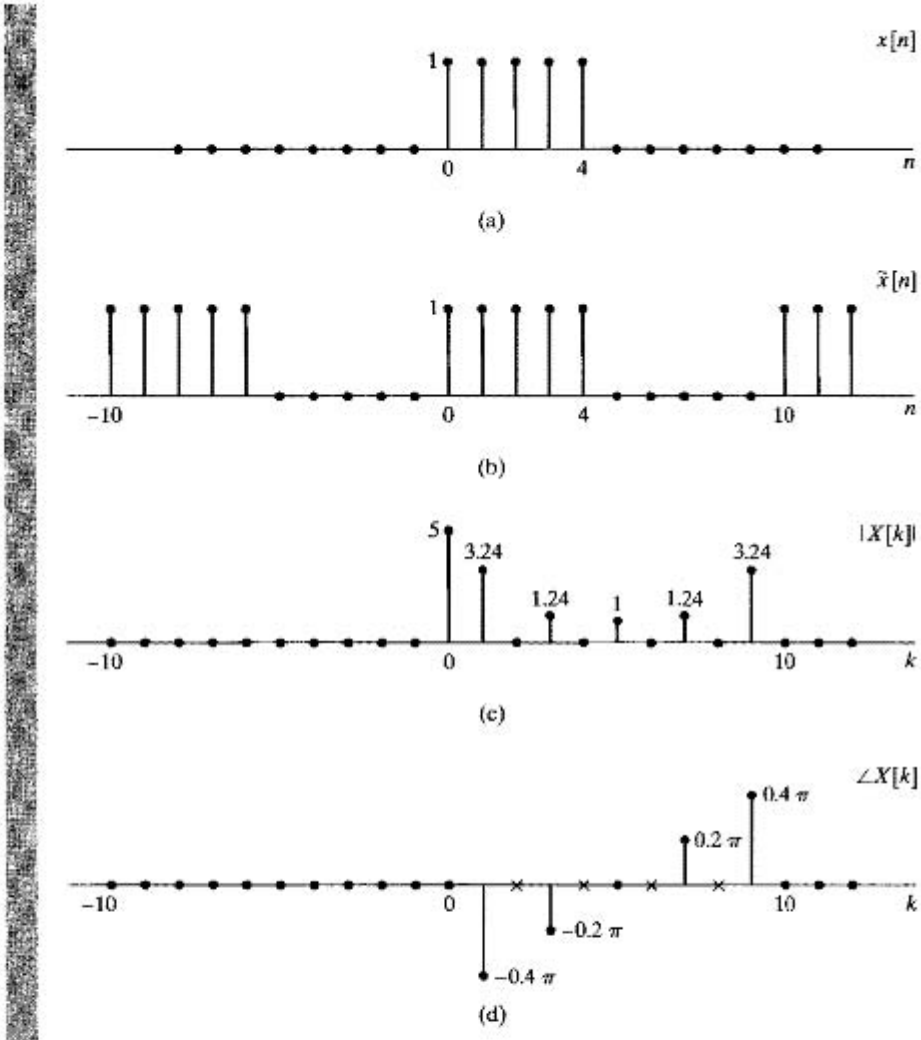

Figure 8.11 Illustration of the DFT. (a) Finite-length sequence $x[n]$. (b) Periodic sequence $\tilde{x}[n]$ formed from $x[n]$ with period $N = 10$. (c) DFT magnitude. (d) DFT phase. (x's indicate indeterminate values.)

The distinction between the finite-duration sequence $x[n]$ and the periodic sequence $\tilde{x}[n]$ related through Eqs. (8.57) and (8.60) may seem minor, since, by using these equations, it is straightforward to construct one from the other. However, the distinction becomes important in considering properties of the DFT and in considering the effect on $x[n]$ of modifications to $X[k]$. This will become evident in the next section, where we discuss the properties of the DFT representation.

8.6 PROPERTIES OF THE DFT

In this section, we consider a number of properties of the DFT for finite-duration sequences. Our discussion parallels the discussion of Section 8.2 for periodic sequences. However, particular attention is paid to the interaction of the finite-length assumption and the implicit periodicity of the DFT representation of finite-length sequences.

8.6.1 Linearity

If two finite-duration sequences $x_1[n]$ and $x_2[n]$ are linearly combined, i.e., if

$$x_3[n] = ax_1[n] + bx_2[n], \tag{8.71}$$

then the DFT of $x_3[n]$ is

$$X_3[k] = aX_1[k] + bX_2[k]. \tag{8.72}$$

Clearly, if $x_1[n]$ has length N_1 and $x_2[n]$ has length N_2, then the maximum length of $x_3[n]$ will be $N_3 = \max(N_1, N_2)$. Thus, in order for Eq. (8.72) to be meaningful, both DFTs must be computed with the same length $N \geq N_3$. If, for example, $N_1 < N_2$, then $X_1[k]$ is the DFT of the sequence $x_1[n]$ augmented by $(N_2 - N_1)$ zeros. That is, the N_2-point DFT of $x_1[n]$ is

$$X_1[k] = \sum_{n=0}^{N_1-1} x_1[n]W_{N_2}^{kn}, \qquad 0 \leq k \leq N_2 - 1, \tag{8.73}$$

and the N_2-point DFT of $x_2[n]$ is

$$X_2[k] = \sum_{n=0}^{N_2-1} x_2[n]W_{N_2}^{kn}, \qquad 0 \leq k \leq N_2 - 1. \tag{8.74}$$

In summary, if

$$x_1[n] \overset{\mathcal{DFT}}{\longleftrightarrow} X_1[k] \tag{8.75a}$$

and

$$x_2[n] \overset{\mathcal{DFT}}{\longleftrightarrow} X_2[k], \tag{8.75b}$$

then

$$ax_1[n] + bx_2[n] \overset{\mathcal{DFT}}{\longleftrightarrow} aX_1[k] + bX_2[k], \tag{8.76}$$

where the lengths of the sequences and their DFTs are all equal to at least the maximum of the lengths of $x_1[n]$ and $x_2[n]$. Of course, DFTs of greater length can be computed by augmenting both sequences with zero-valued samples.

8.6.2 Circular Shift of a Sequence

According to Section 2.9.2 and property 2 in Table 2.2, if $X(e^{j\omega})$ is the discrete-time Fourier transform of $x[n]$, then $e^{-j\omega m}X(e^{j\omega})$ is the Fourier transform of the time-shifted sequence $x[n-m]$. In other words, a shift in the time domain by m points (with positive m corresponding to a time delay and negative m to a time advance) corresponds in the frequency domain to multiplication of the Fourier transform by the linear-phase factor $e^{-j\omega m}$. In Section 8.2.2, we discussed the corresponding property for the DFS coefficients of a periodic sequence; specifically, if a periodic sequence $\tilde{x}[n]$ has Fourier series coefficients $\tilde{X}[k]$, then the shifted sequence $\tilde{x}[n-m]$ has Fourier series coefficients $e^{-j(2\pi k/N)m}\tilde{X}[k]$. Now we will consider the operation in the time domain that corresponds to multiplying the DFT coefficients of a finite-length sequence $x[n]$ by the linear-phase factor $e^{-j(2\pi k/N)m}$. Specifically, let $x_1[n]$ denote the finite-length sequence for which the DFT is $e^{-j(2\pi k/N)m}X[k]$; i.e., if

$$x[n] \overset{\mathcal{DFT}}{\longleftrightarrow} X[k], \tag{8.77}$$

then we are interested in $x_1[n]$ such that

$$x_1[n] \overset{\mathcal{DFT}}{\longleftrightarrow} X_1[k] = e^{-j(2\pi k/N)m}X[k] = W_N^m X[k]. \tag{8.78}$$

Since the N-point DFT represents a finite-duration sequence of length N, both $x[n]$ and $x_1[n]$ must be zero outside the interval $0 \le n \le N-1$, and consequently, $x_1[n]$ cannot result from a simple time shift of $x[n]$. The correct result follows directly from the result of Section 8.2.2 and the interpretation of the DFT as the Fourier series coefficients of the periodic sequence $x_1[((n))_N]$. In particular, from Eqs. (8.59) and (8.62) it follows that

$$\tilde{x}[n] = x[((n))_N] \overset{\mathcal{DFS}}{\longleftrightarrow} \tilde{X}[k] = X[((k))_N], \tag{8.79}$$

and similarly, we can define a periodic sequence $\tilde{x}_1[n]$ such that

$$\tilde{x}_1[n] = x_1[((n))_N] \overset{\mathcal{DFS}}{\longleftrightarrow} \tilde{X}_1[k] = X_1[((k))_N], \tag{8.80}$$

where, by assumption,

$$X_1[k] = e^{-j(2\pi k/N)m}X[k]. \tag{8.81}$$

Therefore, the DFS coefficients of $\tilde{x}_1[n]$ are

$$\tilde{X}_1[k] = e^{-j[2\pi((k))_N/N]m} X[((k))_N]. \tag{8.82}$$

Note that

$$e^{-j[2\pi((k))_N/N]m} = e^{-j(2\pi k/N)m}. \tag{8.83}$$

That is, since $e^{-j(2\pi k/N)m}$ is periodic with period N in both k and m, we can drop the notation $((k))_N$. Hence, Eq. (8.82) becomes

$$\tilde{X}_1[k] = e^{-j(2\pi k/N)m} \tilde{X}[k], \tag{8.84}$$

so that it follows from Section 8.2.2 that

$$\tilde{x}_1[n] = \tilde{x}[n-m] = x[((n-m))_N]. \tag{8.85}$$

Thus, the finite-length sequence $x_1[n]$ whose DFT is given by Eq. (8.81) is

$$x_1[n] = \begin{cases} \tilde{x}_1[n] = x[((n-m))_N], & 0 \le n \le N-1, \\ 0, & \text{otherwise.} \end{cases} \tag{8.86}$$

Equation (8.86) tells us how to construct $x_1[n]$ from $x[n]$.

Example 8.8 Circular Shift of a Sequence

The circular shift procedure is illustrated in Figure 8.12 for $m = -2$; i.e., we want to determine $x_1[n] = x[((n+2))_N]$ for $N = 6$, which we have shown will have DFT $X_1[k] = W_6^{-2k} X[k]$. Specifically, from $x[n]$, we construct the periodic sequence $\tilde{x}[n] = x[((n))_6]$, as indicated in Figure 8.12(b). According to Eq. (8.85), we then shift $\tilde{x}[n]$ by 2 to the left, obtaining $\tilde{x}_1[n] = \tilde{x}[n+2]$ as in Figure 8.12(c). Finally, using Eq. (8.86), we extract one period of $\tilde{x}_1[n]$ to obtain $x_1[n]$, as indicated in Figure 8.12(d).

A comparison of Figures 8.12(a) and (d) indicates clearly that $x_1[n]$ does not correspond to a linear shift of $x[n]$, and in fact, both sequences are confined to the interval between 0 and $(N-1)$. By reference to Figure 8.12, we see that $x_1[n]$ can be formed by shifting $x[n]$, so that as a sequence value leaves the interval 0 to $(N-1)$ at one end, it enters at the other end. Another interesting point is that, for the example shown in Figure 8.12(a), if we form $x_2[n] = x[((n-4))_6]$ by shifting the sequence by 4 to the right modulo 6, we obtain the same sequence as $x_1[n]$. In terms of the DFT, this results because $W_6^{4k} = W_6^{-2k}$ or, more generally, $W_N^{mk} = W_N^{-(N-m)k}$, which implies that an N-point circular shift in one direction by m is the same as a circular shift in the opposite direction by $N-m$.

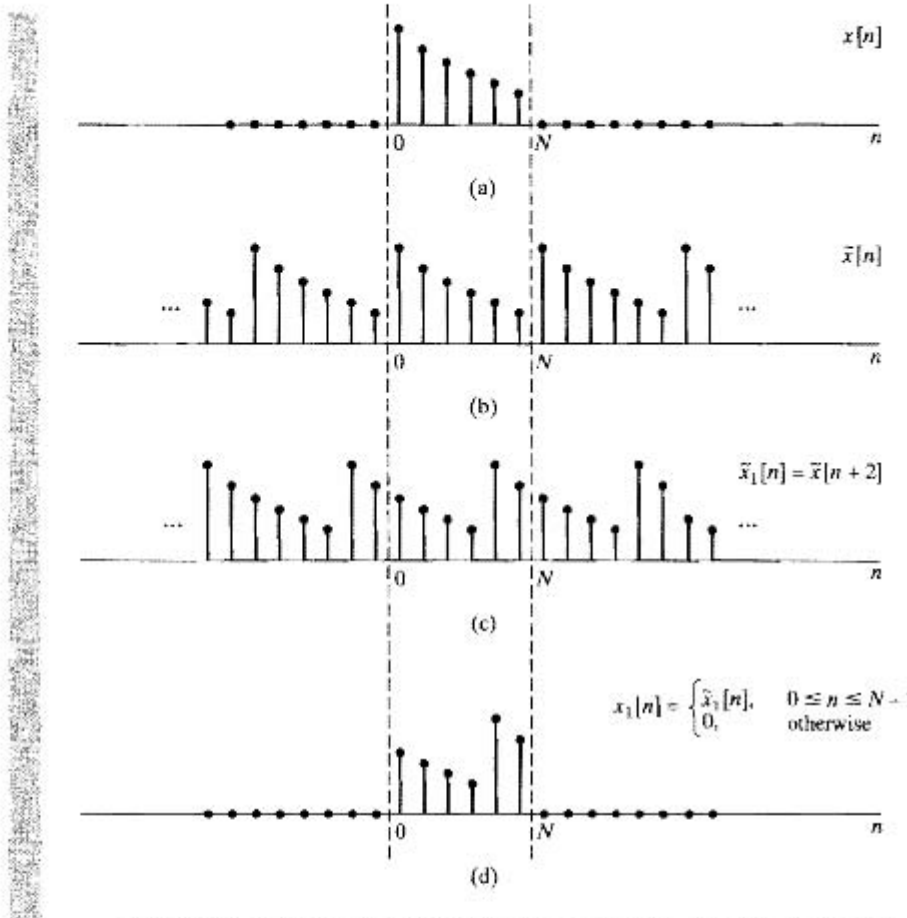

Figure 8.12 Circular shift of a finite-length sequence; i.e., the effect in the time domain of multiplying the DFT of the sequence by a linear-phase factor.

In Section 8.5, we suggested the interpretation of forming the periodic sequence $\tilde{x}[n]$ from the finite-length sequence $x[n]$ by displaying $x[n]$ around the circumference of a cylinder with a circumference of exactly N points. As we repeatedly traverse the circumference of the cylinder, the sequence that we see is the periodic sequence $\tilde{x}[n]$. A linear shift of this sequence corresponds, then, to a rotation of the cylinder. In the context of finite-length sequences and the DFT, such a shift is called a *circular* shift or a *rotation* of the sequence within the interval $0 \le n \le N-1$.

In summary, the circular shift property of the DFT is

$$x[((n-m))_N], \quad 0 \le n \le N-1 \overset{DFT}{\longleftrightarrow} e^{-j(2\pi k/N)m} X[k] = W_N^m X[k]. \tag{8.87}$$

8.6.3 Duality

Since the DFT is so closely associated with the DFS, we would expect the DFT to exhibit a duality property similar to that of the DFS discussed in Section 8.2.3. In fact, from an examination of Eqs. (8.67) and (8.68), we see that the analysis and synthesis equations differ only in the factor $1/N$ and the sign of the exponent of the powers of W_N.

The DFT duality property can be derived by exploiting the relationship between the DFT and the DFS as in our derivation of the circular shift property. Toward this end, consider $x[n]$ and its DFT $X[k]$, and construct the periodic sequences

$$\tilde{x}[n] = x[((n))_N], \tag{8.88a}$$

$$\tilde{X}[k] = X[((k))_N], \tag{8.88b}$$

so that

$$\tilde{x}[n] \overset{\mathcal{DFS}}{\longleftrightarrow} \tilde{X}[k]. \tag{8.89}$$

From the duality property given in Eqs. (8.25),

$$\tilde{X}[n] \overset{\mathcal{DFS}}{\longleftrightarrow} N\tilde{x}[-k]. \tag{8.90}$$

If we define the periodic sequence $\tilde{x}_1[n] = \tilde{X}[n]$, one period of which is the finite-length sequence $x_1[n] = X[n]$, then the DFS coefficients of $\tilde{x}_1[n]$ are $\tilde{X}_1[k] = N\tilde{x}[-k]$. Therefore, the DFT of $x_1[n]$ is

$$X_1[k] = \begin{cases} N\tilde{x}[-k], & 0 \le k \le N-1, \\ 0, & \text{otherwise}, \end{cases} \tag{8.91}$$

or, equivalently,

$$X_1[k] = \begin{cases} Nx[((-k))_N], & 0 \le k \le N-1, \\ 0, & \text{otherwise}. \end{cases} \tag{8.92}$$

Consequently, the duality property for the DFT can be expressed as follows: If

$$x[n] \overset{\mathcal{DFT}}{\longleftrightarrow} X[k], \tag{8.93a}$$

then

$$X[n] \overset{\mathcal{DFT}}{\longleftrightarrow} Nx[((-k))_N], \qquad 0 \le k \le N-1. \tag{8.93b}$$

The sequence $Nx[((-k))_N]$ is $Nx[k]$ index reversed, modulo N. Index-reversing modulo N corresponds specifically to $((-k))_N = N-k$ for $1 \le k \le N-1$ and $((-k))_N = ((k))_N$ for $k = 0$. As in the case of shifting modulo N, the process of index-reversing modulo N is usually best visualized in terms of the underlying periodic sequences.

Example 8.9 The Duality Relationship for the DFT

To illustrate the duality relationship in Eqs. (8.93), let us consider the sequence $x[n]$ of Example 8.7. Figure 8.13(a) shows the finite-length sequence $x[n]$, and Figures 8.13(b) and 8.13(c) are the real and imaginary parts, respectively, of the corresponding 10-point DFT $X[k]$. By simply relabeling the horizontal axis, we obtain the complex sequence $x_1[n] = X[n]$, as shown in Figures 8.13(d) and 8.13(e). According to the duality relation in Eqs. (8.93), the 10-point DFT of the (complex-valued) sequence $X[n]$ is the sequence shown in Figure 8.13(f).

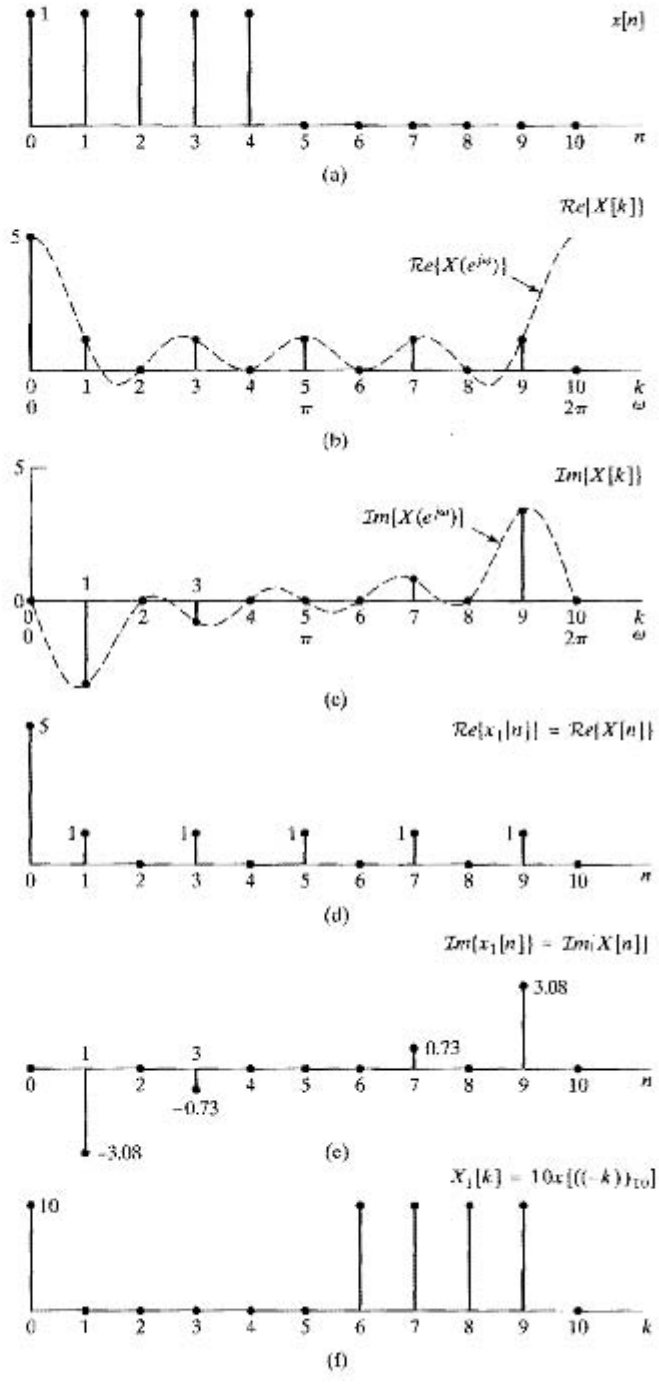

Figure 8.13 Illustration of duality. (a) Real finite-length sequence $x[n]$. (b) and (c) Real and imaginary parts of corresponding DFT $X[k]$. (d) and (e) The real and imaginary parts of the dual sequence $x_1[n] = X[n]$. (f) The DFT of $x_1[n]$.

8.6.4 Symmetry Properties

Since the DFT of $x[n]$ is identical to the DFS coefficients of the periodic sequence $\tilde{x}[n] = x[((n))_N]$, symmetry properties associated with the DFT can be inferred from the symmetry properties of the DFS summarized in Table 8.1 in Section 8.2.6. Specifically, using Eqs. (8.88) together with Properties 9 and 10 in Table 8.1, we have

$$x^*[n] \overset{\mathcal{DFT}}{\longleftrightarrow} X^*[((-k))_N], \qquad 0 \le n \le N-1, \tag{8.94}$$

and

$$x^*[((-n))_N] \overset{\mathcal{DFT}}{\longleftrightarrow} X^*[k], \qquad 0 \le n \le N-1. \tag{8.95}$$

Properties 11–14 in Table 8.1 refer to the decomposition of a periodic sequence into the sum of a conjugate-symmetric and a conjugate-antisymmetric sequence. This suggests the decomposition of the finite-duration sequence $x[n]$ into the two finite-duration sequences of duration N corresponding to one period of the conjugate-symmetric and one period of the conjugate-antisymmetric components of $\tilde{x}[n]$. We will denote these components of $x[n]$ as $x_{ep}[n]$ and $x_{op}[n]$. Thus, with

$$\tilde{x}[n] = x[((n))_N] \tag{8.96}$$

and the conjugate-symmetric part being

$$\tilde{x}_e[n] = \tfrac{1}{2}\{\tilde{x}[n] + \tilde{x}^*[-n]\}, \tag{8.97}$$

and the conjugate-antisymmetric part being

$$\tilde{x}_o[n] = \tfrac{1}{2}\{\tilde{x}[n] - \tilde{x}^*[-n]\}, \tag{8.98}$$

we define $x_{ep}[n]$ and $x_{op}[n]$ as

$$x_{ep}[n] = \tilde{x}_e[n], \qquad 0 \le n \le N-1, \tag{8.99}$$

$$x_{op}[n] = \tilde{x}_o[n], \qquad 0 \le n \le N-1, \tag{8.100}$$

or, equivalently,

$$x_{ep}[n] = \tfrac{1}{2}\{x[((n))_N] + x^*[((-n))_N]\}, \qquad 0 \le n \le N-1, \tag{8.101a}$$

$$x_{op}[n] = \tfrac{1}{2}\{x[((n))_N] - x^*[((-n))_N]\}, \qquad 0 \le n \le N-1, \tag{8.101b}$$

with both $x_{ep}[n]$ and $x_{op}[n]$ being finite-length sequences, i.e., both zero outside the interval $0 \le n \le N-1$. Since $((-n))_N = (N-n)$ and $((n))_N = n$ for $0 \le n \le N-1$, we can also express Eqs. (8.101) as

$$x_{ep}[n] = \tfrac{1}{2}\{x[n] + x^*[N-n]\}, \qquad 1 \le n \le N-1, \tag{8.102a}$$

$$x_{ep}[0] = \mathcal{R}e\{x[0]\}, \tag{8.102b}$$

$$x_{op}[n] = \tfrac{1}{2}\{x[n] - x^*[N-n]\}, \qquad 1 \le n \le N-1, \tag{8.102c}$$

$$x_{op}[0] = j\mathcal{I}m\{x[0]\}. \tag{8.102d}$$

This form of the equations is convenient, since it avoids the modulo N computation of indices.

Clearly, $x_{ep}[n]$ and $x_{op}[n]$ are not equivalent to $x_e[n]$ and $x_o[n]$ as defined by Eqs. (2.149a) and (2.149b). However, it can be shown (see Problem 8.59) that

$$x_{ep}[n] = \{x_e[n] + x_e[n - N]\}, \qquad 0 \le n \le N - 1, \tag{8.103}$$

and

$$x_{op}[n] = \{x_o[n] + x_o[n - N]\}, \qquad 0 \le n \le N - 1. \tag{8.104}$$

In other words, $x_{ep}[n]$ and $x_{op}[n]$ can be generated by time-aliasing $x_e[n]$ and $x_o[n]$ into the interval $0 \le n \le N - 1$. The sequences $x_{ep}[n]$ and $x_{op}[n]$ will be referred to as *the periodic conjugate-symmetric* and *periodic conjugate-antisymmetric* components, respectively, of $x[n]$. When $x_{ep}[n]$ and $x_{op}[n]$ are real, they will be referred to as the *periodic even* and *periodic odd* components, respectively. Note that the sequences $x_{ep}[n]$ and $x_{op}[n]$ are not periodic sequences; they are, however, finite-length sequences that are equal to one period of the periodic sequences $\tilde{x}_e[n]$ and $\tilde{x}_o[n]$, respectively.

Equations (8.101) and (8.102) define $x_{ep}[n]$ and $x_{op}[n]$ in terms of $x[n]$. The inverse relation, expressing $x[n]$ in terms of $x_{ep}[n]$ and $x_{op}[n]$, can be obtained by using Eqs. (8.97) and (8.98) to express $\tilde{x}[n]$ as

$$\tilde{x}[n] = \tilde{x}_e[n] + \tilde{x}_o[n]. \tag{8.105}$$

Thus,

$$x[n] = \tilde{x}[n] = \tilde{x}_e[n] + \tilde{x}_o[n], \qquad 0 \le n \le N - 1. \tag{8.106}$$

Combining Eqs. (8.106) with Eqs. (8.99) and (8.100), we obtain

$$x[n] = x_{ep}[n] + x_{op}[n]. \tag{8.107}$$

Alternatively, Eqs. (8.102), when added, also lead to Eq. (8.107). The symmetry properties of the DFT associated with properties 11–14 in Table 8.1 now follow in a straightforward way:

$$\mathcal{R}e\{x[n]\} \overset{DFT}{\longleftrightarrow} X_{ep}[k], \tag{8.108}$$

$$j\mathcal{I}m\{x[n]\} \overset{DFT}{\longleftrightarrow} X_{op}[k], \tag{8.109}$$

$$x_{ep}[n] \overset{DFT}{\longleftrightarrow} \mathcal{R}e\{X[k]\}, \tag{8.110}$$

$$x_{op}[n] \overset{DFT}{\longleftrightarrow} j\mathcal{I}m\{X[k]\}. \tag{8.111}$$

8.6.5 Circular Convolution

In Section 8.2.5, we showed that multiplication of the DFS coefficients of two periodic sequences corresponds to a periodic convolution of the sequences. Here, we consider two *finite-duration* sequences $x_1[n]$ and $x_2[n]$, both of length N, with DFTs $X_1[k]$ and $X_2[k]$, respectively, and we wish to determine the sequence $x_3[n]$, for which the DFT is $X_3[k] = X_1[k]X_2[k]$. To determine $x_3[n]$, we can apply the results of Section 8.2.5. Specifically, $x_3[n]$ corresponds to one period of $\tilde{x}_3[n]$, which is given by Eq. (8.27). Thus,

$$x_3[n] = \sum_{m=0}^{N-1} \tilde{x}_1[m]\tilde{x}_2[n - m], \qquad 0 \le n \le N - 1, \tag{8.112}$$

or, equivalently,

$$x_3[n] = \sum_{m=0}^{N-1} x_1[((m))_N]x_2[((n-m))_N], \qquad 0 \le n \le N-1. \tag{8.113}$$

Since $((m))_N = m$ for $0 \le m \le N-1$, Eq. (8.113) can be written

$$x_3[n] = \sum_{m=0}^{N-1} x_1[m]x_2[((n-m))_N], \qquad 0 \le n \le N-1. \tag{8.114}$$

Equation (8.114) differs from a linear convolution of $x_1[n]$ and $x_2[n]$ as defined by Eq. (2.49) in some important respects. In linear convolution, the computation of the sequence value $x_3[n]$ involves multiplying one sequence by a time-reversed and linearly shifted version of the other and then summing the values of the product $x_1[m]x_2[n-m]$ over all m. To obtain successive values of the sequence formed by the convolution operation, the two sequences are successively shifted relative to each other along a linear axis. In contrast, for the convolution defined by Eq. (8.114), the second sequence is circularly time reversed and circularly shifted with respect to the first. For this reason, the operation of combining two finite-length sequences according to Eq. (8.114) is called *circular convolution*. More specifically, we refer to Eq. (8.114) as an N-point circular convolution, explicitly identifying the fact that both sequences have length N (or less) and that the sequences are shifted modulo N. Sometimes, the operation of forming a sequence $x_3[n]$ for $0 \le n \le N-1$ using Eq. (8.114) will be denoted

$$x_3[n] = x_1[n] \textcircled{N} x_2[n], \tag{8.115}$$

i.e., the symbol Ⓝ denotes N-point circular convolution.

Since the DFT of $x_3[n]$ is $X_3[k] = X_1[k]X_2[k]$ and since $X_1[k]X_2[k] = X_2[k]X_1[k]$, it follows with no further analysis that

$$x_3[n] = x_2[n] \textcircled{N} x_1[n], \tag{8.116}$$

or, more specifically,

$$x_3[n] = \sum_{m=0}^{N-1} x_2[m]x_1[((n-m))_N]. \tag{8.117}$$

That is, circular convolution, like linear convolution, is a commutative operation.

Since circular convolution is really just periodic convolution, Example 8.4 and Figure 8.3 are also illustrative of circular convolution. However, if we use the notion of circular shifting, it is not necessary to construct the underlying periodic sequences as in Figure 8.3. This is illustrated in the following examples.

Example 8.10 Circular Convolution with a Delayed Impulse Sequence

An example of circular convolution is provided by the result of Section 8.6.2. Let $x_2[n]$ be a finite-duration sequence of length N and

$$x_1[n] = \delta[n - n_0], \tag{8.118}$$

where $0 < n_0 < N$. Clearly, $x_1[n]$ can be considered as the finite-duration sequence

$$x_1[n] = \begin{cases} 0, & 0 \le n < n_0, \\ 1, & n = n_0, \\ 0, & n_0 < n \le N-1. \end{cases} \tag{8.119}$$

as depicted in Figure 8.14 for $n_0 = 1$.

The DFT of $x_1[n]$ is

$$X_1[k] = W_N^{kn_0}. \tag{8.120}$$

If we form the product

$$X_3[k] = W_N^{kn_0} X_2[k], \tag{8.121}$$

we see from Section 8.6.2 that the finite-duration sequence corresponding to $X_3[k]$ is the sequence $x_2[n]$ rotated to the right by n_0 samples in the interval $0 \le n \le N-1$. That is, the circular convolution of a sequence $x_2[n]$ with a single delayed unit impulse results in a rotation of $x_2[n]$ in the interval $0 \le n \le N-1$. This example is illustrated in Figure 8.14 for $N = 5$ and $n_0 = 1$. Here, we show the sequences $x_2[m]$

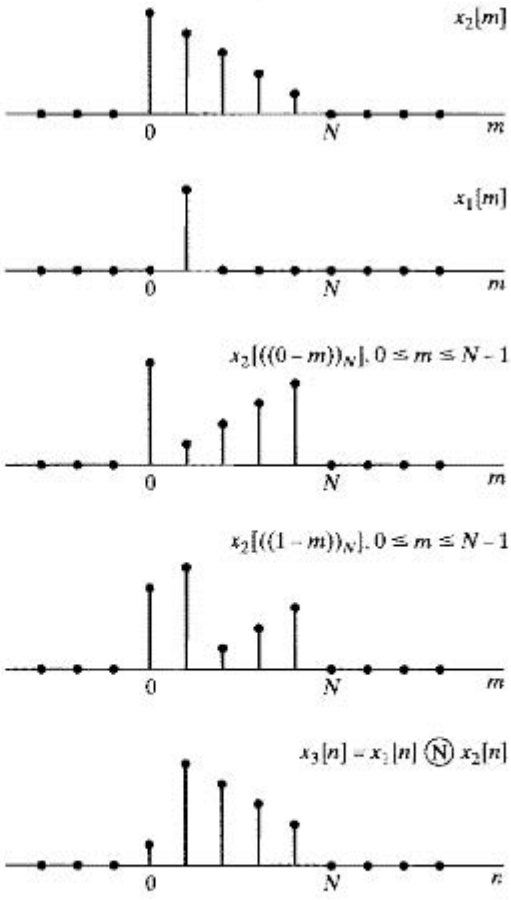

Figure 8.14 Circular convolution of a finite-length sequence $x_2[n]$ with a single delayed impulse, $x_1[n] = \delta[n-1]$.

and $x_1[m]$ and then $x_2[((0-m))_N]$ and $x_2[((1-m))_N]$. It is clear from these two cases that the result of circular convolution of $x_2[n]$ with a single shifted unit impulse will be to circularly shift $x_2[n]$. The last sequence shown is $x_3[n]$, the result of the circular convolution of $x_1[n]$ and $x_2[n]$.

Example 8.11 Circular Convolution of Two Rectangular Pulses

As another example of circular convolution, let

$$x_1[n] = x_2[n] = \begin{cases} 1, & 0 \le n \le L-1, \\ 0, & \text{otherwise,} \end{cases} \tag{8.122}$$

where, in Figure 8.15, $L = 6$. If we let N denote the DFT length, then, for $N = L$, the N-point DFTs are

$$X_1[k] = X_2[k] = \sum_{n=0}^{N-1} W_N^{kn} = \begin{cases} N, & k = 0, \\ 0, & \text{otherwise.} \end{cases} \tag{8.123}$$

If we explicitly multiply $X_1[k]$ and $X_2[k]$, we obtain

$$X_3[k] = X_1[k]X_2[k] = \begin{cases} N^2, & k = 0, \\ 0, & \text{otherwise,} \end{cases} \tag{8.124}$$

from which it follows that

$$x_3[n] = N, \qquad 0 \le n \le N-1. \tag{8.125}$$

This result is depicted in Figure 8.15. Clearly, as the sequence $x_2[((n-m))_N]$ is rotated with respect to $x_1[m]$, the sum of products $x_1[m]x_2[((n-m))_N]$ will always be equal to N.

Of course, it is possible to consider $x_1[n]$ and $x_2[n]$ as $2L$-point sequences by augmenting them with L zeros. If we then perform a $2L$-point circular convolution of the augmented sequences, we obtain the sequence in Figure 8.16, which can be seen to be identical to the linear convolution of the finite-duration sequences $x_1[n]$ and $x_2[n]$. This important observation will be discussed in much more detail in Section 8.7.

Note that for $N = 2L$, as in Figure 8.16,

$$X_1[k] = X_2[k] = \frac{1 - W_N^{Lk}}{1 - W_N^k},$$

so the DFT of the triangular-shaped sequence $x_3[n]$ in Figure 8.16(c) is

$$X_3[k] = \left(\frac{1 - W_N^{Lk}}{1 - W_N^k}\right)^2,$$

with $N = 2L$.

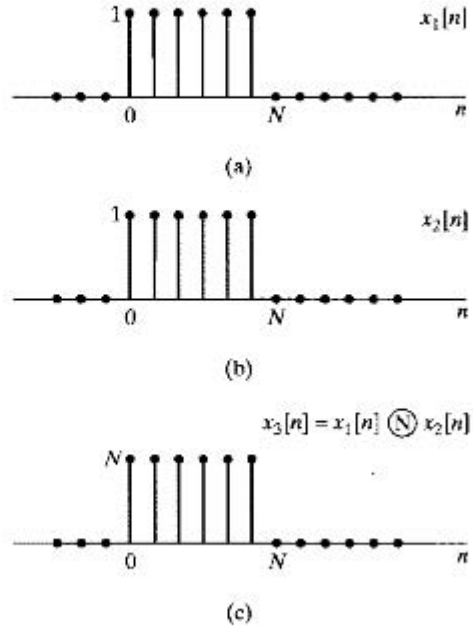

Figure 8.15 N-point circular convolution of two constant sequences of length N.

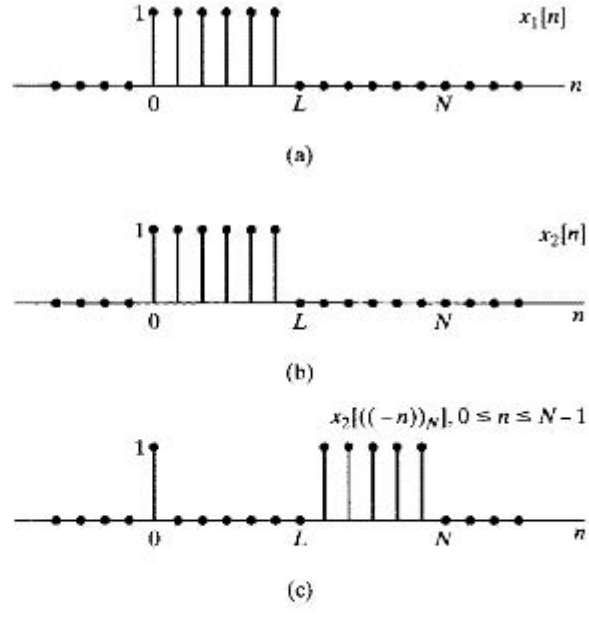

Figure 8.16 $2L$-point circular convolution of two constant sequences of length L.

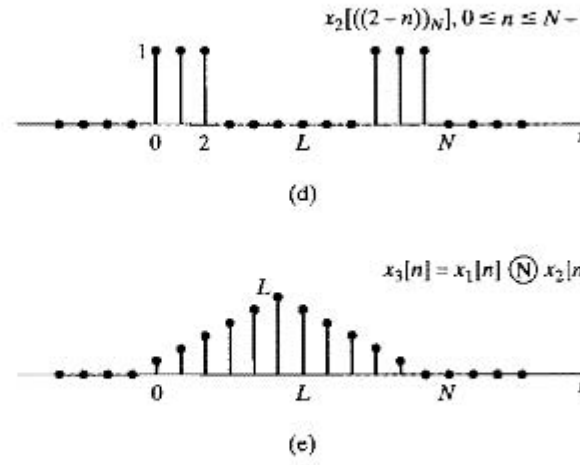

Figure 8.16 *(continued)*

The circular convolution property is represented as

$$x_1[n] \textcircled{N} x_2[n] \overset{\mathcal{DFT}}{\longleftrightarrow} X_1[k]X_2[k]. \tag{8.126}$$

In view of the duality of the DFT relations, it is not surprising that the DFT of a product of two N-point sequences is the circular convolution of their respective DFTs. Specifically, if $x_3[n] = x_1[n]x_2[n]$, then

$$X_3[k] = \frac{1}{N}\sum_{\ell=0}^{N-1} X_1[\ell]X_2[((k-\ell))_N] \tag{8.127}$$

or

$$x_1[n]x_2[n] \overset{\mathcal{DFT}}{\longleftrightarrow} \frac{1}{N}X_1[k] \textcircled{N} X_2[k]. \tag{8.128}$$

8.6.6 Summary of Properties of the DFT

The properties of the DFT that we discussed in Section 8.6 are summarized in Table 8.2. Note that for all of the properties, the expressions given specify $x[n]$ for $0 \le n \le N-1$ and $X[k]$ for $0 \le k \le N-1$. Both $x[n]$ and $X[k]$ are equal to zero outside those ranges.

TABLE 8.2 SUMMARY OF PROPERTIES OF THE DFT

Finite-Length Sequence (Length N)	N-point DFT (Length N)
1. $x[n]$	$X[k]$
2. $x_1[n], x_2[n]$	$X_1[k], X_2[k]$
3. $ax_1[n] + bx_2[n]$	$aX_1[k] + bX_2[k]$
4. $X[n]$	$Nx[((-k))_N]$
5. $x[((n-m))_N]$	$W_N^{km}X[k]$
6. $W_N^{-\ell n}x[n]$	$X[((k-\ell))_N]$
7. $\sum_{m=0}^{N-1} x_1[m]x_2[((n-m))_N]$	$X_1[k]X_2[k]$
8. $x_1[n]x_2[n]$	$\frac{1}{N}\sum_{\ell=0}^{N-1} X_1[\ell]X_2[((k-\ell))_N]$
9. $x^*[n]$	$X^*[((-k))_N]$
10. $x^*[((-n))_N]$	$X^*[k]$
11. $\mathcal{R}e\{x[n]\}$	$X_{ep}[k] = \frac{1}{2}\{X[((k))_N] + X^*[((-k))_N]\}$
12. $j\mathcal{I}m\{x[n]\}$	$X_{op}[k] = \frac{1}{2}\{X[((k))_N] - X^*[((-k))_N]\}$
13. $x_{ep}[n] = \frac{1}{2}\{x[n] + x^*[((-n))_N]\}$	$\mathcal{R}e\{X[k]\}$
14. $x_{op}[n] = \frac{1}{2}\{x[n] - x^*[((-n))_N]\}$	$j\mathcal{I}m\{X[k]\}$
Properties 15–17 apply only when $x[n]$ is real.	
15. Symmetry properties	$\begin{cases} X[k] = X^*[((-k))_N] \\ \mathcal{R}e\{X[k]\} = \mathcal{R}e\{X[((-k))_N]\} \\ \mathcal{I}m\{X[k]\} = -\mathcal{I}m\{X[((-k))_N]\} \\ \lvert X[k]\rvert = \lvert X[((-k))_N]\rvert \\ \angle X[k] = -\angle X[((-k))_N] \end{cases}$
16. $x_{ep}[n] = \frac{1}{2}\{x[n] + x[((-n))_N]\}$	$\mathcal{R}e\{X[k]\}$
17. $x_{op}[n] = \frac{1}{2}\{x[n] - x[((-n))_N]\}$	$j\mathcal{I}m\{X[k]\}$

8.7 COMPUTING LINEAR CONVOLUTION USING THE DFT

We will show in Chapter 9 that efficient algorithms are available for computing the DFT of a finite-duration sequence. These are known collectively as FFT algorithms. Because these algorithms are available, it is computationally efficient to implement a convolution of two sequences by the following procedure:

(a) Compute the N-point DFTs $X_1[k]$ and $X_2[k]$ of the two sequences $x_1[n]$ and $x_2[n]$, respectively.

(b) Compute the product $X_3[k] = X_1[k]X_2[k]$ for $0 \leq k \leq N-1$.

(c) Compute the sequence $x_3[n] = x_1[n] \textcircled{N} x_2[n]$ as the inverse DFT of $X_3[k]$.

In many DSP applications, we are interested in implementing a linear convolution of two sequences; i.e., we wish to implement an LTI system. This is certainly true, for example, in filtering a sequence such as a speech waveform or a radar signal or in computing the autocorrelation function of such signals. As we saw in Section 8.6.5, the multiplication of DFTs corresponds to a circular convolution of the sequences. To obtain a linear convolution, we must ensure that circular convolution has the effect of linear convolution. The discussion at the end of Example 8.11 hints at how this might be done. We now present a more detailed analysis.

8.7.1 Linear Convolution of Two Finite-Length Sequences

Consider a sequence $x_1[n]$ whose length is L points and a sequence $x_2[n]$ whose length is P points, and suppose that we wish to combine these two sequences by linear convolution to obtain a third sequence

$$x_3[n] = \sum_{m=-\infty}^{\infty} x_1[m]x_2[n-m]. \tag{8.129}$$

Figure 8.17(a) shows a typical sequence $x_1[m]$ and Figure 8.17(b) shows a typical sequence $x_2[n-m]$ for the three cases $n = -1$, for $0 \le n \le L-1$, and $n = L+P-1$. Clearly, the product $x_1[m]x_2[n-m]$ is zero for all m whenever $n < 0$ and $n > L+P-2$; i.e., $x_3[n] \neq 0$ for $0 \le n \le L+P-2$. Therefore, $(L+P-1)$ is the maximum length of the sequence $x_3[n]$ resulting from the linear convolution of a sequence of length L with a sequence of length P.

8.7.2 Circular Convolution as Linear Convolution with Aliasing

As Examples 8.10 and 8.11 show, whether a circular convolution corresponding to the product of two N-point DFTs is the same as the linear convolution of the corresponding finite-length sequences depends on the length of the DFT in relation to the length of the finite-length sequences. An extremely useful interpretation of the relationship between circular convolution and linear convolution is in terms of time aliasing. Since this interpretation is so important and useful in understanding circular convolution, we will develop it in several ways.

In Section 8.4, we observed that if the Fourier transform $X(e^{j\omega})$ of a sequence $x[n]$ is sampled at frequencies $\omega_k = 2\pi k/N$, then the resulting sequence corresponds to the DFS coefficients of the periodic sequence

$$\tilde{x}[n] = \sum_{r=-\infty}^{\infty} x[n-rN]. \tag{8.130}$$

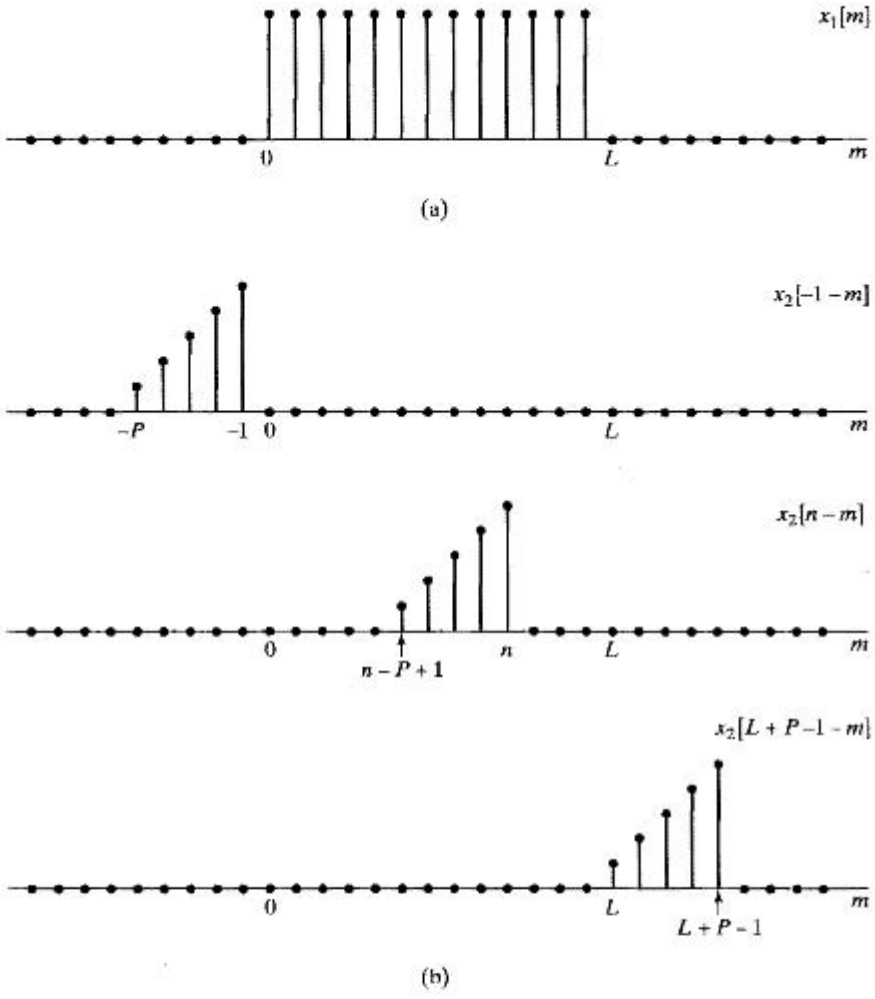

Figure 8.17 Example of linear convolution of two finite-length sequences showing that the result is such that $x_3[n] = 0$ for $n \leq -1$ and for $n \geq L + P - 1$. (a) Finite-length sequence $x_1[m]$. (b) $x_2[n - m]$ for several values of n.

From our discussion of the DFT, it follows that the finite-length sequence

$$X[k] = \begin{cases} X(e^{j(2\pi k/N)}), & 0 \leq k \leq N-1, \\ 0, & \text{otherwise}, \end{cases} \tag{8.131}$$

is the DFT of one period of $\tilde{x}[n]$, as given by Eq. (8.130); i.e.,

$$x_p[n] = \begin{cases} \tilde{x}[n], & 0 \leq n \leq N-1, \\ 0, & \text{otherwise}. \end{cases} \tag{8.132}$$

Obviously, if $x[n]$ has length less than or equal to N, no time aliasing occurs and $x_p[n] = x[n]$. However, if the length of $x[n]$ is greater than N, $x_p[n]$ may not be equal to $x[n]$ for some or all values of n. We will henceforth use the subscript p to denote

that a sequence is one period of a periodic sequence resulting from an inverse DFT of a sampled Fourier transform. The subscript can be dropped if it is clear that time aliasing is avoided.

The sequence $x_3[n]$ in Eq. (8.129) has Fourier transform

$$X_3(e^{j\omega}) = X_1(e^{j\omega})X_2(e^{j\omega}). \tag{8.133}$$

If we define a DFT

$$X_3[k] = X_3(e^{j(2\pi k/N)}), \qquad 0 \le k \le N-1, \tag{8.134}$$

then it is clear from Eqs. (8.133) and (8.134) that, also

$$X_3[k] = X_1(e^{j(2\pi k/N)})X_2(e^{j(2\pi k/N)}), \qquad 0 \le k \le N-1, \tag{8.135}$$

and therefore,

$$X_3[k] = X_1[k]X_2[k]. \tag{8.136}$$

That is, the sequence resulting as the inverse DFT of $X_3[k]$ is

$$x_{3p}[n] = \begin{cases} \displaystyle\sum_{r=-\infty}^{\infty} x_3[n+rN], & 0 \le n \le N-1, \\ 0, & \text{otherwise}, \end{cases} \tag{8.137}$$

and from Eq. (8.136), it follows that

$$x_{3p}[n] = x_1[n] \textcircled{N} x_2[n]. \tag{8.138}$$

Thus, the circular convolution of two finite-length sequences is equivalent to linear convolution of the two sequences, followed by time aliasing according to Eq. (8.137).

Note that if N is greater than or equal to either L or P, $X_1[k]$ and $X_2[k]$ represent $x_1[n]$ and $x_2[n]$ exactly, but $x_{3p}[n] = x_3[n]$ for all n only if N is greater than or equal to the length of the sequence $x_3[n]$. As we showed in Section 8.7.1, if $x_1[n]$ has length L and $x_2[n]$ has length P, then $x_3[n]$ has maximum length $(L+P-1)$. Therefore, the circular convolution corresponding to $X_1[k]X_2[k]$ is identical to the linear convolution corresponding to $X_1(e^{j\omega})X_2(e^{j\omega})$ if N, the length of the DFTs, satisfies $N \ge L+P-1$.

Example 8.12 Circular Convolution as Linear Convolution with Aliasing

The results of Example 8.11 are easily understood in light of the interpretation just discussed. Note that $x_1[n]$ and $x_2[n]$ are identical constant sequences of length $L = P = 6$, as shown in Figure 8.18(a). The linear convolution of $x_1[n]$ and $x_2[n]$ is of length $L+P-1 = 11$ and has the triangular shape shown in Figure 8.18(b). In Figures 8.18(c) and (d) are shown two of the shifted versions $x_3[n-rN]$ in Eq. (8.137), $x_3[n-N]$ and $x_3[n+N]$ for $N = 6$. The N-point circular convolution of $x_1[n]$ and $x_2[n]$ can be formed by using Eq. (8.137). This is shown in Figure 8.18(e) for $N = L = 6$ and in Figure 8.18(f) for $N = 2L = 12$. Note that for $N = L = 6$, only $x_3[n]$ and $x_3[n+N]$ contribute to the result. For $N = 2L = 12$, only $x_3[n]$ contributes to the result. Since the length of the linear convolution is $(2L-1)$, the result of the circular convolution for $N = 2L$ is identical to the result of linear convolution for all $0 \le n \le N-1$. In

fact, this would be true for $N = 2L - 1 = 11$ as well.

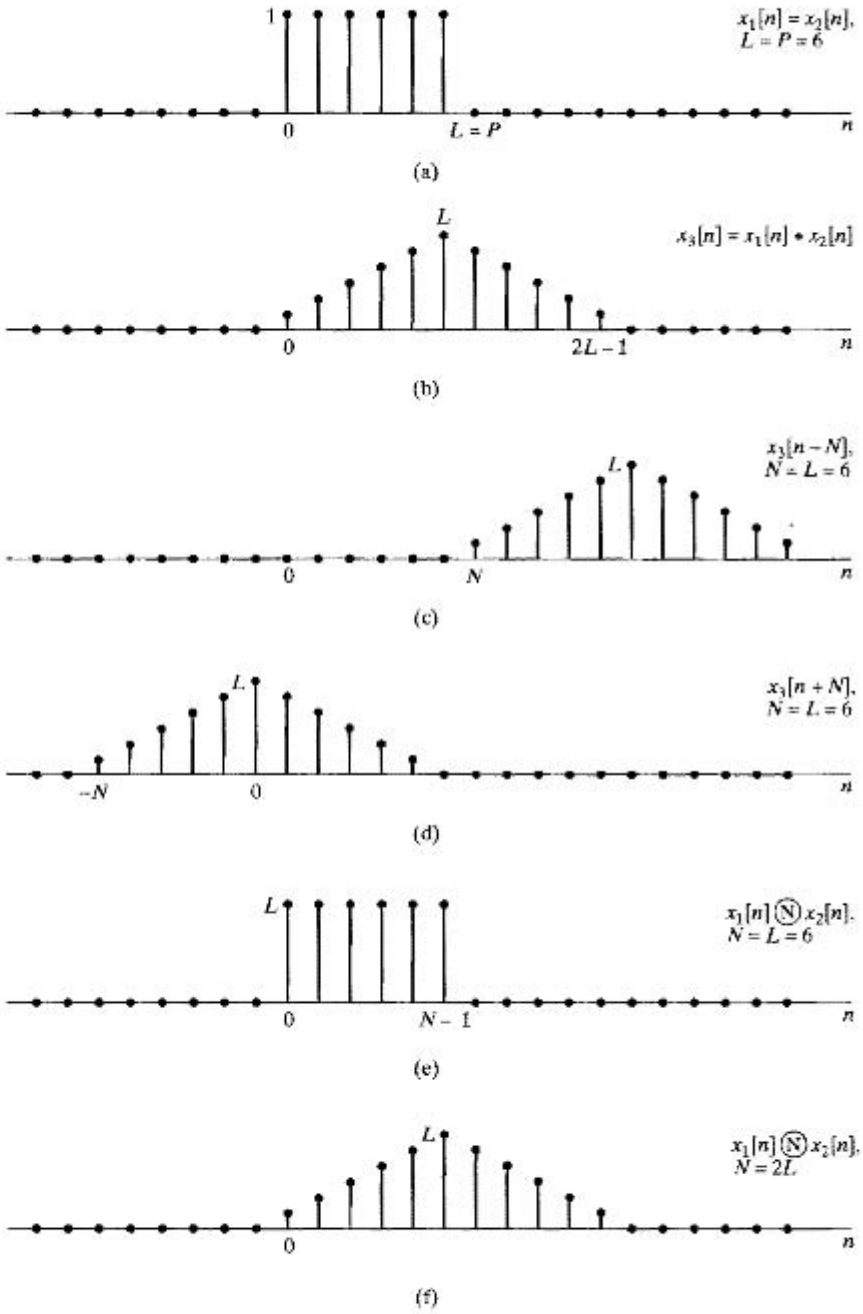

Figure 8.18 Illustration that circular convolution is equivalent to linear convolution followed by aliasing. (a) The sequences $x_1[n]$ and $x_2[n]$ to be convolved. (b) The linear convolution of $x_1[n]$ and $x_2[n]$. (c) $x_3[n - N]$ for $N = 6$. (d) $x_3[n + N]$ for $N = 6$. (e) $x_1[n]$ (6) $x_2[n]$, which is equal to the sum of (b), (c), and (d) in the interval $0 \le n \le 5$. (f) $x_1[n]$ (12) $x_2[n]$.

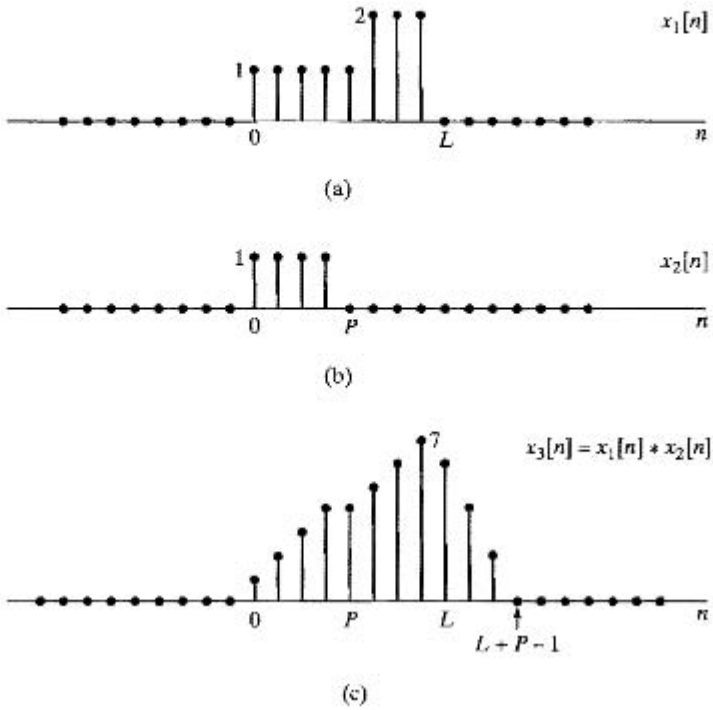

Figure 8.19 An example of linear convolution of two finite-length sequences.

As Example 8.12 points out, time aliasing in the circular convolution of two finite-length sequences can be avoided if $N \geq L + P - 1$. Also, it is clear that if $N = L = P$, all of the sequence values of the circular convolution may be different from those of the linear convolution. However, if $P < L$, some of the sequence values in an L-point circular convolution will be equal to the corresponding sequence values of the linear convolution. The time-aliasing interpretation is useful for showing this.

Consider two finite-duration sequences $x_1[n]$ and $x_2[n]$, with $x_1[n]$ of length L and $x_2[n]$ of length P, where $P < L$, as indicated in Figures 8.19(a) and 8.19(b), respectively. Let us first consider the L-point circular convolution of $x_1[n]$ and $x_2[n]$ and inquire as to which sequence values in the circular convolution are identical to values that would be obtained from a linear convolution and which are not. The linear convolution of $x_1[n]$ with $x_2[n]$ will be a finite-length sequence of length $(L + P - 1)$, as indicated in Figure 8.19(c). To determine the L-point circular convolution, we use Eqs. (8.137) and (8.138) so that

$$x_{3p}[n] = \begin{cases} x_1[n] \textcircled{L} x_2[n] = \displaystyle\sum_{r=-\infty}^{\infty} x_3[n - rL], & 0 \leq n \leq L-1, \\ 0, & \text{otherwise.} \end{cases} \tag{8.139}$$

Figure 8.20(a) shows the term in Eq. (8.139) for $r = 0$, and Figures 8.20(b) and 8.20(c) show the terms for $r = -1$ and $r = +1$, respectively. From Figure 8.20, it should be clear that in the interval $0 \leq n \leq L - 1$, $x_{3p}[n]$ is influenced only by $x_3[n]$ and $x_3[n + L]$.

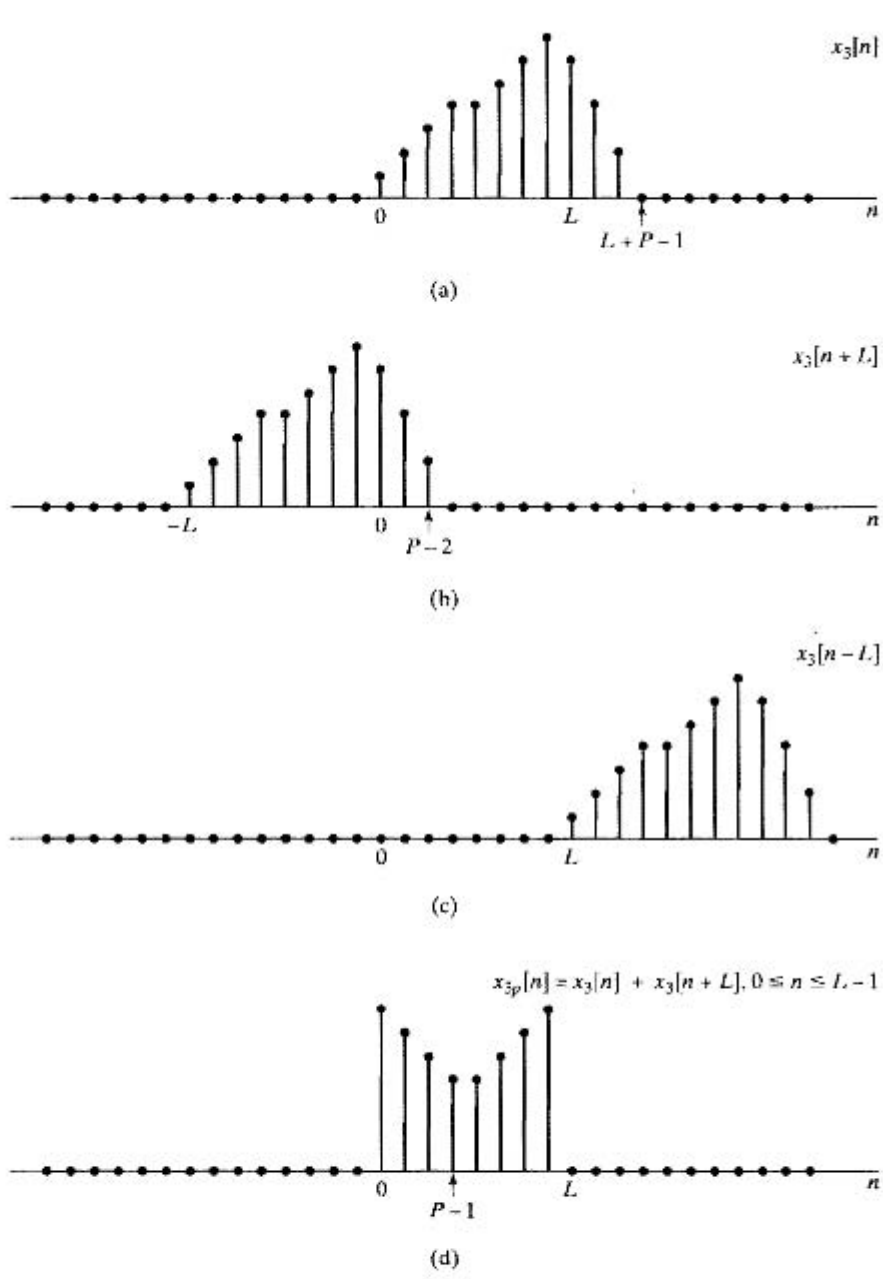

Figure 8.20 Interpretation of circular convolution as linear convolution followed by aliasing for the circular convolution of the two sequences $x_1[n]$ and $x_2[n]$ in Figure 8.19.

In general, whenever $P < L$, only the term $x_3[n + L]$ will alias into the interval $0 \le n \le L-1$. More specifically, when these terms are summed, the last $(P-1)$ points of $x_3[n+L]$, which extend from $n = 0$ to $n = P-2$, will be added to the first $(P-1)$ points of $x_3[n]$, and the last $(P-1)$ points of $x_3[n]$, extending from $n = L$ to $n = L+P-2$, will contribute only to the next period of the underlying periodic result $\tilde{x}_3[n]$. Then, $x_{3p}[n]$ is formed by extracting the portion for $0 \le n \le L-1$. Since the last $(P-1)$ points of $x_3[n+L]$ and the last $(P-1)$ points of $x_3[n]$ are identical, we can alternatively view the process of forming the circular convolution $x_{3p}[n]$ through linear convolution plus aliasing, as taking the $(P-1)$ values of $x_3[n]$ from $n = L$ to $n = L+P-2$ and adding them to the first $(P-1)$ values of $x_3[n]$. This process is illustrated in Figure 8.21 for the case $P = 4$ and $L = 8$. Figure 8.21(a) shows the linear convolution $x_3[n]$, with the points for $n \ge L$ denoted by open symbols. Note that only $(P-1)$ points for $n \ge L$ are nonzero. Figure 8.21(b) shows the formation of $x_{3p}[n]$ by "wrapping $x_3[n]$ around on itself." The first $(P-1)$ points are corrupted by the time aliasing, and the remaining points from $n = P-1$ to $n = L-1$ (i.e., the last $L-P+1$ points) are not corrupted; that is, they are identical to what would be obtained with a linear convolution.

From this discussion, it should be clear that if the circular convolution is of sufficient length relative to the lengths of the sequences $x_1[n]$ and $x_2[n]$, then aliasing with nonzero values can be avoided, in which case the circular convolution and linear convolution will be identical. Specifically, if, for the case just considered, $x_3[n]$ is replicated with period $N \ge L+P-1$, then no nonzero overlap will occur. Figures 8.21(c) and 8.21(d) illustrate this case, again for $P = 4$ and $L = 8$, with $N = 11$.

8.7.3 Implementing Linear Time-Invariant Systems Using the DFT

The previous discussion focused on ways of obtaining a linear convolution from a circular convolution. Since LTI systems can be implemented by convolution, this implies that circular convolution (implemented by the procedure suggested at the beginning of Section 8.7) can be used to implement these systems. To see how this can be done, let us first consider an L-point input sequence $x[n]$ and a P-point impulse response $h[n]$. The linear convolution of these two sequences, which will be denoted by $y[n]$, has finite duration with length $(L+P-1)$. Consequently, as discussed in Section 8.7.2, for the circular convolution and linear convolution to be identical, the circular convolution must have a length of at least $(L+P-1)$ points. The circular convolution can be achieved by multiplying the DFTs of $x[n]$ and $h[n]$. Since we want the product to represent the DFT of the linear convolution of $x[n]$ and $h[n]$, which has length $(L+P-1)$, the DFTs that we compute must also be of at least that length, i.e., both $x[n]$ and $h[n]$ must be augmented with sequence values of zero amplitude. This process is often referred to as *zero-padding*.

This procedure permits the computation of the linear convolution of two finite-length sequences using the DFT; i.e., the output of an FIR system whose input also has finite length can be computed with the DFT. In many applications, such as filtering a speech waveform, the input signal is of indefinite duration. Theoretically, while we might be able to store the entire waveform and then implement the procedure just discussed using a DFT for a large number of points, such a DFT might be impractical to compute.

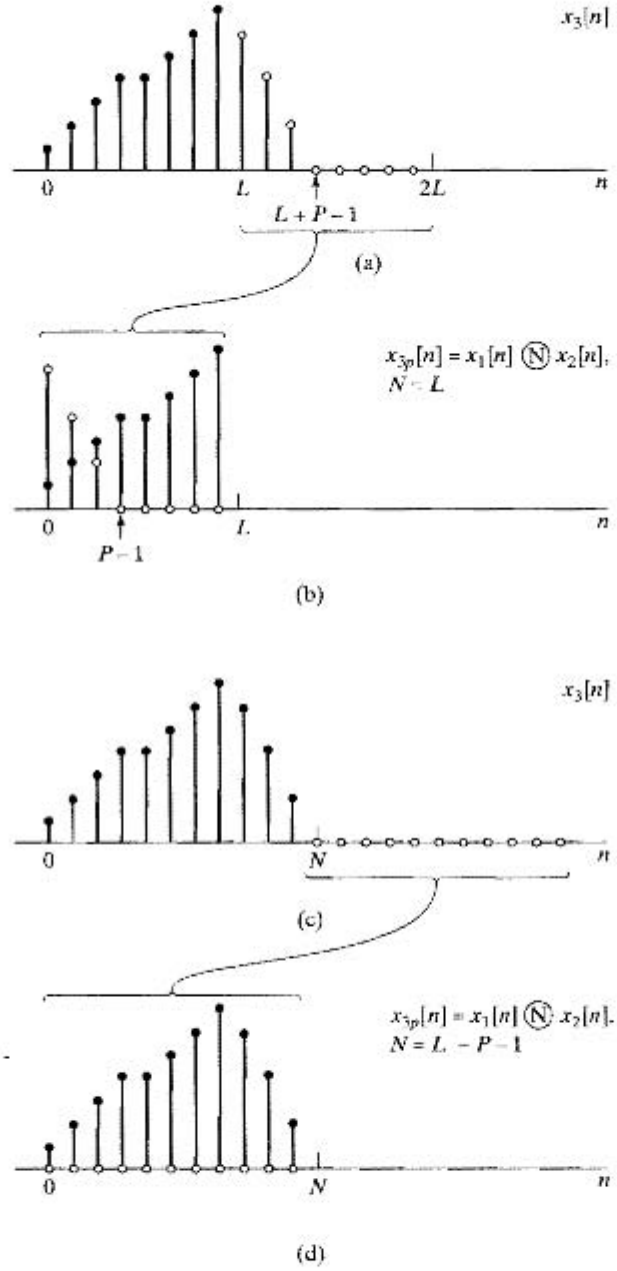

Figure 8.21 Illustration of how the result of a circular convolution "wraps around." (a) and (b) $N = L$, so the aliased "tail" overlaps the first $(P - 1)$ points. (c) and (d) $N = (L + P - 1)$, so no overlap occurs.

Another consideration is that for this method of filtering, no filtered samples can be computed until all the input samples have been collected. Generally, we would like to avoid such a large delay in processing. The solution to both of these problems is to use *block convolution*, in which the signal to be filtered is segmented into sections of length L. Each section can then be convolved with the finite-length impulse response and the

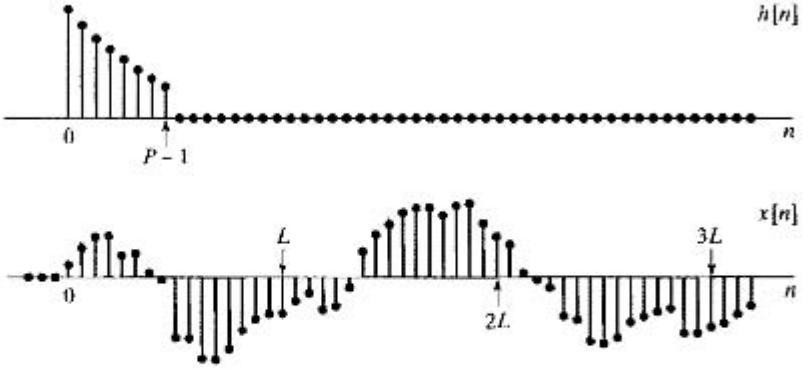

Figure 8.22 Finite-length impulse response $h[n]$ and indefinite-length signal $x[n]$ to be filtered.

filtered sections fitted together in an appropriate way. The linear filtering of each block can then be implemented using the DFT.

To illustrate the procedure and to develop the procedure for fitting the filtered sections together, consider the impulse response $h[n]$ of length P and the signal $x[n]$ depicted in Figure 8.22. Henceforth, we will assume that $x[n] = 0$ for $n < 0$ and that the length of $x[n]$ is much greater than P. The sequence $x[n]$ can be represented as a sum of shifted nonoverlapping finite-length segments of length L; i.e.,

$$x[n] = \sum_{r=0}^{\infty} x_r[n - rL], \tag{8.140}$$

where

$$x_r[n] = \begin{cases} x[n + rL], & 0 \le n \le L - 1, \\ 0, & \text{otherwise.} \end{cases} \tag{8.141}$$

Figure 8.23(a) illustrates this segmentation for $x[n]$ in Figure 8.22. Note that within each segment $x_r[n]$, the first sample is at $n = 0$; however, the zero$^{\text{th}}$ sample of $x_r[n]$ is the rL^{th} sample of the sequence $x[n]$. This is shown in Figure 8.23(a) by plotting the segments in their shifted positions but with the redefined time origin indicated.

Because convolution is an LTI operation, it follows from Eq. (8.140) that

$$y[n] = x[n] * h[n] = \sum_{r=0}^{\infty} y_r[n - rL], \tag{8.142}$$

where

$$y_r[n] = x_r[n] * h[n]. \tag{8.143}$$

Since the sequences $x_r[n]$ have only L nonzero points and $h[n]$ is of length P, each of the terms $y_r[n] = x_r[n] * h[n]$ has length $(L + P - 1)$. Thus, the linear convolution $x_r[n] * h[n]$ can be obtained by the procedure described earlier using N-point DFTs, wherein $N \ge L + P - 1$. Since the beginning of each input section is separated from its neighbors by L points and each filtered section has length $(L + P - 1)$, the nonzero points in the filtered sections will overlap by $(P - 1)$ points, and these overlap samples

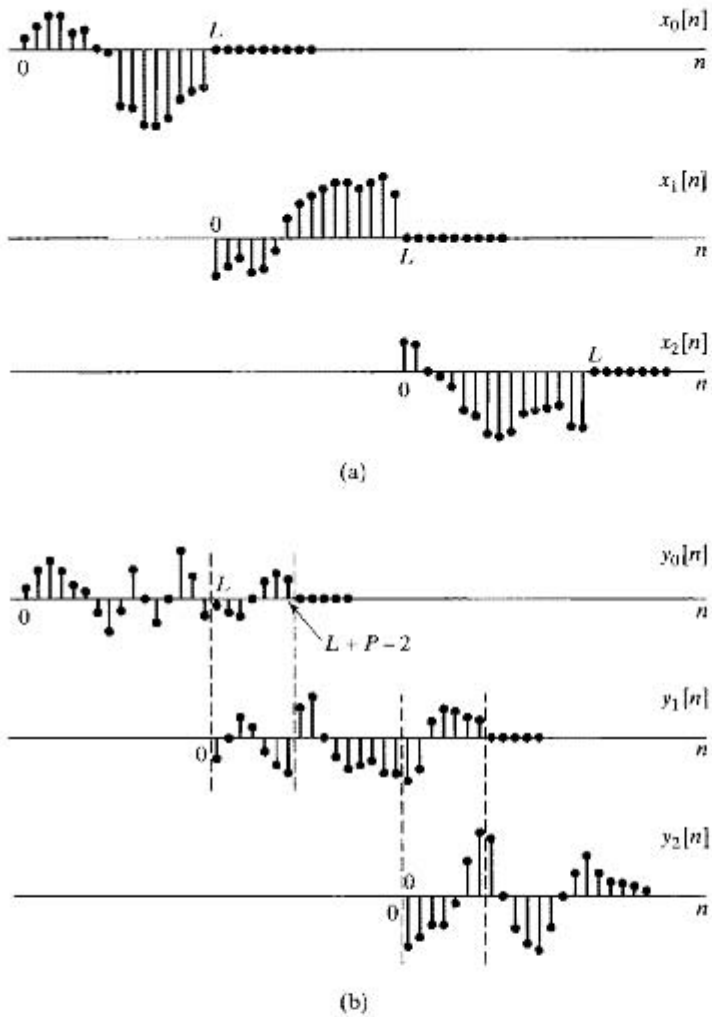

Figure 8.23 (a) Decomposition of $x[n]$ in Figure 8.22 into nonoverlapping sections of length L. (b) Result of convolving each section with $h[n]$.

must be added in carrying out the sum required by Eq. (8.142). This is illustrated in Figure 8.23(b), which illustrates the filtered sections, $y_r[n] = x_r[n] * h[n]$. Just as the input waveform is reconstructed by adding the delayed waveforms in Figure 8.23(a), the filtered result $x[n] * h[n]$ is constructed by adding the delayed filtered sections depicted in Figure 8.23(b). This procedure for constructing the filtered output from filtered sections is often referred to as the *overlap–add method*, because the filtered sections are overlapped and added to construct the output. The overlapping occurs because the linear convolution of each section with the impulse response is, in general, longer than the length of the section. The *overlap–add method* of block convolution is not tied to the DFT and circular convolution. Clearly, all that is required is that the smaller convolutions be computed and the results combined appropriately.

An alternative block convolution procedure, commonly called the *overlap–save method*, corresponds to implementing an L-point circular convolution of a P-point impulse response $h[n]$ with an L-point segment $x_r[n]$ and identifying the part of the circular convolution that corresponds to a linear convolution. The resulting output segments are then "patched together" to form the output. Specifically, we showed that if an L-point sequence is circularly convolved with a P-point sequence ($P < L$), then the first $(P-1)$ points of the result are incorrect due to time aliasing, whereas the remaining points are identical to those that would be obtained had we implemented a linear convolution. Therefore, we can divide $x[n]$ into sections of length L so that each input section overlaps the preceding section by $(P-1)$ points. That is, we define the sections as

$$x_r[n] = x[n + r(L - P + 1) - P + 1], \qquad 0 \le n \le L - 1, \tag{8.144}$$

wherein, as before, we have defined the time origin for each section to be at the beginning of that section rather than at the origin of $x[n]$. This method of sectioning is depicted in Figure 8.24(a). The circular convolution of each section with $h[n]$ is denoted $y_{rp}[n]$, the extra subscript p indicating that $y_{rp}[n]$ is the result of a circular convolution in which time aliasing has occurred. These sequences are depicted in Figure 8.24(b). The portion of each output section in the region $0 \le n \le P-2$ is the part that must be discarded. The remaining samples from successive sections are then abutted to construct the final filtered output. That is,

$$y[n] = \sum_{r=0}^{\infty} y_r[n - r(L - P + 1) + P - 1], \tag{8.145}$$

where

$$y_r[n] = \begin{cases} y_{rp}[n], & P-1 \le n \le L-1, \\ 0, & \text{otherwise.} \end{cases} \tag{8.146}$$

This procedure is called the overlap–save method because the input segments overlap, so that each succeeding input section consists of $(L - P + 1)$ new points and $(P-1)$ points saved from the previous section.

The utility of the overlap–add and the overlap–save methods of block convolution may not be immediately apparent. In Chapter 9, we consider highly efficient algorithms for computing the DFT. These algorithms, collectively called the FFT, are so efficient that, for FIR impulse responses of even modest length (on the order of 25 or 30), it may be more efficient to carry out block convolution using the DFT than to implement the linear convolution directly. The length P at which the DFT method becomes more efficient is, of course, dependent on the hardware and software available to implement the computations. (See Stockham, 1966, and Helms, 1967.)

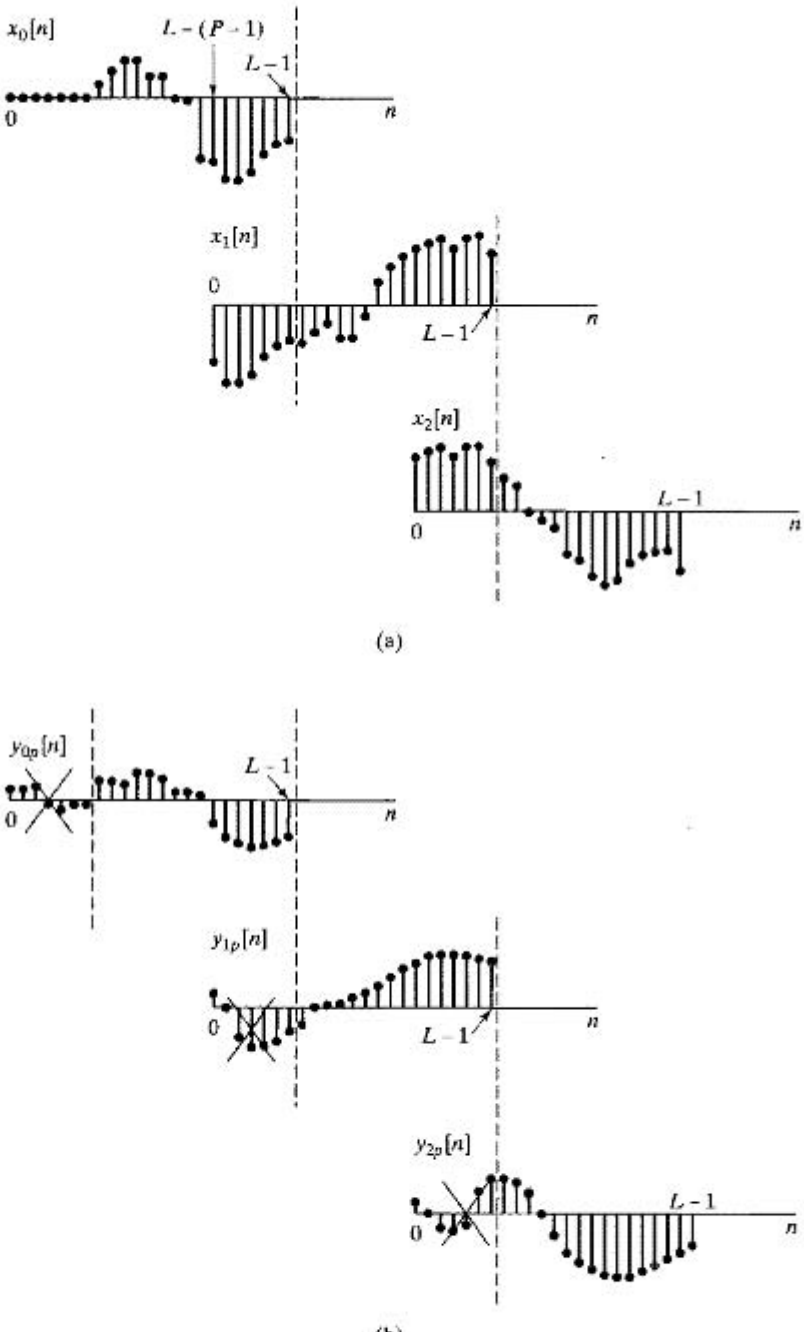

Figure 8.24 (a) Decomposition of $x[n]$ in Figure 8.22 into overlapping sections of length L. (b) Result of convolving each section with $h[n]$. The portions of each filtered section to be discarded in forming the linear convolution are indicated.

8.8 THE DISCRETE COSINE TRANSFORM (DCT)

The DFT is perhaps the most common example of a general class of finite-length transform representations of the form

$$A[k] = \sum_{n=0}^{N-1} x[n]\phi_k^*[n], \tag{8.147}$$

$$x[n] = \frac{1}{N}\sum_{k=0}^{N-1} A[k]\phi_k[n], \tag{8.148}$$

where the sequences $\phi_k[n]$, referred to as the *basis sequences*, are orthogonal to one another; i.e.,

$$\frac{1}{N}\sum_{n=0}^{N-1} \phi_k[n]\phi_m^*[n] = \begin{cases} 1, & m = k, \\ 0, & m \neq k. \end{cases} \tag{8.149}$$

In the case of the DFT, the basis sequences are the complex periodic sequences $e^{j2\pi kn/N}$, and the sequence $A[k]$ is, in general, complex even if the sequence $x[n]$ is real. It is natural to inquire as to whether there exist sets of real-valued basis sequences that would yield a real-valued transform sequence $A[k]$ when $x[n]$ is real. This has led to the definition of a number of other orthogonal transform representations, such as Haar transforms, Hadamard transforms (see Elliott and Rao, 1982), and Hartley transforms (Bracewell, 1983, 1984, 1989). (The definition and properties of the Hartley transform are explored in Problem 8.68.) Another orthogonal transform for real sequences is the discrete cosine transform (DCT). (See Ahmed, Natarajan and Rao, 1974 and Rao and Yip, 1990.) The DCT is closely related to the DFT and has become especially useful and important in a number of signal-processing applications, particularly speech and image compression. In this section, we conclude our discussion of the DFT by introducing the DCT and showing its relationship to the DFT.

8.8.1 Definitions of the DCT

The DCT is a transform in the form of Eqs. (8.147) and (8.148) with basis sequences $\phi_k[n]$ that are cosines. Since cosines are both periodic and have even symmetry, the extension of $x[n]$ outside the range $0 \leq n \leq (N-1)$ in the synthesis Eq. (8.148) will be both periodic and symmetric. In other words, just as the DFT involves an implicit assumption of periodicity, the DCT involves implicit assumptions of both periodicity and *even symmetry*.

In the development of the DFT, we represented finite-length sequences by first forming periodic sequences from which the finite-length sequence can be uniquely recovered and then using an expansion in terms of periodic complex exponentials. In a similar style, the DCT corresponds to forming a periodic, symmetric sequence from a finite-length sequence in such a way that the original finite-length sequence can be uniquely recovered. Because there are many ways to do this, there are many definitions of the DCT. In Figure 8.25, we show 17 samples for each of four examples of symmetric periodic extensions of a four-point sequence. The original finite-length sequence is shown in each subfigure as the samples with solid dots. These sequences are all periodic

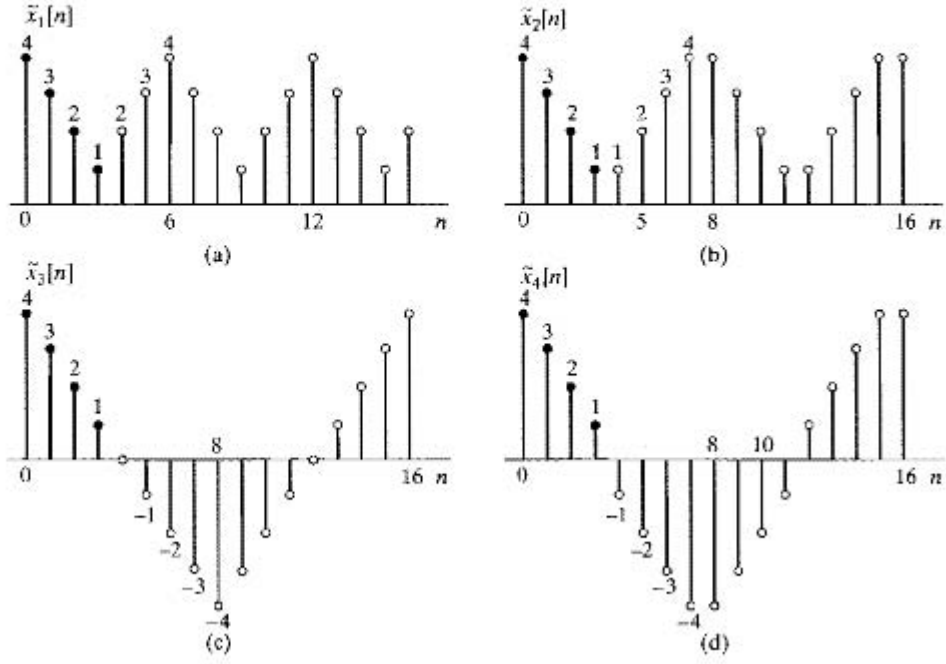

Figure 8.25 Four ways to extend a four-point sequence $x[n]$ both periodically and symmetrically. The finite-length sequence $x[n]$ is plotted with solid dots. (a) Type-1 periodic extension for DCT-1. (b) Type-2 periodic extension for DCT-2. (c) Type-3 periodic extension for DCT-3. (d) Type-4 periodic extension for DCT-4.

(with period 16 or less) and also have even symmetry. In each case, the finite-length sequence is easily extracted as the first four points of one period. For convenience, we denote the periodic sequences obtained by replicating with period 16 each of the four subsequences in Figure 8.25(a), (b), (c), and (d) as $\tilde{x}_1[n]$, $\tilde{x}_2[n]$, $\tilde{x}_3[n]$, and $\tilde{x}_4[n]$, respectively. We note that $\tilde{x}_1[n]$ has period $(2N-2)=6$ and has even symmetry about both $n=0$ and $n=(N-1)=3$. The sequence $\tilde{x}_2[n]$ has period $2N=8$ and has even symmetry about the "half sample" points $n=-\frac{1}{2}$ and $\frac{7}{2}$. The sequence $\tilde{x}_3[n]$ has period $4N=16$ and has even symmetry about $n=0$ and $n=8$. The sequence $\tilde{x}_4[n]$ also has period $4N=16$ and even symmetry about the "half sample" points $n=-\frac{1}{2}$ and $n=(2N-\frac{1}{2})=\frac{15}{2}$.

The four different cases shown in Figure 8.25 illustrate the periodicity that is implicit in the four common forms of the DCT, which are referred to as DCT-1, DCT-2, DCT-3, and DCT-4 respectively. It can be shown (see Martucci, 1994) that there are four more ways to create an even periodic sequence from $x[n]$. This implies four other possible DCT representations. Furthermore, it is also possible to create eight odd-symmetric periodic real sequences from $x[n]$, leading to eight different versions of the *discrete sine transform* (DST), wherein the basis sequences in the orthonormal representation are sine functions. These transforms make up a family of 16 orthonormal transforms for real sequences. Of these, the DCT-1 and DCT-2 representations are the most used, and we shall focus on them in the remainder of our discussion.

8.8.2 Definition of the DCT-1 and DCT-2

All of the periodic extensions leading to different forms of the DCT can be thought of as a sum of shifted copies of the N-point sequences $\pm x[n]$ and $\pm x[-n]$. The differences between the extensions for the DCT-1 and DCT-2 depend on whether the endpoints overlap with shifted versions of themselves and, if so, which of the endpoints overlap. For the DCT-1, $x[n]$ is first modified at the endpoints and then extended to have period $2N-2$. The resulting periodic sequence is

$$\tilde{x}_1[n] = x_\alpha[((n))_{2N-2}] + x_\alpha[((-n))_{2N-2}], \tag{8.150}$$

where $x_\alpha[n]$ is the modified sequence $x_\alpha[n] = \alpha[n]x[n]$, with

$$\alpha[n] = \begin{cases} \frac{1}{2}, & n = 0 \text{ and } N-1, \\ 1, & 1 \le n \le N-2. \end{cases} \tag{8.151}$$

The weighting of the endpoints compensates for the doubling that occurs when the two terms in Eq. (8.150) overlap at $n = 0$, $n = (N-1)$, and at the corresponding points spaced from these by integer multiples of $(2N-2)$. With this weighting, it is easily verified that $x[n] = \tilde{x}_1[n]$ for $n = 0, 1, \ldots, N-1$. The resulting periodic sequence $\tilde{x}_1[n]$ has even periodic symmetry about the points $n = 0$ and $n = N-1, 2N-2$, etc., which we refer to as *Type-1* periodic symmetry. Figure 8.25 (a) is an example of Type-1 symmetry where $N = 4$ and the periodic sequence $\tilde{x}_1[n]$ has period $2N-2 = 6$. The DCT-1 is defined by the transform pair

$$X^{c1}[k] = 2\sum_{n=0}^{N-1} \alpha[n]x[n]\cos\left(\frac{\pi kn}{N-1}\right), \qquad 0 \le k \le N-1, \tag{8.152}$$

$$x[n] = \frac{1}{N-1}\sum_{k=0}^{N-1} \alpha[k]X^{c1}[k]\cos\left(\frac{\pi kn}{N-1}\right), \qquad 0 \le n \le N-1, \tag{8.153}$$

where $\alpha[n]$ is defined in Eq. (8.151).

For the DCT-2, $x[n]$ is extended to have period $2N$, and the periodic sequence is given by

$$\tilde{x}_2[n] = x[((n))_{2N}] + x[((-n-1))_{2N}], \tag{8.154}$$

Because the endpoints do not overlap, no modification of them is required to ensure that $x[n] = \tilde{x}_2[n]$ for $n = 0, 1, \ldots, N-1$. In this case, which we call *Type-2* periodic symmetry, the periodic sequence $\tilde{x}_2[n]$ has even periodic symmetry about the "half sample" points $-1/2$, $N-1/2$, $2N-1/2$, etc. This is illustrated by Figure 8.25(b) for $N = 4$ and period $2N = 8$. The DCT-2 is defined by the transform pair

$$X^{c2}[k] = 2\sum_{n=0}^{N-1} x[n]\cos\left(\frac{\pi k(2n+1)}{2N}\right), \qquad 0 \le k \le N-1, \tag{8.155}$$

$$x[n] = \frac{1}{N}\sum_{k=0}^{N-1} \beta[k]X^{c2}[k]\cos\left(\frac{\pi k(2n+1)}{2N}\right), \qquad 0 \le n \le N-1, \tag{8.156}$$

where the inverse DCT-2 involves the weighting function

$$\beta[k] = \begin{cases} \frac{1}{2}, & k = 0 \\ 1, & 1 \le k \le N-1. \end{cases} \tag{8.157}$$

In many treatments, the DCT definitions include normalization factors that make the transforms *unitary*.[4] For example, the DCT-2 form is often defined as

$$\tilde{X}^{c2}[k] = \sqrt{\frac{2}{N}}\tilde{\beta}[k]\sum_{n=0}^{N-1} x[n]\cos\left(\frac{\pi k(2n+1)}{2N}\right), \qquad 0 \le k \le N-1, \tag{8.158}$$

$$x[n] = \sqrt{\frac{2}{N}}\sum_{k=0}^{N-1} \tilde{\beta}[k]\tilde{X}^{c2}[k]\cos\left(\frac{\pi k(2n+1)}{2N}\right), \qquad 0 \le n \le N-1, \tag{8.159}$$

where

$$\tilde{\beta}[k] = \begin{cases} \frac{1}{\sqrt{2}}, & k = 0, \\ 1, & k = 1, 2, \ldots, N-1. \end{cases} \tag{8.160}$$

Comparing these equations with Eqs. (8.155) and (8.156), we see that the multiplicative factors 2, $1/N$, and $\beta[k]$ have been redistributed between the direct and inverse transforms. (A similar normalization can be applied to define a normalized version of the DCT-1.) While this normalization creates a unitary transform representation, the definitions in Eqs. (8.152) and (8.153) and Eqs. (8.155) and (8.156) are simpler to relate to the DFT as we have defined it in this chapter. Therefore, in the following discussions, we use our definitions rather than the normalized definitions that are found, for example, in Rao and Yip (1990) and many other texts.

Although we normally evaluate the DCT only for $0 \le k \le N-1$, nothing prevents our evaluating the DCT equations outside that interval, as illustrated in Figure 8.26, wherein the DCT values for $0 \le k \le N-1$ are shown as solid dots. These figures illustrate that the DCTs also are even periodic sequences. However, the symmetry of the transform sequence is not always the same as the symmetry of the implicit periodic input sequence. While $\tilde{x}_1[n]$ and the extension of $X^{c1}[k]$ both have Type-1 symmetry with the same period, we see from a comparison of Figures 8.25(c) and 8.26(b) that the extended $X^{c2}[k]$ has the same symmetry as $\tilde{x}_3[n]$ rather than $\tilde{x}_2[n]$. Furthermore, $X^{c2}[n]$ extends with period $4N$ while $\tilde{x}_2[n]$ has period $2N$.

Since the DCTs are orthogonal transform representations, they have properties similar in form to those of the DFT. These properties are elaborated on in some detail in Ahmed, Natarajan and Rao (1974) and Rao and Yip (1990).

8.8.3 Relationship between the DFT and the DCT-1

As might be expected, there is a close relationship between the DFT and the various classes of the DCT of a finite-length sequence. To develop this relationship, we note that,

[4] The DCT would be a unitary transform if it is orthonormal and also has the property that $\sum_{n=0}^{N-1}(x[n])^2 = \sum_{k=0}^{N-1}(X^{c2}[k])^2$.

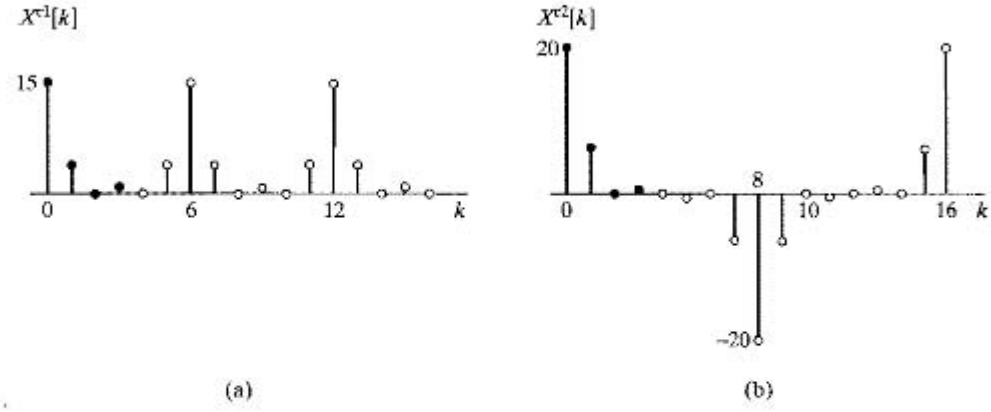

Figure 8.26 DCT-1 and DCT-2 for the four-point sequence used in Figure 8.25. (a) DCT-1. (b) DCT-2.

since, for the DCT-1, $\tilde{x}_1[n]$ is constructed from $x_1[n]$ through Eqs. (8.150) and (8.151), one period of the periodic sequence $\tilde{x}_1[n]$ defines the finite-length sequence

$$x_1[n] = x_\alpha[((n))_{2N-2}] + x_\alpha[((-n))_{2N-2}] = \tilde{x}_1[n], \qquad n = 0, 1, \ldots, 2N-3, \quad (8.161)$$

where $x_\alpha[n] = \alpha[n]x[n]$ is the N-point real sequence with endpoints divided by 2. From Eq. (8.161), it follows that the $(2N-2)$-point DFT of the $(2N-2)$-point sequence $x_1[n]$ is

$$X_1[k] = X_\alpha[k] + X_\alpha^*[k] = 2\mathcal{R}e\{X_\alpha[k]\}, \qquad k = 0, 1, \ldots, 2N-3. \quad (8.162)$$

where $X_\alpha[k]$ is the $(2N-2)$-point DFT of the N-point sequence $\alpha[n]x[n]$; i.e., $\alpha[n]x[n]$ is padded with $(N-2)$ zero samples. Using the definition of the $(2N-2)$-point DFT of the padded sequence, we obtain for $k = 0, 1 \ldots, N-1$,

$$X_1[k] = 2\mathcal{R}e\{X_\alpha[k]\} = 2\sum_{n=0}^{N-1} \alpha[n]x[n]\cos\left(\frac{2\pi kn}{2N-2}\right) = X^{c1}[k]. \quad (8.163)$$

Therefore, the DCT-1 of an N-point sequence is identical to the first N points of $X_1[k]$, the $(2N-2)$-point DFT of the symmetrically extended sequence $x_1[n]$, and it is also identical to twice the real part of the first N points of $X_\alpha[k]$, the $(2N-2)$-point DFT of the weighted sequence $x_\alpha[n]$.

Since, as discussed in Chapter 9, fast computational algorithms exist for the DFT, they can be used to compute the DFTs $X_\alpha[k]$ or $X_1[k]$ in Eq. (8.163), thus providing a convenient and readily available fast computation of the DCT-1. Since the definition of the DCT-1 involves only real-valued coefficients, there are also efficient algorithms for computing the DCT-1 of real sequences more directly without requiring the use of complex multiplications and additions. (See Ahmed, Natarajan and Rao, 1974 and Chen and Fralick, 1977.)

The inverse DCT-1 can also be computed using the inverse DFT. It is only necessary to use Eq. (8.163) to construct $X_1[k]$ from $X^{c1}[k]$ and then compute the inverse $(2N-2)$-point DFT. Specifically,

$$X_1[k] = \begin{cases} X^{c1}[k], & k = 0, \ldots, N-1, \\ X^{c1}[2N-2-k], & k = N, \ldots, 2N-3, \end{cases} \quad (8.164)$$

and, using the definition of the $(2N-2)$-point inverse DFT, we can compute the symmetrically extended sequence

$$x_1[n] = \frac{1}{2N-2}\sum_{k=0}^{2N-3} X_1[k]e^{j2\pi kn/(2N-2)}, \qquad n = 0, 1, \ldots, 2N-3, \tag{8.165}$$

from which we can obtain $x[n]$ by extracting the first N points, i.e., $x[n] = x_1[n]$ for $n = 0, 1, \ldots, N-1$. By substitution of Eq. (8.164) into Eq. (8.165), it also follows that the inverse DCT-1 relation can be expressed in terms of $X^{c1}[k]$ and cosine functions, as in Eq. (8.153). This is suggested as an exercise in Problem 8.71.

8.8.4 Relationship between the DFT and the DCT-2

It is also possible to express the DCT-2 of a finite-length sequence $x[n]$ in terms of the DFT. To develop this relationship, observe that one period of the periodic sequence $\tilde{x}_2[n]$ defines the $2N$-point sequence

$$x_2[n] = x[((n))_{2N}] + x[((-n-1))_{2N}] = \tilde{x}_2[n], \qquad n = 0, 1, \ldots, 2N-1, \tag{8.166}$$

where $x[n]$ is the original N-point real sequence. From Eq. (8.166), it follows that the $2N$-point DFT of the $2N$-point sequence $x_2[n]$ is

$$X_2[k] = X[k] + X^*[k]e^{j2\pi k/(2N)}, \qquad k = 0, 1, \ldots, 2N-1, \tag{8.167}$$

where $X[k]$ is the $2N$-point DFT of the N-point sequence $x[n]$; i.e., in this case, $x[n]$ is padded with N zero samples. From Eq. (8.167), we obtain

$$\begin{aligned} X_2[k] &= X[k] + X^*[k]e^{j2\pi k/(2N)} \\ &= e^{j\pi k/(2N)}\left(X[k]e^{-j\pi k/(2N)} + X^*[k]e^{j\pi k/(2N)}\right) \\ &= e^{j\pi k/(2N)}2\mathcal{R}e\left\{X[k]e^{-j\pi k/(2N)}\right\}. \end{aligned} \tag{8.168}$$

From the definition of the $2N$-point DFT of the padded sequence, it follows that

$$\mathcal{R}e\left\{X[k]e^{-j\pi k/(2N)}\right\} = \sum_{n=0}^{N-1} x[n]\cos\left(\frac{\pi k(2n+1)}{2N}\right). \tag{8.169}$$

Therefore, using Eqs. (8.155), (8.167), and (8.169), we can express $X^{c2}[k]$ in terms of $X[k]$, the $2N$-point DFT of the N-point sequence $x[n]$, as

$$X^{c2}[k] = 2\mathcal{R}e\left\{X[k]e^{-j\pi k/(2N)}\right\}, \qquad k = 0, 1, \ldots, N-1, \tag{8.170}$$

or in terms of the $2N$-point DFT of the $2N$-point symmetrically extended sequence $x_2[n]$ defined by Eq. (8.166) as

$$X^{c2}[k] = e^{-j\pi k/(2N)}X_2[k], \qquad k = 0, 1, \ldots, N-1, \tag{8.171}$$

and equivalently,

$$X_2[k] = e^{j\pi k/(2N)}X^{c2}[k], \qquad k = 0, 1, \ldots, N-1. \tag{8.172}$$

As in the case of the DCT-1, fast algorithms can be used to compute the $2N$-point DFTs $X[k]$ and $X_2[k]$ in Eqs. (8.170) and (8.171), respectively. Makhoul (1980) discusses other ways that the DFT can be used to compute the DCT-2. (See also Problem 8.72.) In addition, special fast algorithms for the computation of the DCT-2 have been developed (Rao and Yip, 1990).

The inverse DCT-2 can also be computed using the inverse DFT. The procedure utilizes Eq. (8.172) together with a symmetry property of the DCT-2. Specifically, it is easily verified by direct substitution into Eq. (8.155) that

$$X^{c2}[2N-k] = -X^{c2}[k], \qquad k = 0, 1, \ldots, 2N-1, \tag{8.173}$$

from which it follows that

$$X_2[k] = \begin{cases} X^{c2}[0], & k = 0, \\ e^{j\pi k/(2N)} X^{c2}[k], & k = 1, \ldots, N-1, \\ 0, & k = N, \\ -e^{j\pi k/(2N)} X^{c2}[2N-k], & k = N+1, N+2, \ldots, 2N-1. \end{cases} \tag{8.174}$$

Using the inverse DFT, we can compute the symmetrically extended sequence

$$x_2[n] = \frac{1}{2N} \sum_{k=0}^{2N-1} X_2[k] e^{j2\pi kn/(2N)}, \qquad n = 0, 1, \ldots, 2N-1, \tag{8.175}$$

from which we can obtain $x[n] = x_2[n]$ for $n = 0, 1, \ldots, N-1$. By substituting Eq. (8.174) into Eq. (8.175), we can easily show that the inverse DCT-2 relation is that given by Eq. (8.156). (See Problem 8.73.)

8.8.5 Energy Compaction Property of the DCT-2

The DCT-2 is used in many data compression applications in preference to the DFT because of a property that is frequently referred to as "energy compaction." Specifically, the DCT-2 of a finite-length sequence often has its coefficients more highly concentrated at low indices than the DFT does. The importance of this flows from Parseval's theorem, which, for the DCT-1, is

$$\sum_{n=0}^{N-1} \alpha[n] |x[n]|^2 = \frac{1}{2N-2} \sum_{k=0}^{N-1} \alpha[k] |X^{c1}[k]|^2, \tag{8.176}$$

and, for the DCT-2, is

$$\sum_{n=0}^{N-1} |x[n]|^2 = \frac{1}{N} \sum_{k=0}^{N-1} \beta[k] |X^{c2}[k]|^2, \tag{8.177}$$

where $\beta[k]$ is defined in Eq. (8.157). The DCT can be said to be concentrated in the low indices of the DCT if the remaining DCT coefficients can be set to zero without a significant impact on the energy of the signal. We illustrate the energy compaction property in the following example.

Example 8.13 Energy Compaction in the DCT-2

Consider a test input of the form

$$x[n] = a^n \cos(\omega_0 n + \phi), \qquad n = 0, 1, \ldots, N-1. \tag{8.178}$$

Such a signal is illustrated in Figure 8.27 for $a = .9$, $\omega_0 = 0.1\pi$, $\phi = 0$, and $N = 32$.

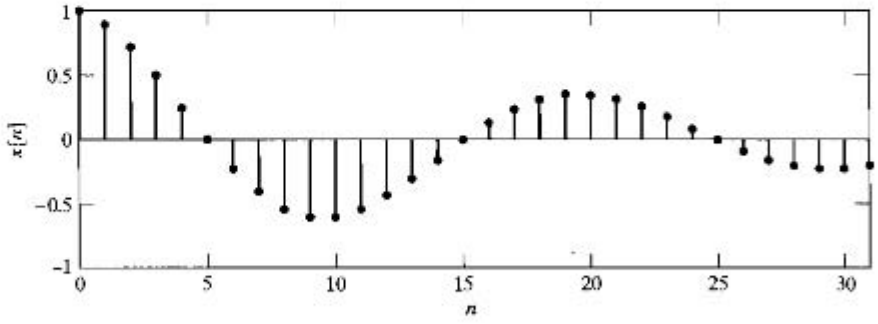

Figure 8.27 Test signal for comparing DFT and DCT.

The real and imaginary parts of the 32-point DFT of the 32-point sequence in Figure 8.27 are shown in Figures 8.28(a) and (b), respectively, and the DCT-2 of the sequence is shown in Figure 8.28(c). In the case of the DFT, the real and imaginary parts are shown for $k = 0, 1, \ldots, 16$. Since the signal is real, $X[0]$ and $X[16]$ are real. The remaining values are complex and conjugate symmetric. Thus, the 32 real numbers shown in Figures 8.28(a) and (b) completely specify the 32-point DFT. In the case of the DCT-2, we show all 32 of the real DCT-2 values. Clearly, the DCT-2 values are highly concentrated at low indices, so Parseval's theorem suggests that the energy of the sequence is more concentrated in the DCT-2 representation than in the DFT representation.

This energy concentration property can be quantified by truncating the two representations and comparing the mean-squared approximation error for the two representations when both use the same number of real coefficient values. To do this, we define

$$x_m^{\text{dft}}[n] = \frac{1}{N} \sum_{k=0}^{N-1} T_m[k] X[k] e^{j2\pi kn/N}, \qquad n = 0, 1, \ldots, N-1, \tag{8.179}$$

where, in this case, $X[k]$ is the N-point DFT of $x[n]$ and

$$T_m[k] = \begin{cases} 1, & 0 \le k \le (N-1-m)/2, \\ 0, & (N+1-m)/2 \le k \le (N-1+m)/2, \\ 1, & (N+1+m)/2 \le k \le N-1. \end{cases}$$

If $m = 1$, the term $X[N/2]$ is removed. If $m = 3$, then the terms $X[N/2]$ and $X[N/2-1]$ and its corresponding complex conjugate $X[N/2+1]$ are removed, and so forth; i.e., $x_m^{\text{dft}}[n]$ for $m = 1, 3, 5, \ldots, N-1$ is the sequence that is synthesized by symmetrically omitting m DFT coefficients.[5] With the exception of the DFT value, $X[N/2]$, which is

[5] For simplicity, we assume that N is an even integer.

real, each omitted complex DFT value and its corresponding complex conjugate actually corresponds to omitting two real numbers. For example, $m = 5$ would correspond to setting the coefficients $X[14]$, $X[15]$, $X[16]$, $X[17]$, and $X[18]$ to zero in synthesizing $x_5^{\text{dft}}[n]$ from the 32-point DFT shown in Figures 8.28(a) and (b).

Likewise, we can truncate the DCT-2 representation, obtaining

$$x_m^{\text{dct}}[n] = \frac{1}{N} \sum_{k=0}^{N-1-m} \beta[k] X^{c2}[k] \cos\left(\frac{\pi k(2n+1)}{2N}\right), \qquad 0 \le n \le N-1. \tag{8.180}$$

In this case, if $m = 5$, we omit the DCT-2 coefficients $X^{c2}[27], \ldots, X^{c2}[31]$ in the synthesis of $x_m^{\text{dct}}[n]$ from the DCT-2 shown in Figure 8.28(c). Since these coefficients are very small, $x_5^{\text{dct}}[n]$ should differ only slightly from $x[n]$.

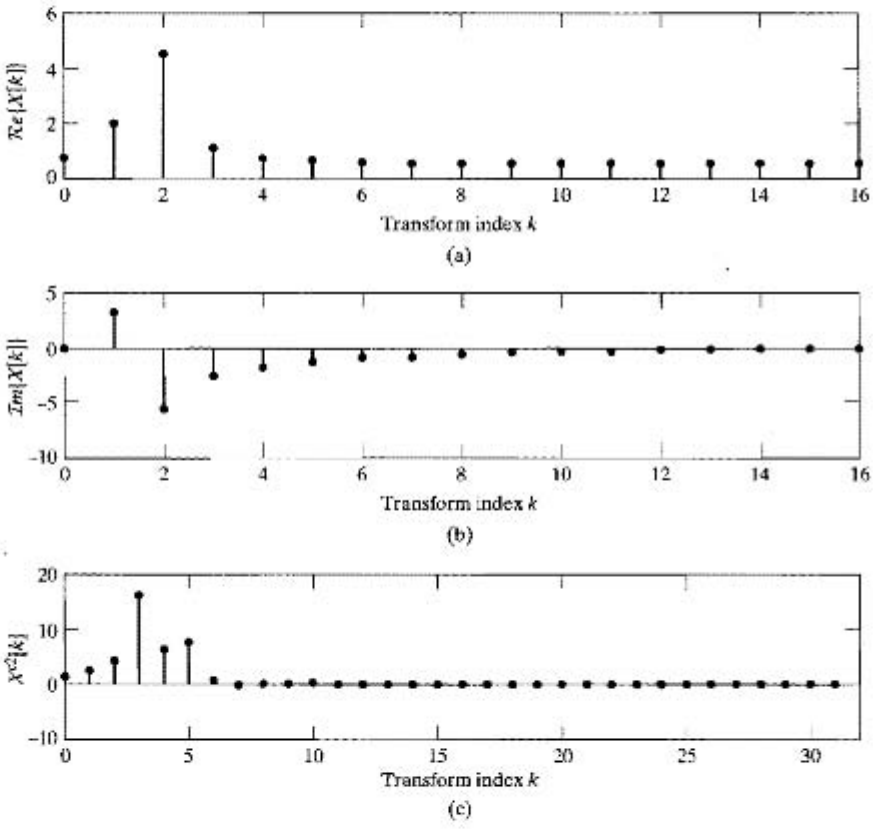

Figure 8.28 (a) Real part of 32-point DFT; (b) Imaginary part of 32-point DFT; (c) 32-point DCT-2 of the test signal plotted in Figure 8.27.

To show how the approximation errors depend on m for the DFT and the DCT-2, we define

$$E^{\text{dft}}[m] = \frac{1}{N}\sum_{n=0}^{N-1} |x[n] - x_m^{\text{dft}}[n]|^2$$

and

$$E^{\text{dct}}[m] = \frac{1}{N}\sum_{n=0}^{N-1} |x[n] - x_m^{\text{dct}}[n]|^2$$

to be the mean-squared approximation errors for the truncated DFT and DCT, respectively. These errors are plotted in Figure 8.29, with $E^{\text{dft}}[m]$ indicated with ∘ and $E^{\text{dct}}[m]$ shown with •. For the special cases $m = 0$ (no truncation) and $m = N-1$ (only the DC value is retained), the DFT truncation function is $T_0[k] = 1$ for $0 \le k \le N-1$ and $T_{N-1}[k] = 0$ for $1 \le k \le N-1$ and $T_{N-1}[0] = 1$. In these cases, both representations give the same error. For values $1 \le m \le 30$, the DFT error grows steadily as m increases, whereas the DCT error remains very small—up to about $m = 25$—implying that the 32 numbers of the sequence $x[n]$ can be represented with slight error by only seven DCT-2 coefficients.

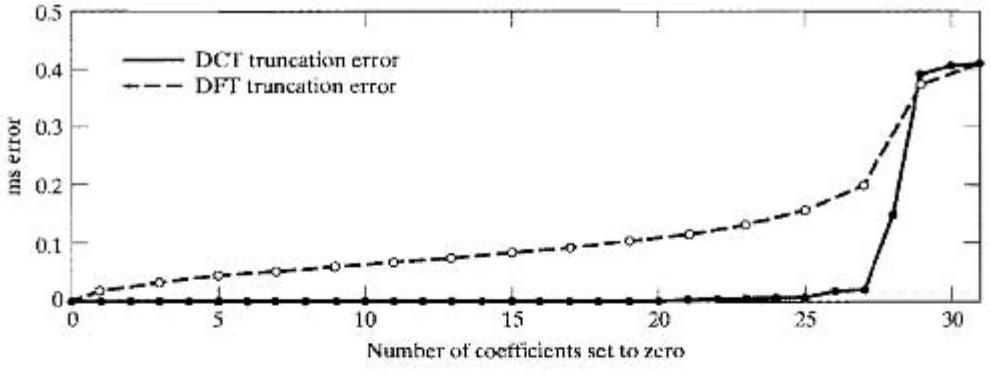

Figure 8.29 Comparison of truncation errors for DFT and DCT-2.

The signal in Example 8.13 is a low frequency exponentially decaying signal with zero phase. We have chosen this example very carefully to emphasize the energy compaction property. Not every choice of $x[n]$ will give such dramatic results. Highpass signals and even some signals of the form of Eq. (8.178) with different parameters do not show this dramatic difference. Nevertheless, in many cases of interest in data compression, the DCT-2 provides a distinct advantage over the DFT. It can be shown (Rao and Yip, 1990) that the DCT-2 is nearly optimum in the sense of minimum mean-squared truncation error for sequences with exponential correlation functions.

8.8.6 Applications of the DCT

The major application of the DCT-2 is in signal compression, where it is a key part of many standardized algorithms. (See Jayant and Noll, 1984, Pau, 1995, Rao and Hwang,

1996, Taubman and Marcellin, 2002, Bosi and Goldberg, 2003 and Spanias, Painter and Atti, 2007.) In this application, the blocks of the signal are represented by their cosine transforms. The popularity of the DCT in signal compression is mainly as a result of its energy concentration property, which we demonstrated by a simple example in the previous section.

The DCT representations, being orthogonal transforms like the DFT, have many properties similar to those of the DFT that make them very flexible for manipulating the signals that they represent. One of the most important properties of the DFT is that periodic convolution of two finite-length sequences corresponds to multiplication of their corresponding DFTs. We have seen in Section 8.7 that it is possible to exploit this property to compute linear convolutions by doing only DFT computations. In the case of the DCT, the corresponding result is that multiplication of DCTs corresponds to periodic convolution of the underlying symmetrically extended sequences. However, there are additional complications. For example, the periodic convolution of two Type-2 symmetric periodic sequences is not a Type-2 sequence, but rather, a Type-1 sequence. Alternatively, periodic convolution of a Type-1 sequence with a Type-2 sequence of the same implied period is a Type-2 sequence. Thus, a mixture of DCTs is required to effect periodic symmetric convolution by inverse transformation of the product of DCTs. There are many more ways to do this, because we have many different DCT definitions from which to choose. Each different combination would correspond to periodic convolution of a pair of symmetrically extended finite sequences. Martucci (1994) provides a complete discussion of the use of DCT and DST transforms in implementing symmetric periodic convolution.

Multiplication of DCTs corresponds to a special type of periodic convolution that has some features that may be useful in some applications. As we have seen for the DFT, periodic convolution is characterized by end effects, or "wrap around" effects. Indeed, even linear convolution of two finite-length sequences has end effects as the impulse response engages and disengages from the input. The end effects of periodic symmetric convolution are different from ordinary convolution and from periodic convolution as implemented by multiplying DFTs. The symmetric extension creates symmetry at the endpoints. The "smooth" boundaries that this implies often mitigate the end effects encountered in convolving finite-length sequences. One area in which symmetric convolution is particularly useful is image filtering, where objectionable edge effects are perceived as blocking artifacts. In such representations, the DCT may be superior to the DFT or even ordinary linear convolution. In doing periodic symmetric convolution by multiplication of DCTs, we can force the same result as ordinary convolution by extending the sequences with a sufficient number of zero samples placed at both the beginning and the end of each sequence.

8.9 SUMMARY

In this chapter, we have discussed discrete Fourier representations of finite-length sequences. Most of our discussion focused on the discrete Fourier transform (DFT), which is based on the DFS representation of periodic sequences. By defining a periodic sequence for which each period is identical to the finite-length sequence, the DFT becomes

identical to one period of the DFS coefficients. Because of the importance of this underlying periodicity, we first examined the properties of DFS representations and then interpreted those properties in terms of finite-length sequences. An important result is that the DFT values are equal to samples of the z-transform at equally spaced points on the unit circle. This leads to the notion of time aliasing in the interpretation of DFT properties, a concept we used extensively in the study of circular convolution and its relation to linear convolution. We then used the results of this study to show how the DFT could be employed to implement the linear convolution of a finite-length impulse response with an indefinitely long input signal.

The chapter concluded with an introduction to the DCT. It was shown that the DCT and DFT are closely related and that they share an implicit assumption of periodicity. The energy compaction property, which is the main reason for the popularity of the DCT in data compression, was demonstrated with an example.

Problems

Basic Problems with Answers

8.1. Suppose $x_c(t)$ is a periodic continuous-time signal with period 1 ms and for which the Fourier series is

$$x_c(t) = \sum_{k=-9}^{9} a_k e^{j(2000\pi kt)}.$$

The Fourier series coefficients a_k are zero for $|k| > 9$. $x_c(t)$ is sampled with a sample spacing $T = \frac{1}{6} \times 10^{-3}$ s to form $x[n]$. That is,

$$x[n] = x_c\left(\frac{n}{6000}\right).$$

(a) Is $x[n]$ periodic and, if so, with what period?
(b) Is the sampling rate above the Nyquist rate? That is, is T sufficiently small to avoid aliasing?
(c) Find the DFS coefficients of $x[n]$ in terms of a_k.

8.2. Suppose $\tilde{x}[n]$ is a periodic sequence with period N. Then $\tilde{x}[n]$ is also periodic with period $3N$. Let $\tilde{X}[k]$ denote the DFS coefficients of $\tilde{x}[n]$ considered as a periodic sequence with period N, and let $\tilde{X}_3[k]$ denote the DFS coefficients of $\tilde{x}[n]$ considered as a periodic sequence with period $3N$.

(a) Express $\tilde{X}_3[k]$ in terms of $\tilde{X}[k]$.
(b) By explicitly calculating $\tilde{X}[k]$ and $\tilde{X}_3[k]$, verify your result in part (a) when $\tilde{x}[n]$ is as given in Figure P8.2.

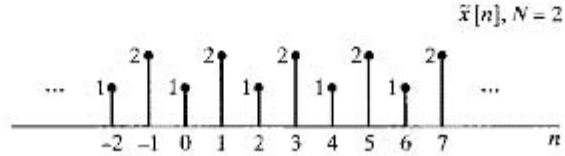

Figure P8.2

8.3. Figure P8.3 shows three periodic sequences $\tilde{x}_1[n]$ through $\tilde{x}_3[n]$. These sequences can be expressed in a Fourier series as

$$\tilde{x}[n] = \frac{1}{N}\sum_{k=0}^{N-1} \tilde{X}[k]e^{j(2\pi/N)kn}.$$

(a) For which sequences can the time origin be chosen such that all the $\tilde{X}[k]$ are real?
(b) For which sequences can the time origin be chosen such that all the $\tilde{X}[k]$ (except for k an integer multiple of N) are imaginary?
(c) For which sequences does $\tilde{X}[k] = 0$ for $k = \pm 2, \pm 4, \pm 6$?

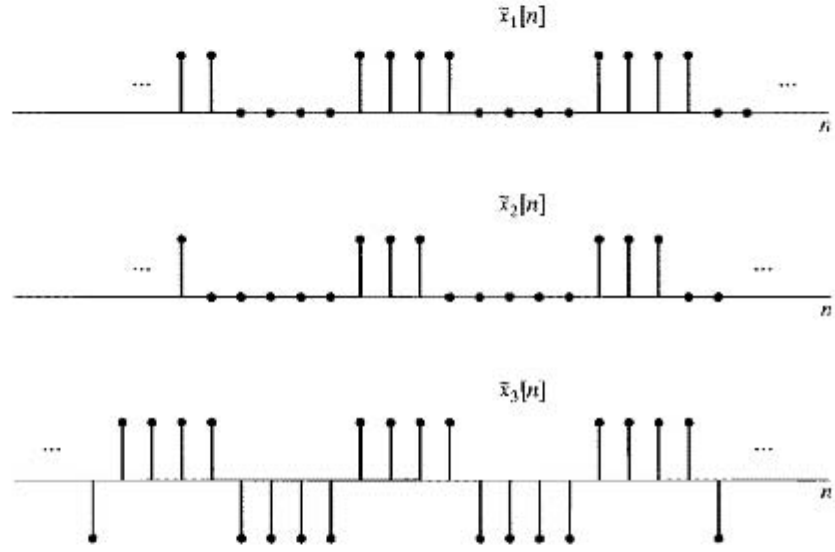

Figure P8.3

8.4. Consider the sequence $x[n]$ given by $x[n] = \alpha^n u[n]$. Assume $|\alpha| < 1$. A periodic sequence $\tilde{x}[n]$ is constructed from $x[n]$ in the following way:

$$\tilde{x}[n] = \sum_{r=-\infty}^{\infty} x[n + rN].$$

(a) Determine the Fourier transform $X(e^{j\omega})$ of $x[n]$.
(b) Determine the DFS coefficients $\tilde{X}[k]$ for the sequence $\tilde{x}[n]$.
(c) How is $\tilde{X}[k]$ related to $X(e^{j\omega})$?

8.5. Compute the DFT of each of the following finite-length sequences considered to be of length N (where N is even):

(a) $x[n] = \delta[n]$,
(b) $x[n] = \delta[n - n_0], \quad 0 \le n_0 \le N-1$,
(c) $x[n] = \begin{cases} 1, & n \text{ even}, \quad 0 \le n \le N-1, \\ 0, & n \text{ odd}, \quad 0 \le n \le N-1, \end{cases}$
(d) $x[n] = \begin{cases} 1, & 0 \le n \le N/2 - 1, \\ 0, & N/2 \le n \le N-1. \end{cases}$

(e) $x[n] = \begin{cases} a^n, & 0 \le n \le N-1, \\ 0, & \text{otherwise.} \end{cases}$

8.6. Consider the complex sequence

$$x[n] = \begin{cases} e^{j\omega_0 n}, & 0 \le n \le N-1, \\ 0, & \text{otherwise.} \end{cases}$$

(a) Find the Fourier transform $X(e^{j\omega})$ of $x[n]$.
(b) Find the N-point DFT $X[k]$ of the finite-length sequence $x[n]$.
(c) Find the DFT of $x[n]$ for the case $\omega_0 = 2\pi k_0/N$, where k_0 is an integer.

8.7. Consider the finite-length sequence $x[n]$ in Figure P8.7. Let $X(z)$ be the z-transform of $x[n]$. If we sample $X(z)$ at $z = e^{j(2\pi/4)k}$, $k = 0, 1, 2, 3$, we obtain

$$X_1[k] = X(z)\big|_{z=e^{j(2\pi/4)k}}, \qquad k = 0, 1, 2, 3.$$

Sketch the sequence $x_1[n]$ obtained as the inverse DFT of $X_1[k]$.

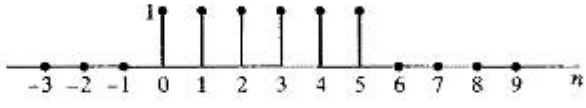

Figure P8.7

8.8. Let $X(e^{j\omega})$ denote the Fourier transform of the sequence $x[n] = (0.5)^n u[n]$. Let $y[n]$ denote a finite-duration sequence of length 10; i.e., $y[n] = 0$, $n < 0$, and $y[n] = 0$, $n \ge 10$. The 10-point DFT of $y[n]$, denoted by $Y[k]$, corresponds to 10 equally spaced samples of $X(e^{j\omega})$; i.e., $Y[k] = X(e^{j2\pi k/10})$. Determine $y[n]$.

8.9. Consider a 20-point finite-duration sequence $x[n]$ such that $x[n] = 0$ outside $0 \le n \le 19$, and let $X(e^{j\omega})$ represent the discrete-time Fourier transform of $x[n]$.

(a) If it is desired to evaluate $X(e^{j\omega})$ at $\omega = 4\pi/5$ by computing one M-point DFT, determine the smallest possible M, and develop a method to obtain $X(e^{j\omega})$ at $\omega = 4\pi/5$ using the smallest M.
(b) If it is desired to evaluate $X(e^{j\omega})$ at $\omega = 10\pi/27$ by computing one L-point DFT, determine the smallest possible L, and develop a method to obtain $X(e^{j10\pi/27})$ using the smallest L.

8.10. The two eight-point sequences $x_1[n]$ and $x_2[n]$ shown in Figure P8.10 have DFTs $X_1[k]$ and $X_2[k]$, respectively. Determine the relationship between $X_1[k]$ and $X_2[k]$.

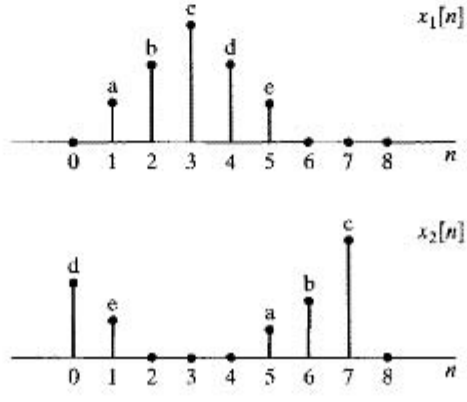

Figure P8.10

8.11. Figure P8.11 shows two finite-length sequences $x_1[n]$ and $x_2[n]$. Sketch their six-point circular convolution.

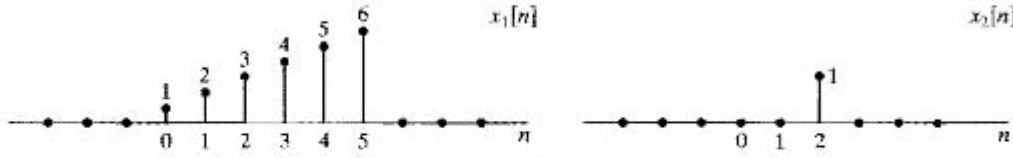

Figure P8.11

8.12. Suppose we have two four-point sequences $x[n]$ and $h[n]$ as follows:

$$x[n] = \cos\left(\frac{\pi n}{2}\right), \quad n = 0, 1, 2, 3,$$
$$h[n] = 2^n, \quad n = 0, 1, 2, 3.$$

(a) Calculate the four-point DFT $X[k]$.
(b) Calculate the four-point DFT $H[k]$.
(c) Calculate $y[n] = x[n] \textcircled{4} h[n]$ by doing the circular convolution directly.
(d) Calculate $y[n]$ of part (c) by multiplying the DFTs of $x[n]$ and $h[n]$ and performing an inverse DFT.

8.13. Consider the finite-length sequence $x[n]$ in Figure P8.13. The five-point DFT of $x[n]$ is denoted by $X[k]$. Plot the sequence $y[n]$ whose DFT is

$$Y[k] = W_5^{-2k} X[k].$$

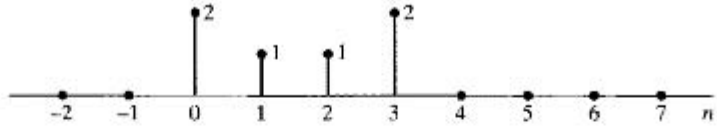

Figure P8.13

8.14. Two finite-length signals, $x_1[n]$ and $x_2[n]$, are sketched in Figure P8.14. Assume that $x_1[n]$ and $x_2[n]$ are zero outside of the region shown in the figure. Let $x_3[n]$ be the eight-point circular convolution of $x_1[n]$ with $x_2[n]$; i.e., $x_3[n] = x_1[n] \textcircled{8} x_2[n]$. Determine $x_3[2]$.

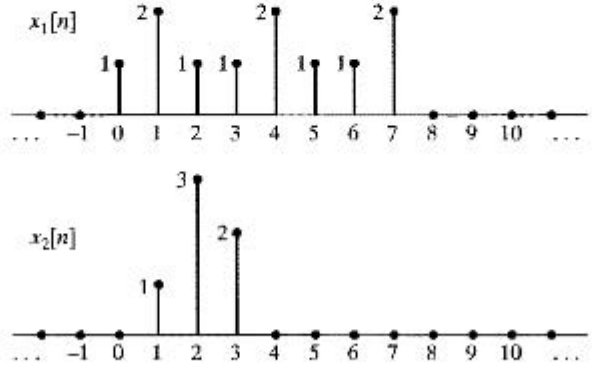

Figure P8.14

8.15. Figure P8.15-1 shows two sequences $x_1[n]$ and $x_2[n]$. The value of $x_2[n]$ at time $n = 3$ is not known, but is shown as a variable a. Figure P8.15-2 shows $y[n]$, the four-point circular convolution of $x_1[n]$ and $x_2[n]$. Based on the graph of $y[n]$, can you specify a uniquely? If so, what is a? If not, give two possible values of a that would yield the sequence $y[n]$ as shown.

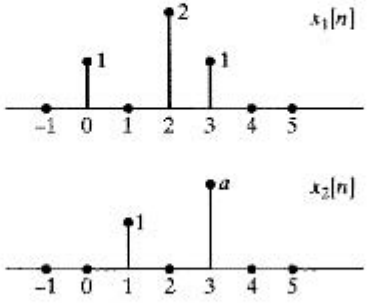

Figure P8.15-1

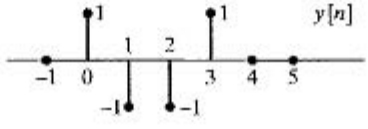

Figure P8.15-2

8.16. Figure P8.16-1 shows a six-point discrete-time sequence $x[n]$. Assume that $x[n] = 0$ outside the interval shown. The value of $x[4]$ is not known and is represented as b. Note that the sample shown for b in the figure is not necessarily to scale. Let $X(e^{j\omega})$ be the DTFT of $x[n]$ and $X_1[k]$ be samples of $X(e^{j\omega})$ every $\pi/2$; i.e.,

$$X_1[k] = X(e^{j\omega})|_{\omega=(\pi/2)k}, \qquad 0 \le k \le 3.$$

The four-point sequence $x_1[n]$ that results from taking the four-point inverse DFT of $X_1[k]$ is shown in Figure P8.16-2. Based on this figure, can you determine b uniquely? If so, give the value for b.

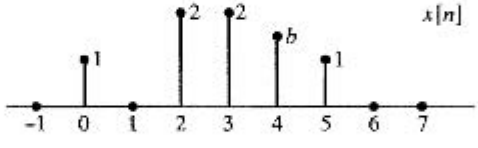

Figure P8.16-1

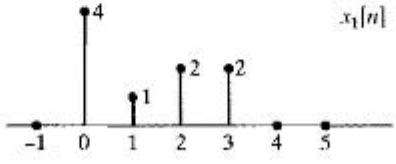

Figure P8.16-2

8.17. Figure P8.17 shows two finite-length sequences $x_1[n]$ and $x_2[n]$. What is the smallest N such that the N-point circular convolution of $x_1[n]$ and $x_2[n]$ are equal to the linear convolution of these sequences, i.e., such that $x_1[n] \textcircled{N} x_2[n] = x_1[n] * x_2[n]$?

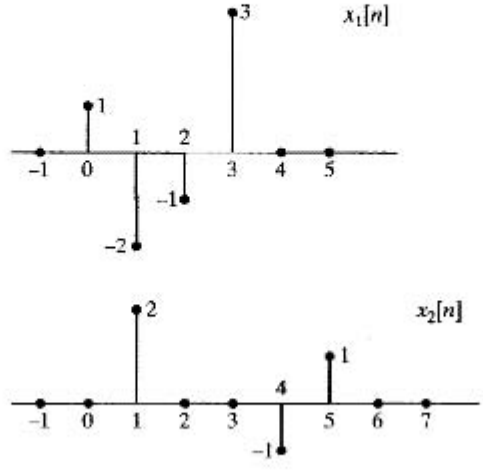

Figure P8.17

8.18. Figure P8.18-1 shows a sequence $x[n]$ for which the value of $x[3]$ is an unknown constant c. The sample with amplitude c is not necessarily drawn to scale. Let

$$X_1[k] = X[k]e^{j2\pi 3k/5},$$

where $X[k]$ is the five-point DFT of $x[n]$. The sequence $x_1[n]$ plotted in Figure P8.18-2 is the inverse DFT of $X_1[k]$. What is the value of c?

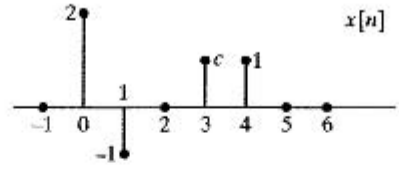

Figure P8.18-1

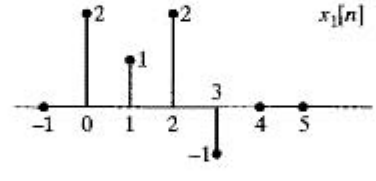

Figure P8.18-2

8.19. Two finite-length sequences $x[n]$ and $x_1[n]$ are shown in Figure P8.19. The DFTs of these sequences, $X[k]$ and $X_1[k]$, respectively, are related by the equation

$$X_1[k] = X[k]e^{-j(2\pi km/6)},$$

where m is an unknown constant. Can you determine a value of m consistent with Figure P8.19? Is your choice of m unique? If so, justify your answer. If not, find another choice of m consistent with the information given.

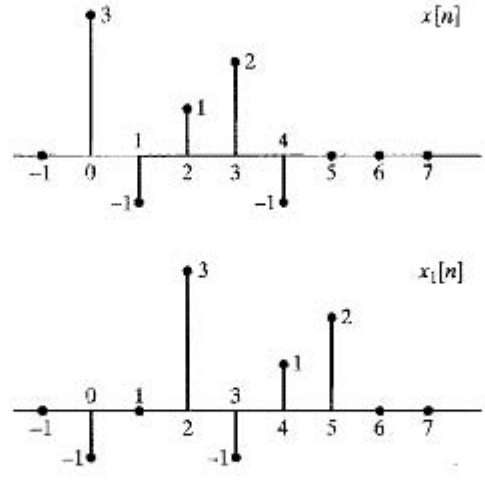

Figure P8.19

8.20. Two finite-length sequences $x[n]$ and $x_1[n]$ are shown in Figure P8.20. The N-point DFTs of these sequences, $X[k]$ and $X_1[k]$, respectively, are related by the equation

$$X_1[k] = X[k]e^{j2\pi k2/N},$$

where N is an unknown constant. Can you determine a value of N consistent with Figure P8.20? Is your choice for N unique? If so, justify your answer. If not, find another choice of N consistent with the information given.

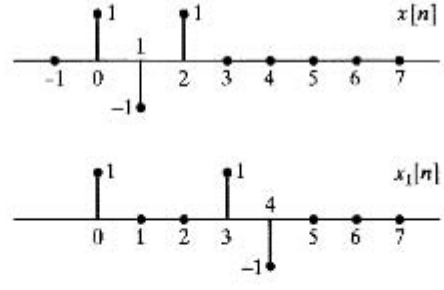

Figure P8.20

Basic Problems

8.21. **(a)** Figure P8.21-1 shows two periodic sequences, $\tilde{x}_1[n]$ and $\tilde{x}_2[n]$, with period $N = 7$. Find a sequence $\tilde{y}_1[n]$ whose DFS is equal to the product of the DFS of $\tilde{x}_1[n]$ and the DFS of $\tilde{x}_2[n]$, i.e.,

$$\tilde{Y}_1[k] = \tilde{X}_1[k]\tilde{X}_2[k].$$

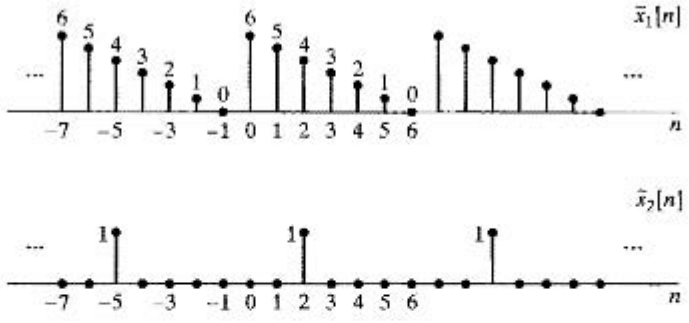

Figure P8.21-1

(b) Figure P8.21-2 shows a periodic sequence $\tilde{x}_3[n]$ with period $N = 7$. Find a sequence $\tilde{y}_2[n]$ whose DFS is equal to the product of the DFS of $\tilde{x}_1[n]$ and the DFS of $\tilde{x}_3[n]$, i.e.,

$$\tilde{Y}_2[k] = \tilde{X}_1[k]\tilde{X}_3[k].$$

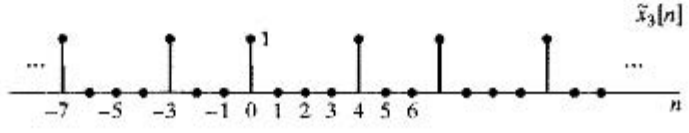

Figure P8.21-2

8.22. Consider an N-point sequence $x[n]$, i.e.,

$$x[n] = 0 \text{ for } n > N-1 \text{ and } n < 0.$$

The discrete-time Fourier transform of $x[n]$ is $X(e^{j\omega})$, and the N-point DFT of $x[n]$ is $X[k]$.

If $\mathcal{R}e\{X[k]\} = 0$ for $k = 0, 1, \ldots, N-1$, can we conclude that $\mathcal{R}e\left\{X(e^{j\omega})\right\} = 0$ for $-\pi \leq \omega \leq \pi$? If your answer is yes, explicitly show why. If not, give a simple counterexample.

8.23. Consider the real finite-length sequence $x[n]$ shown in Figure P8.23.

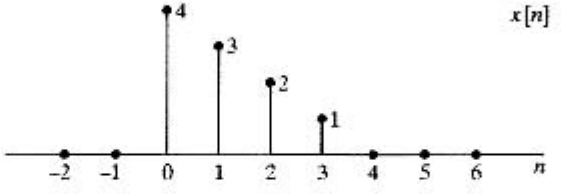

Figure P8.23

(a) Sketch the finite-length sequence $y[n]$ whose six-point DFT is

$$Y[k] = W_6^{5k} X[k],$$

where $X[k]$ is the six-point DFT of $x[n]$.

(b) Sketch the finite-length sequence $w[n]$ whose six-point DFT is

$$W[k] = \mathcal{I}m\{X[k]\}.$$

(c) Sketch the finite-length sequence $q[n]$ whose three-point DFT is

$$Q[k] = X[2k+1], \qquad k = 0, 1, 2.$$

8.24. Figure P8.24 shows a finite-length sequence $x[n]$. Sketch the sequences

$$x_1[n] = x[((n-2))_4], \qquad 0 \le n \le 3,$$

and

$$x_2[n] = x[((-n))_4], \qquad 0 \le n \le 3.$$

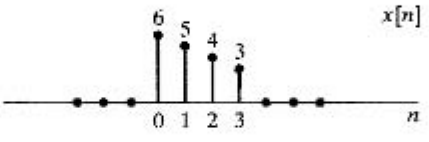

Figure P8.24

8.25. Consider the signal $x[n] = \delta[n-4] + 2\delta[n-5] + \delta[n-6]$.

(a) Find $X(e^{j\omega})$ the discrete-time Fourier transform of $x[n]$. Write expressions for the magnitude and phase of $X(e^{j\omega})$, and sketch these functions.

(b) Find all values of N for which the N-point DFT is a set of real numbers.

(c) Can you find a three-point causal signal $x_1[n]$ (i.e., $x_1[n] = 0$ for $n < 0$ and $n > 2$) for which the three-point DFT of $x_1[n]$ is:

$$X_1[k] = |X[k]| \qquad k = 0, 1, 2$$

where $X[k]$ is the three-point DFT of $x[n]$?

8.26. We have shown that the DFT $X[k]$ of a finite-length sequence $x[n]$ is identical to samples of the DTFT $X(e^{j\omega})$ of that sequence at frequencies $\omega_k = (2\pi/N)k$; i.e., $X[k] = X(e^{j(2\pi/N)k})$ for $k = 0, 1, \ldots, N-1$. Now consider a sequence $y[n] = e^{-j(\pi/N)n}x[n]$ whose DFT is $Y[k]$.

(a) Determine the relationship between the DFT $Y[k]$ and the DTFT $X(e^{j\omega})$.

(b) The result of part (a) shows that $Y[k]$ is a differently sampled version of $X(e^{j\omega})$. What are the frequencies at which $X(e^{j\omega})$ is sampled?

(c) Given the modified DFT $Y[k]$, how would you recover the original sequence $x[n]$?

8.27. The 10-point DFT of a 10-point sequence $g[n]$ is

$$G[k] = 10\,\delta[k].$$

Find $G(e^{j\omega})$, the DTFT of $g[n]$.

8.28. Consider the six-point sequence

$$x[n] = 6\delta[n] + 5\delta[n-1] + 4\delta[n-2] + 3\delta[n-3] + 2\delta[n-4] + \delta[n-5]$$

shown in Figure P8.28.

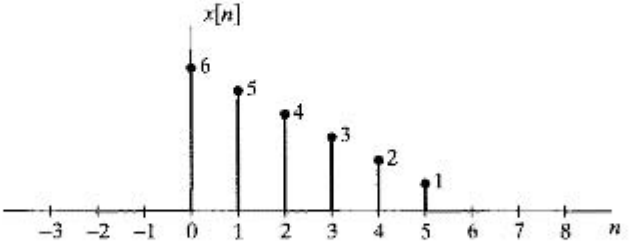

Figure P8.28

(a) Determine $X[k]$, the six-point DFT of $x[n]$. Express your answer in terms of $W_6 = e^{-j2\pi/6}$.

(b) Plot the sequence $w[n]$, $n = 0, 1, \ldots, 5$, that is obtained by computing the inverse six-point DFT of $W[k] = W_6^{-2k} X[k]$.

(c) Use any convenient method to evaluate the six-point circular convolution of $x[n]$ with the sequence $h[n] = \delta[n] + \delta[n-1] + \delta[n-2]$. Sketch the result.

(d) If we convolve the given $x[n]$ with the given $h[n]$ by N-point circular convolution, how should N be chosen so that the result of the circular convolution is identical to the result of linear convolution? That is, choose N so that

$$y_p[n] = x[n] \textcircled{N} h[n] = \sum_{m=0}^{N-1} x[m]h[((n-m))_N]$$

$$= x[n] * h[n] = \sum_{m=-\infty}^{\infty} x[m]h[n-m] \quad \text{for } 0 \le n \le N-1.$$

(e) In certain applications, such as multicarrier communication systems (see Starr et al, 1999), the linear convolution of a finite-length signal $x[n]$ of length L samples with a shorter finite-length impulse response $h[n]$ is required to be identical (over $0 \le n \le L-1$) to what would have been obtained by L-point circular convolution of $x[n]$ with $h[n]$. This can be achieved by augmenting the sequence $x[n]$ appropriately. Starting with the graph of Figure P8.28, where $L = 6$, add samples to the given sequence $x[n]$ to produce a new sequence $x_1[n]$ such that with the sequence $h[n]$ given in part (c), the ordinary convolution $y_1[n] = x_1[n] * h[n]$ satisfies the equation

$$y_1[n] = x_1[n] * h[n] = \sum_{m=-\infty}^{\infty} x_1[m]h[n-m]$$

$$= y_p[n] = x[n] \textcircled{L} h[n] = \sum_{m=0}^{5} x[m]h[((n-m))_6] \quad \text{for } 0 \le n \le 5.$$

(f) Generalize the result of part (e) for the case where $h[n]$ is nonzero for $0 \le n \le M$ and $x[n]$ is nonzero for $0 \le n \le L-1$, where $M < L$; i.e., show how to construct a sequence $x_1[n]$ from $x[n]$ such that the linear convolution $x_1[n] * h[n]$ is equal to the circular convolution $x[n] \textcircled{L} h[n]$ for $0 \le n \le L-1$.

8.29. Consider the real five-point sequence

$$x[n] = \delta[n] + \delta[n-1] + \delta[n-2] - \delta[n-3] + \delta[n-4].$$

The deterministic autocorrelation of this sequence is the inverse DTFT of

$$C(e^{j\omega}) = X(e^{j\omega})X^*(e^{j\omega}) = |X(e^{j\omega})|^2,$$

where $X^*(e^{j\omega})$ is the complex conjugate of $X(e^{j\omega})$. For the given $x[n]$, the autocorrelation can be found to be

$$c[n] = x[n] * x[-n].$$

(a) Plot the sequence $c[n]$. Observe that $c[-n] = c[n]$ for all n.

(b) Now assume that we compute the seven-point DFT ($N = 5$) of the sequence $x[n]$. Call this DFT $X_5[k]$. Then, we compute the inverse DFT of $C_5[k] = X_5[k]X_5^*[k]$. Plot the resulting sequence $c_5[n]$. How is $c_5[n]$ related to $c[n]$ from part (a)?

(c) Now assume that we compute the 10-point DFT ($N = 10$) of the sequence $x[n]$. Call this DFT $X_{10}[k]$. Then, we compute the inverse DFT of $C_{10}[k] = X_{10}[k]X_{10}^*[k]$. Plot the resulting sequence $c_{10}[n]$.

(d) Now suppose that we use $X_{10}[k]$ to form $D_{10}[k] = W_{10}^{5k}C_{10}[k] = W_{10}^{5k}X_{10}[k]X_{10}^*[k]$, where $W_{10} = e^{-j(2\pi/10)}$. Then, we compute the inverse DFT of $D_{10}[k]$. Plot the resulting sequence $d_{10}[n]$.

8.30. Consider two sequences $x[n]$ and $h[n]$, and let $y[n]$ denote their ordinary (linear) convolution, $y[n] = x[n] * h[n]$. Assume that $x[n]$ is zero outside the interval $21 \le n \le 31$, and $h[n]$ is zero outside the interval $18 \le n \le 31$.

(a) The signal $y[n]$ will be zero outside of an interval $N_1 \le n \le N_2$. Determine numerical values for N_1 and N_2.

(b) Now suppose that we compute the 32-point DFTs of

$$x_1[n] = \begin{cases} 0 & n = 0, 1, \ldots, 20 \\ x[n] & n = 21, 22, \ldots, 31 \end{cases}$$

and

$$h_1[n] = \begin{cases} 0 & n = 0, 1, \ldots, 17 \\ h[n] & n = 18, 19, \ldots, 31 \end{cases}$$

(i.e., the zero samples at the beginning of each sequence are included). Then, we form the product $Y_1[k] = X_1[k]H_1[k]$. If we define $y_1[n]$ to be the 32-point inverse DFT of $Y_1[k]$, how is $y_1[n]$ related to the ordinary convolution $y[n]$? That is, give an equation that expresses $y_1[n]$ in terms of $y[n]$ for $0 \le n \le 31$.

(c) Suppose that you are free to choose the DFT length (N) in part (b) so that the sequences are also zero-padded at their ends. What is the *minimum* value of N so that $y_1[n] = y[n]$ for $0 \le n \le N - 1$?

8.31. Consider the sequence $x[n] = 2\delta[n] + \delta[n-1] - \delta[n-2]$.

(a) Determine the DTFT $X(e^{j\omega})$ of $x[n]$ and the DTFT $Y(e^{j\omega})$ of the sequence $y[n] = x[-n]$.

(b) Using your results from part (a) find an expression for

$$W(e^{j\omega}) = X(e^{j\omega})Y(e^{j\omega}).$$

(c) Using the result of part (b) make a plot of $w[n] = x[n] * y[n]$.

(d) Now plot the sequence $y_p[n] = x[((-n))_4]$ as a function of n for $0 \le n \le 3$.

(e) Now use any convenient method to evaluate the four-point circular convolution of $x[n]$ with $y_p[n]$. Call your answer $w_p[n]$ and plot it.

(f) If we convolve $x[n]$ with $y_p[n] = x[((-n))_N]$, how should N be chosen to avoid time-domain aliasing?

8.32. Consider a finite-duration sequence $x[n]$ of length P such that $x[n] = 0$ for $n < 0$ and $n \ge P$. We want to compute samples of the Fourier transform at the N equally spaced frequencies

$$\omega_k = \frac{2\pi k}{N}, \qquad k = 0, 1, \ldots, N-1.$$

Determine and justify procedures for computing the N samples of the Fourier transform using only one N-point DFT for the following two cases:

(a) $N > P$.

(b) $N < P$.

8.33. An FIR filter has a 10-point impulse response, i.e.,

$$h[n] = 0 \qquad \text{for } n < 0 \text{ and for } n > 9.$$

Given that the 10-point DFT of $h[n]$ is given by

$$H[k] = \frac{1}{5}\delta[k-1] + \frac{1}{3}\delta[k-7],$$

find $H(e^{j\omega})$, the DTFT of $h[n]$.

8.34. Suppose that $x_1[n]$ and $x_2[n]$ are two finite-length sequences of length N, i.e., $x_1[n] = x_2[n] = 0$ outside $0 \le n \le N-1$. Denote the z-transform of $x_1[n]$ by $X_1(z)$, and denote the N-point DFT of $x_2[n]$ by $X_2[k]$. The two transforms $X_1(z)$ and $X_2[k]$ are related by:

$$X_2[k] = X_1(z)\Big|_{z=\frac{1}{2}e^{-j\frac{2\pi k}{N}}}, \qquad k = 0, 1, \ldots, N-1$$

Determine the relationship between $x_1[n]$ and $x_2[n]$.

Advanced Problems

8.35. Figure P8.35-1 illustrates a six-point discrete-time sequence $x[n]$. Assume that $x[n]$ is zero outside the interval shown.

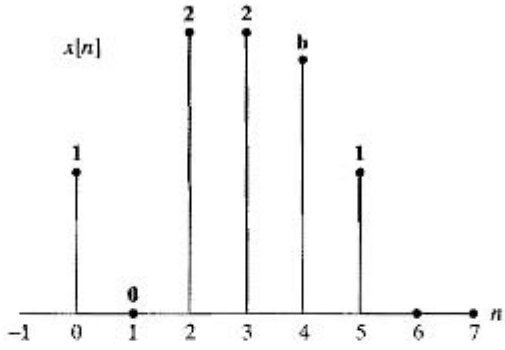

Figure P8.35-1

The value of $x[4]$ is not known and is represented as b. The sample in the figure is not shown to scale. Let $X(e^{j\omega})$ be the DTFT of $x[n]$ and $X_1[k]$ be samples of $X(e^{j\omega})$ at $\omega_k = 2\pi k/4$, i.e.,

$$X_1[k] = X(e^{j\omega})|_{\omega=\frac{\pi k}{2}}, \qquad 0 \le k \le 3.$$

The four-point sequence $x_1[n]$ that results from taking the four-point inverse DFT of $X_1[k]$ is shown in Figure P8.35-2. Based on the figure can you determine b uniquely? If so, give the value of b.

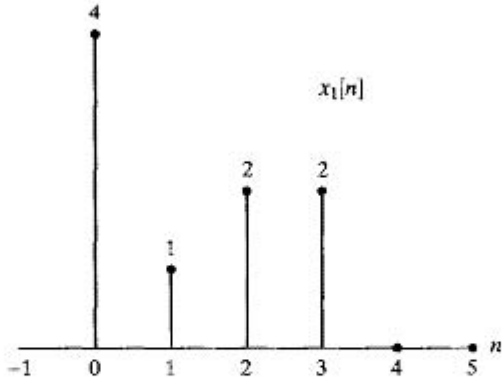

Figure P8.35-2

8.36. **(a)** $X(e^{j\omega})$ is the DTFT of the discrete-time signal

$$x[n] = (1/2)^n u[n].$$

Find a length-5 sequence $g[n]$ whose five-point DFT $G[k]$ is identical to samples of the DTFT of $x[n]$ at $\omega_k = 2\pi k/5$, i.e.,

$$g[n] = 0 \text{ for } n < 0, \quad n > 4$$

and

$$G[k] = X(e^{j2\pi k/5}) \text{ for } k = 0, 1, \ldots, 4.$$

(b) Let $w[n]$ be a sequence that is strictly nonzero for $0 \le n \le 9$ and zero elsewhere, i.e.,

$$w[n] \neq 0, \quad 0 \le n \le 9$$
$$w[n] = 0 \quad \text{otherwise}$$

Determine a choice for $w[n]$ such that its DTFT $W(e^{j\omega})$ is equal to $X(e^{j\omega})$ at the frequencies $\omega = 2\pi k/5$, $k = 0, 1, \ldots, 4$, i.e.,

$$W(e^{j2\pi k/5}) = X(e^{j2\pi k/5}) \text{ for } k = 0, 1, \ldots, 4.$$

8.37. A discrete-time LTI filter S is to be implemented using the overlap–save method. In the overlap–save method, the input is divided into *overlapping* blocks, as opposed to the overlap–add method where the input blocks are nonoverlapping. For this implementation, the input signal $x[n]$ will be divided into overlapping 256-point blocks $x_r[n]$. Adjacent blocks will overlap by 255 points so that they differ by only one sample. This is represented by Eq. (P8.37-1) which is a relation between $x_r[n]$ and $x[n]$,

$$x_r[n] = \begin{cases} x[n+r] & 0 \le n \le 255 \\ 0 & \text{otherwise,} \end{cases} \tag{P8.37-1}$$

where r ranges over all integers and we obtain a different block $x_r[n]$ for each value of r.

Each block is processed by computing the 256-point DFT of $x_r[n]$, multiplying the result with $H[k]$ given in Eq. (P8.37-2), and computing the 256-point inverse DFT of the product.

$$H[k] = \begin{cases} 1 & 0 \le k \le 31 \\ 0 & 32 \le k \le 224 \\ 1 & 225 \le k \le 255 \end{cases} \qquad \text{(P8.37-2)}$$

One sample from each block computation (in this case only a single sample per block) is then "saved" as part of the overall output.

(a) Is S an ideal frequency-selective filter? Justify your answer.
(b) Is the impulse response of S real valued? Justify your answer.
(c) Determine the impulse response of S.

8.38. $x[n]$ is a real-valued finite-length sequence of length 512, i.e.,

$$x[n] = 0 \qquad n < 0, n \ge 512$$

and has been stored in a 512-point data memory. It is known that $X[k]$ the 512-point DFT of $x[n]$ has the property

$$X[k] = 0 \qquad 250 \le k \le 262.$$

In storing the data, one data point at most may have been corrupted. Specifically, if $s[n]$ denotes the stored data, $s[n] = x[n]$ except possibly at one unknown memory location n_0. To test and possibly correct the data, you are able to examine $S[k]$, the 512-point DFT of $s[n]$.

(a) Specify whether, by examining $S[k]$, it is possible and if so, how, to *detect* whether an error has been made in one data point, i.e., whether or not $s[n] = x[n]$ for all n.

In parts (b) and (c), assume that you know for sure that one data point has been corrupted, i.e., that $s[n] = x[n]$ *except* at $n = n_0$.

(b) In this part, assume the value of n_0 is unknown. Specify a procedure for determining from $S[k]$ the value of n_0.
(c) In this part, assume that you know the value of n_0. Specify a procedure for determining $x[n_0]$ from $S[k]$.

8.39. In the system shown in the Figure P8.39, $x_1[n]$ and $x_2[n]$ are both causal, 32-point sequences, i.e., they are both zero outside the interval $0 \le n \le 31$. $y[n]$ denotes the linear convolution of $x_1[n]$ and $x_2[n]$, i.e., $y[n] = x_1[n] * x_2[n]$.

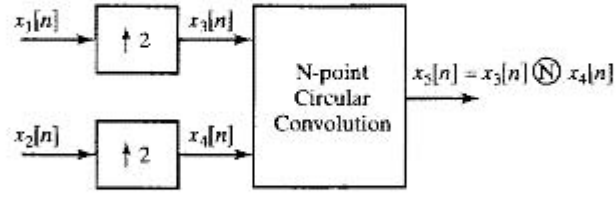

Figure P8.39

(a) Determine the values of N for which all the values of $y[n]$ can be completely recovered from $x_5[n]$.
(b) Specify explicitly how to recover $y[n]$ from $x_5[n]$ for the *smallest* value of N which you determined in part (a).

8.40. Three real-valued seven-point sequences ($x_1[n], x_2[n]$, and $x_3[n]$) are shown in Figure P8.40. For each of these sequences, specify whether the seven-point DFT can be written in the form

$$X_i[k] = A_i[k]e^{-j(2\pi k/7)k\alpha_i} \qquad k = 0, 1, \ldots, 6$$

where $A_i[k]$ is real-valued and $2\alpha_i$ is an integer. Include a brief explanation. For each sequence which can be written in this form, specify all corresponding values of α_i for $0 \leq \alpha_i < 7$.

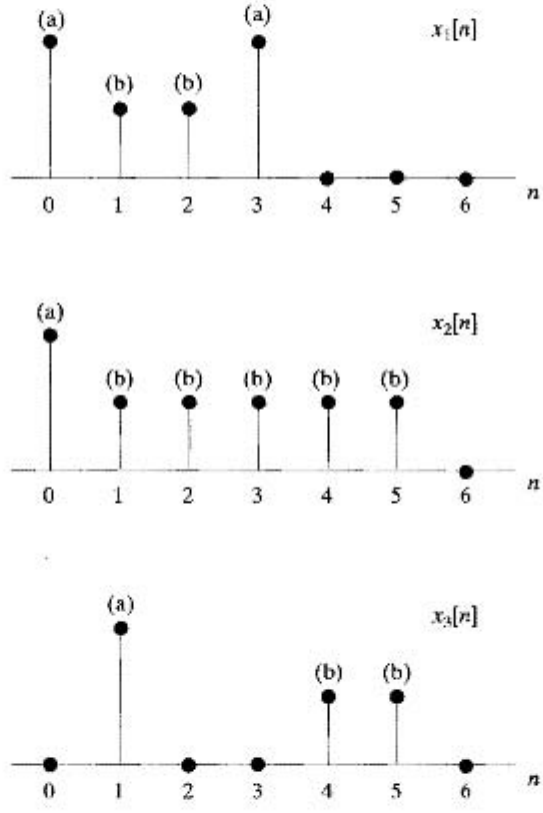

Figure P8.40

8.41. Suppose $x[n]$ is the eight-point complex-valued sequence with real part $x_r[n]$ and imaginary part $x_i[n]$ shown in Figure P8.41 (i.e., $x[n] = x_r[n] + jx_i[n]$). Let $y[n]$ be the four-point complex-valued sequence such that $Y[k]$, the four-point DFT of $y[n]$, is equal to the odd-indexed values of $X[k]$, the eight-point DFT of $x[n]$ (the odd-indexed values of $X[k]$ are those for which $k = 1, 3, 5, 7$).

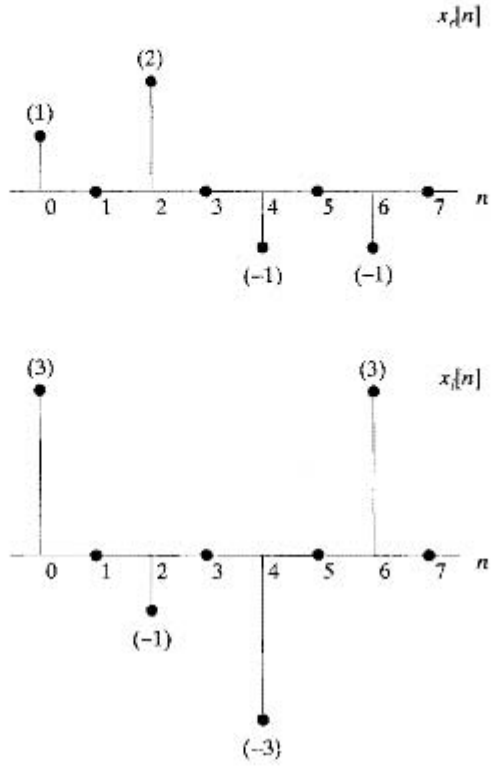

Figure P8.41

Determine the numerical values of $y_r[n]$ and $y_i[n]$, and the real and imaginary parts of $y[n]$.

8.42. $x[n]$ is a finite-length sequence of length 1024, i.e.,

$$x[n] = 0 \text{ for } n < 0, \; n > 1023.$$

The autocorrelation of $x[n]$ is defined as

$$c_{xx}[m] = \sum_{n=-\infty}^{\infty} x[n]x[n+m],$$

and $X_N[k]$ is defined as the N-point DFT of $x[n]$, with $N \geq 1024$.

We are interested in computing $c_{xx}[m]$. A proposed procedure begins by first computing the N-point inverse DFT of $|X_N[k]|^2$ to obtain an N-point sequence $g_N[n]$, i.e.,

$$g_N[n] = N\text{-point IDFT}\left\{|X_N[k]|^2\right\}.$$

(a) Determine the minimum value of N so that $c_{xx}[m]$ can be obtained from $g_N[n]$. Also specify how you would obtain $c_{xx}[m]$ from $g_N[n]$.

(b) Determine the minimum value of N so that $c_{xx}[m]$ for $|m| \leq 10$ can be obtained from $g_N[n]$. Also specify how you would obtain these values from $g_N[n]$.

8.43. In Figure P8.43, $x[n]$ is a finite-length sequence of length 1024. The sequence $R[k]$ is obtained by taking the 1024-point DFT of $x[n]$ and compressing the result by 2.

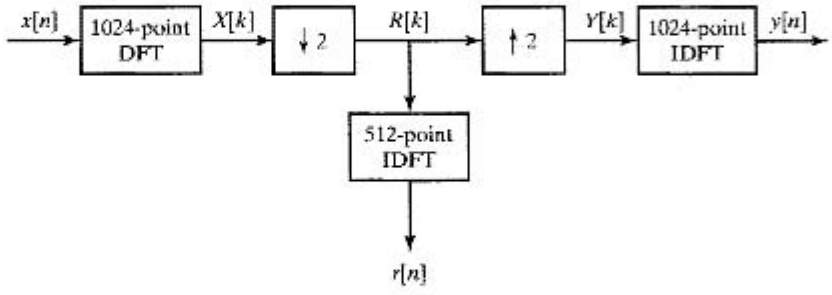

Figure P8.43

(a) Choose the most accurate statement for $r[n]$, the 512-point inverse DFT of $R[k]$. Justify your choice in a few concise sentences.

(i) $r[n] = x[n],\ 0 \le n \le 511$

(ii) $r[n] = x[2n],\ 0 \le n \le 511$

(iii) $r[n] = x[n] + x[n + 512],\ 0 \le n \le 511$

(iv) $r[n] = x[n] + x[-n + 512],\ 0 \le n \le 511$

(v) $r[n] = x[n] + x[1023 - n],\ 0 \le n \le 511$

In all cases $r[n] = 0$ outside $0 \le n \le 511$.

(b) The sequence $Y[k]$ is obtained by expanding $R[k]$ by 2. Choose the most accurate statement for $y[n]$, the 1024-point inverse DFT of $Y[k]$. Justify your choice in a few concise sentences.

(i) $y[n] = \begin{cases} \frac{1}{2}(x[n] + x[n + 512]), & 0 \le n \le 511 \\ \frac{1}{2}(x[n] + x[n - 512]), & 512 \le n \le 1023 \end{cases}$

(ii) $y[n] = \begin{cases} x[n], & 0 \le n \le 511 \\ x[n - 512], & 512 \le n \le 1023 \end{cases}$

(iii) $y[n] = \begin{cases} x[n], & n \text{ even} \\ 0, & n \text{ odd} \end{cases}$

(iv) $y[n] = \begin{cases} x[2n], & 0 \le n \le 511 \\ x[2(n - 512)], & 512 \le n \le 1023 \end{cases}$

(v) $y[n] = \frac{1}{2}(x[n] + x[1023 - n]),\ 0 \le n \le 1023$

In all cases $y[n] = 0$ outside $0 \le n \le 1023$.

8.44. Figure P8.44 shows two finite-length sequences $x_1[n]$ and $x_2[n]$ of length 7. $X_i(e^{j\omega})$ denotes the DTFT of $x_i[n]$, and $X_i[k]$ denotes the seven-point DFT of $x_i[n]$.

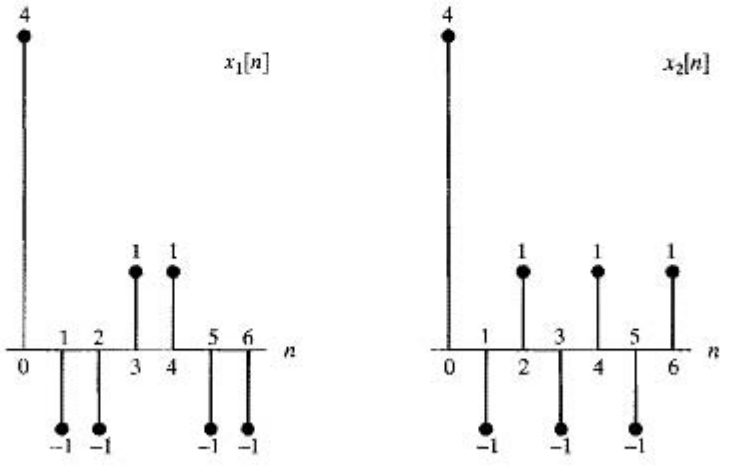

Figure P8.44

For each of the sequences $x_1[n]$ and $x_2[n]$, indicate whether each one of the following properties holds:

(a) $X_i(e^{j\omega})$ can be written in the form

$$X_i(e^{j\omega}) = A_i(\omega)e^{j\alpha_i\omega}, \quad \text{for } \omega \in (-\pi, \pi),$$

where $A_i(\omega)$ is real and α_i is a constant.

(b) $X_i[k]$ can be written in the form

$$X_i[k] = B_i[k]e^{j\beta_i k},$$

where $B_i[k]$ is real and β_i is a constant.

8.45. The sequence $x[n]$ is a 128-point sequence (i.e., $x[n] = 0$ for $n < 0$ and for $n > 127$), and $x[n]$ has at least one nonzero sample. The DTFT of $x[n]$ is denoted $X(e^{j\omega})$. What is the largest integer M such that it is possible for $X(e^{j2\pi k/M})$ to be zero for all integer values of k? Construct an example for the maximal M that you have found.

8.46. Each part of this problem may be solved independently. All parts use the signal $x[n]$ given by

$$x[n] = 3\delta[n] - \delta[n-1] + 2\delta[n-3] + \delta[n-4] - \delta[n-6].$$

(a) Let $X\left(e^{j\omega}\right)$ be the DTFT of $x[n]$. Define

$$R[k] = X\left(e^{j\omega}\right)\Big|_{\omega=\frac{2\pi k}{4}}, \qquad 0 \le k \le 3$$

Plot the signal $r[n]$ which is the four-point inverse DFT of $R[k]$.

(b) Let $X[k]$ be the eight-point DFT of $x[n]$, and let $H[k]$ be the eight-point DFT of the impulse response $h[n]$ given by

$$h[n] = \delta[n] - \delta[n-4].$$

Define $Y[k] = X[k]H[k]$ for $0 \le k \le 7$. Plot $y[n]$, the eight-point DFT of $Y[k]$.

8.47. Consider a time-limited continuous-time signal $x_c(t)$ whose duration is 100 ms. Assume that this signal has a bandlimited Fourier transform such that $X_c(j\Omega) = 0$ for $|\Omega| \geq 2\pi(10,000)$ rad/s; i.e., assume that aliasing is negligible. We want to compute samples of $X_c(j\Omega)$ with 5 Hz spacing over the interval $0 \leq \Omega \leq 2\pi(10,000)$. This can be done with a 4000-point DFT. Specifically, we want to obtain a 4000-point sequence $x[n]$ for which the 4000-point DFT is related to $X_c(j\Omega)$ by:

$$X[k] = \alpha X_c(j2\pi \cdot 5 \cdot k), \qquad k = 0, 1, \ldots, 1999, \tag{P8.47-1}$$

where α is a known scale factor. The following method is proposed to obtain a 4000-point sequence whose DFT gives the desired samples of $X_c(j\Omega)$. First, $x_c(t)$ is sampled with a sampling period of $T = 50\mu s$. Next, the resulting 2000-point sequence is used to form the sequence $\hat{x}[n]$ as follows:

$$\hat{x}[n] = \begin{cases} x_c(nT), & 0 \leq n \leq 1999, \\ x_c((n-2000)T), & 2000 \leq n \leq 3999, \\ 0, & \text{otherwise.} \end{cases} \tag{P8.47-2}$$

Finally, the 4000-point DFT $\hat{X}[k]$ of this sequence is computed. For this method, determine how $\hat{X}[k]$ is related to $X_c(j\Omega)$. Indicate this relationship in a sketch for a "typical" Fourier transform $X_c(j\Omega)$. Explicitly state whether or not $\hat{X}[k]$ is the desired result, i.e., whether $\hat{X}[k]$ equals $X[k]$ as specified in Eq. (P8.47-1).

8.48. $x[n]$ is a real-valued finite length sequence of length 1024, i.e.,

$$x[n] = 0 \qquad n < 0, n \geq 1023.$$

Only the following samples of the 1024-point DFT of $x[n]$ are known

$$X[k] \qquad k = 0, 16, 16 \times 2, 16 \times 3, \ldots, 16 \times (64 - 1)$$

Also, we observe $s[n]$ which is a corrupted version of $x[n]$, with first 64 points corrupted, i.e., $s[n] = x[n]$ for $n \geq 64$, and $s[n] \neq x[n]$, for $0 \leq n \leq 63$. Describe a procedure to recover the first 64 samples of $x[n]$ using only 1024-point DFT and IDFT blocks, multipliers, and adders.

8.49. The deterministic crosscorrelation function between two real sequences is defined as

$$c_{xy}[n] = \sum_{m=-\infty}^{\infty} y[m]x[n+m] = \sum_{m=-\infty}^{\infty} y[-m]x[n-m] = y[-n] * x[n] \qquad -\infty < n < \infty$$

(a) Show that the DTFT of $c_{xy}[n]$ is $C_{xy}(e^{j\omega}) = X(e^{j\omega})Y^*(e^{j\omega})$.

(b) Suppose that $x[n] = 0$ for $n < 0$ and $n > 99$ and $y[n] = 0$ for $n < 0$ and $n > 49$. The corresponding crosscorrelation function $c_{xy}[n]$ will be nonzero only in a finite-length interval $N_1 \leq n \leq N_2$. What are N_1 and N_2?

(c) Suppose that we wish to compute values of $c_{xy}[n]$ in the interval $0 \leq n \leq 20$ using the following procedure:

(i) Compute $X[k]$, the N-point DFT of $x[n]$
(ii) Compute $Y[k]$, the N-point DFT of $y[n]$
(iii) Compute $C[k] = X[k]Y^*[k]$ for $0 \leq k \leq N-1$
(iv) Compute $c[n]$, the inverse DFT of $C[k]$

What is the *minimum* value of N such that $c[n] = c_{xy}[n]$, $0 \leq n \leq 20$? Explain your reasoning.

8.50. The DFT of a finite-duration sequence corresponds to samples of its z-transform on the unit circle. For example, the DFT of a 10-point sequence $x[n]$ corresponds to samples of $X(z)$ at the 10 equally spaced points indicated in Figure P8.50-1. We wish to find the equally spaced samples of $X(z)$ on the contour shown in Figure P8.50-2; i.e., we wish to obtain

$$X(z)\big|_{z=0.5e^{j((2\pi k/10)+(\pi/10))}}.$$

Show how to modify $x[n]$ to obtain a sequence $x_1[n]$ such that the DFT of $x_1[n]$ corresponds to the desired samples of $X(z)$.

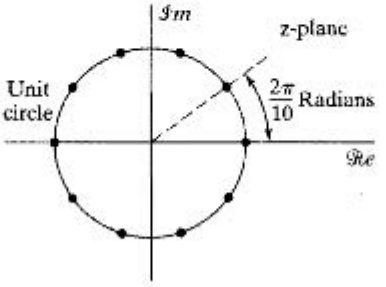

Figure P8.50-1

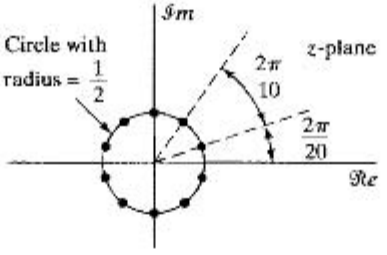

Figure P8.50-2

8.51. Let $w[n]$ denote the linear convolution of $x[n]$ and $y[n]$. Let $g[n]$ denote the 40-point circular convolution of $x[n]$ and $y[n]$:

$$w[n] = x[n] * y[n] = \sum_{k=-\infty}^{\infty} x[k]y[n-k],$$

$$g[n] = x[n] \textcircled{40} y[n] = \sum_{k=0}^{39} x[k]y[((n-k))_{40}].$$

(a) Determine the values of n for which $w[n]$ can be nonzero.

(b) Determine the values of n for which $w[n]$ can be obtained from $g[n]$. Explicitly specify at what index values n in $g[n]$ these values of $w[n]$ appear.

8.52. Let $x[n] = 0, \quad n < 0, n > 7$, be a real eight-point sequence, and let $X[k]$ be its eight-point DFT.

(a) Evaluate

$$\left(\frac{1}{8}\sum_{k=0}^{7} X[k]e^{j(2\pi/8)kn}\right)\Bigg|_{n=9}$$

in terms of $x[n]$.

(b) Let $v[n] = 0, \quad n < 0, n > 7$, be an eight-point sequence, and let $V[k]$ be its eight-point DFT.
If $V[k] = X(z)$ at $z = 2\exp(j(2\pi k + \pi)/8)$ for $k = 0, \ldots, 7$, where $X(z)$ is the z-transform of $x[n]$, express $v[n]$ in terms of $x[n]$.

(c) Let $w[n] = 0, \quad n < 0, n > 3$, be a four-point sequence, and let $W[k]$ be its four-point DFT.
If $W[k] = X[k] + X[k+4]$, express $w[n]$ in terms of $x[n]$.

(d) Let $y[n] = 0, \quad n < 0, n > 7$, be an eight-point sequence, and let $Y[k]$ be its eight-point DFT.
If

$$Y[k] = \begin{cases} 2X[k], & k = 0, 2, 4, 6, \\ 0, & k = 1, 3, 5, 7, \end{cases}$$

express $y[n]$ in terms of $x[n]$.

8.53. Read each part of this problem carefully to note the differences among parts.

(a) Consider the signal

$$x[n] = \begin{cases} 1 + \cos(\pi n/4) - 0.5\cos(3\pi n/4), & 0 \le n \le 7, \\ 0, & \text{otherwise}, \end{cases}$$

which can be represented by the IDFT equation as

$$x[n] = \begin{cases} \frac{1}{8}\sum_{k=0}^{7} X_8[k]e^{j(2\pi k/8)n}, & 0 \le n \le 7, \\ 0, & \text{otherwise}, \end{cases}$$

where $X_8[k]$ is the eight-point DFT of $x[n]$. Plot $X_8[k]$ for $0 \le k \le 7$.

(b) Determine $V_{16}[k]$, the 16-point DFT of the 16-point sequence

$$v[n] = \begin{cases} 1 + \cos(\pi n/4) - 0.5\cos(3\pi n/4), & 0 \le n \le 15, \\ 0, & \text{otherwise}. \end{cases}$$

Plot $V_{16}[k]$ for $0 \le k \le 15$.

(c) Finally, consider $|X_{16}[k]|$, the magnitude of the 16-point DFT of the eight-point sequence

$$x[n] = \begin{cases} 1 + \cos(\pi n/4) - 0.5\cos(3\pi n/4), & 0 \le n \le 7, \\ 0, & \text{otherwise}. \end{cases}$$

Plot $|X_{16}[k]|$ for $0 \le k \le 15$ *without explicitly evaluating the DFT expression*. You will not be able to find all values of $|X_{16}[k]|$ by inspection as in parts (a) and (b), but you should be able to find some of the values exactly. Plot all the values you know exactly with a solid circle, and plot estimates of the other values with an open circle.

Extension Problems

8.54. In deriving the DFS analysis Eq. (8.11), we used the identity of Eq. (8.7). To verify this identity, we will consider the two conditions $k - r = mN$ and $k - r \neq mN$ separately.

(a) For $k - r = mN$, show that $e^{j(2\pi/N)(k-r)n} = 1$ and, from this, that

$$\frac{1}{N}\sum_{n=0}^{N-1} e^{j(2\pi/N)(k-r)n} = 1 \qquad \text{for } k - r = mN. \tag{P8.54-1}$$

(b) Since k and r are both integers in Eq. (8.7), we can make the substitution $k - r = \ell$ and consider the summation

$$\frac{1}{N}\sum_{n=0}^{N-1} e^{j(2\pi/N)\ell n} = \frac{1}{N}\sum_{n=0}^{N-1} [e^{j(2\pi/N)\ell}]^n. \tag{P8.54-2}$$

Because this is the sum of a finite number of terms in a geometric series, it can be expressed in closed form as

$$\frac{1}{N}\sum_{n=0}^{N-1} [e^{j(2\pi/N)\ell}]^n = \frac{1}{N}\frac{1 - e^{j(2\pi/N)\ell N}}{1 - e^{j(2\pi/N)\ell}}. \tag{P8.54-3}$$

For what values of ℓ is the right-hand side of Eq. (P8.54-3) equation indeterminate? That is, are the numerator and denominator both zero?

(c) From the result in part (b), show that if $k - r \neq mN$, then

$$\frac{1}{N}\sum_{n=0}^{N-1} e^{j(2\pi/N)(k-r)n} = 0. \tag{P8.54-4}$$

8.55. In Section 8.2, we stated the property that if

$$\tilde{x}_1[n] = \tilde{x}[n - m],$$

then

$$\tilde{X}_1[k] = W_N^{km}\tilde{X}[k],$$

where $\tilde{X}[k]$ and $\tilde{X}_1[k]$ are the DFS coefficients of $\tilde{x}[n]$ and $\tilde{x}_1[n]$, respectively. In this problem, we consider the proof of that property.

(a) Using Eq. (8.11) together with an appropriate substitution of variables, show that $\tilde{X}_1[k]$ can be expressed as

$$\tilde{X}_1[k] = W_N^{km}\sum_{r=-m}^{N-1-m} \tilde{x}[r]W_N^{kr}. \tag{P8.55-1}$$

(b) The summation in Eq. (P8.55-1) can be rewritten as

$$\sum_{r=-m}^{N-1-m} \tilde{x}[r]W_N^{kr} = \sum_{r=-m}^{-1} \tilde{x}[r]W_N^{kr} + \sum_{r=0}^{N-1-m} \tilde{x}[r]W_N^{kr}. \tag{P8.55-2}$$

Using the fact that $\tilde{x}[r]$ and W_N^{kr} are both periodic, show that

$$\sum_{r=-m}^{-1} \tilde{x}[r]W_N^{kr} = \sum_{r=N-m}^{N-1} \tilde{x}[r]W_N^{kr}. \tag{P8.55-3}$$

(c) From your results in parts (a) and (b), show that

$$\tilde{X}_1[k] = W_N^{km} \sum_{r=0}^{N-1} \tilde{x}[r] W_N^{kr} = W_N^{km} \tilde{X}[k].$$

8.56. **(a)** Table 8.1 lists a number of symmetry properties of the DFS for periodic sequences, several of which we repeat here. Prove that each of these properties is true. In carrying out your proofs, you may use the definition of the DFS and any previous property in the list. (For example, in proving property 3, you may use properties 1 and 2.)

Sequence	*DFS*
1. $\tilde{x}^*[n]$	$\tilde{X}^*[-k]$
2. $\tilde{x}^*[-n]$	$\tilde{X}^*[k]$
3. $\mathcal{R}e\{\tilde{x}[n]\}$	$\tilde{X}_e[k]$
4. $j\mathcal{I}m\{\tilde{x}[n]\}$	$\tilde{X}_o[k]$

(b) From the properties proved in part (a), show that for a real periodic sequence $\tilde{x}[n]$, the following symmetry properties of the DFS hold:

1. $\mathcal{R}e\{\tilde{X}[k]\} = \mathcal{R}e\{\tilde{X}[-k]\}$
2. $\mathcal{I}m\{\tilde{X}[k]\} = -\mathcal{I}m\{\tilde{X}[-k]\}$
3. $|\tilde{X}[k]| = |\tilde{X}[-k]|$
4. $\angle\tilde{X}[k] = -\angle\tilde{X}[-k]$

8.57. We stated in Section 8.4 that a direct relationship between $X(e^{j\omega})$ and $\tilde{X}[k]$ can be derived, where $\tilde{X}[k]$ is the DFS coefficients of a periodic sequence and $X(e^{j\omega})$ is the Fourier transform of one period. Since $\tilde{X}[k]$ corresponds to samples of $X(e^{j\omega})$, the relationship then corresponds to an interpolation formula.

One approach to obtaining the desired relationship is to rely on the discussion of Section 8.4, the relationship of Eq. (8.54), and the modulation property of Section 2.9.7. The procedure is as follows:

1. With $\tilde{X}[k]$ denoting the DFS coefficients of $\tilde{x}[n]$, express the Fourier transform $\tilde{X}(e^{j\omega})$ of $\tilde{x}[n]$ as an impulse train; i.e., scaled and shifted impulse functions $S(\omega)$.
2. From Eq. (8.57), $x[n]$ can be expressed as $x[n] = \tilde{x}[n]w[n]$, where $w[n]$ is an appropriate finite-length window.
3. Since $x[n] = \tilde{x}[n]w[n]$, from Section 2.9.7, $X(e^{j\omega})$ can be expressed as the (periodic) convolution of $\tilde{X}(e^{j\omega})$ and $W(e^{j\omega})$.

By carrying out the details in this procedure, show that $X(e^{j\omega})$ can be expressed as

$$X(e^{j\omega}) = \frac{1}{N} \sum_k \tilde{X}[k] \frac{\sin[(\omega N - 2\pi k)/2]}{\sin[(\omega - (2\pi k/N))/2]} e^{-j[(N-1)/2][\omega - 2\pi k/N]}.$$

Specify explicitly the limits on the summation.

8.58. Let $X[k]$ denote the N-point DFT of the N-point sequence $x[n]$.

(a) Show that if

$$x[n] = -x[N-1-n],$$

then $X[0] = 0$. Consider separately the cases of N even and N odd.

(b) Show that if N is even and if

$$x[n] = x[N-1-n],$$

then $X[N/2] = 0$.

8.59. In Section 2.8, the conjugate-symmetric and conjugate-antisymmetric components of a sequence $x[n]$ were defined, respectively, as

$$x_e[n] = \frac{1}{2}(x[n] + x^*[-n]),$$

$$x_o[n] = \frac{1}{2}(x[n] - x^*[-n]).$$

In Section 8.6.4, we found it convenient to define respectively the periodic conjugate-symmetric and periodic conjugate-antisymmetric components of a sequence of finite duration N as

$$x_{ep}[n] = \tfrac{1}{2}\{x[((n))_N] + x^*[((-n))_N]\}, \qquad 0 \le n \le N-1,$$

$$x_{op}[n] = \tfrac{1}{2}\{x[((n))_N] - x^*[((-n))_N]\}, \qquad 0 \le n \le N-1.$$

(a) Show that $x_{ep}[n]$ can be related to $x_e[n]$ and that $x_{op}[n]$ can be related to $x_o[n]$ by the relations

$$x_{ep}[n] = (x_e[n] + x_e[n-N]), \qquad 0 \le n \le N-1,$$

$$x_{op}[n] = (x_o[n] + x_o[n-N]), \qquad 0 \le n \le N-1.$$

(b) $x[n]$ is considered to be a sequence of length N, and in general, $x_e[n]$ cannot be recovered from $x_{ep}[n]$, and $x_o[n]$ cannot be recovered from $x_{op}[n]$. Show that with $x[n]$ considered as a sequence of length N, but with $x[n] = 0, n > N/2$, $x_e[n]$ can be obtained from $x_{ep}[n]$, and $x_o[n]$ can be obtained from $x_{op}[n]$.

8.60. Show from Eqs. (8.65) and (8.66) that with $x[n]$ as an N-point sequence and $X[k]$ as its N-point DFT,

$$\sum_{n=0}^{N-1} |x[n]|^2 = \frac{1}{N}\sum_{k=0}^{N-1} |X[k]|^2.$$

This equation is commonly referred to as *Parseval's relation* for the DFT.

8.61. $x[n]$ is a real-valued, nonnegative, finite-length sequence of length N; i.e., $x[n]$ is real and nonnegative for $0 \le n \le N-1$ and is zero otherwise. The N-point DFT of $x[n]$ is $X[k]$, and the Fourier transform of $x[n]$ is $X(e^{j\omega})$.

Determine whether each of the following statements is true or false. For each statement, if you indicate that it is true, clearly show your reasoning. If you state that it is false, construct a counterexample.

(a) If $X(e^{j\omega})$ is expressible in the form

$$X(e^{j\omega}) = B(\omega)e^{j\alpha\omega},$$

where $B(\omega)$ is real and α is a real constant, then $X[k]$ can be expressed in the form

$$X[k] = A[k]e^{j\gamma k},$$

where $A[k]$ is real and γ is a real constant.

(b) If $X[k]$ is expressible in the form

$$X[k] = A[k]e^{j\gamma k},$$

where $A[k]$ is real and γ is a real constant, then $X(e^{j\omega})$ can be expressed in the form

$$X(e^{j\omega}) = B(\omega)e^{j\alpha\omega},$$

where $B(\omega)$ is real and α is a real constant.

8.62. $x[n]$ and $y[n]$ are two real-valued, positive, finite-length sequences of length 256; i.e.,

$$\begin{aligned} x[n] &> 0, \qquad 0 \le n \le 255, \\ y[n] &> 0, \qquad 0 \le n \le 255, \\ x[n] = y[n] &= 0, \qquad \text{otherwise.} \end{aligned}$$

$r[n]$ denotes the *linear* convolution of $x[n]$ and $y[n]$. $R(e^{j\omega})$ denotes the Fourier transform of $r[n]$. $R_s[k]$ denotes 128 equally spaced samples of $R(e^{j\omega})$; i.e.,

$$R_s[k] = R(e^{j\omega})\Big|_{\omega=2\pi k/128}, \qquad k = 0, 1, \ldots, 127.$$

Given $x[n]$ and $y[n]$, we want to obtain $R_s[k]$ as efficiently as possible. The *only* modules available are those shown in Figure P8.62. The costs associated with each module are as follows:

Modules I and II are free.
Module III costs 10 units.
Module IV costs 50 units.
Module V costs 100 units.

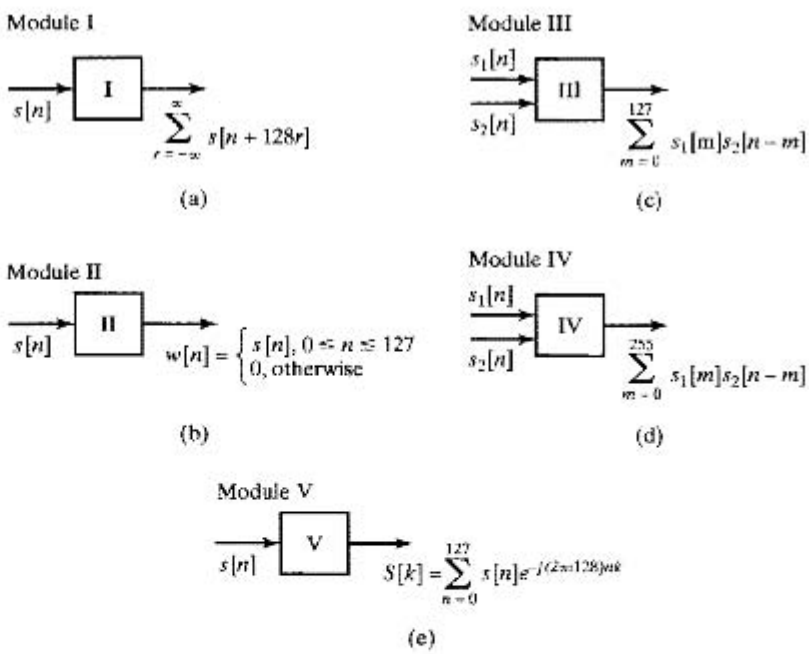

Figure P8.62

By appropriately connecting one or several of each module, construct a system for which the inputs are $x[n]$ and $y[n]$ and the output is $R_s[k]$. The important considerations are (a) whether the system works and (b) how efficient it is. The lower the *total* cost, the more efficient the system is.

8.63. $y[n]$ is the output of a stable LTI system with system function $H(z) = 1/(z - bz^{-1})$, where b is a known constant. We would like to recover the input signal $x[n]$ by operating on $y[n]$.

The following procedure is proposed for recovering part of $x[n]$ from the data $y[n]$:

1. Using $y[n]$, $0 \le n \le N-1$, calculate $Y[k]$, the N-point DFT of $y[n]$.
2. Form

$$V[k] = (W_N^{-k} - bW_N^k)Y[k].$$

3. Calculate the inverse DFT of $V[k]$ to obtain $v[n]$.

For which values of the index n in the range $n = 0, 1, \ldots, N-1$ are we guaranteed that

$$x[n] = v[n]?$$

8.64. A modified discrete Fourier transform (MDFT) was proposed (Vernet, 1971) that computes samples of the z-transform on the unit circle offset from those computed by the DFT. In particular, with $X_M[k]$ denoting the MDFT of $x(n)$,

$$X_M[k] = X(z)\Big|_{z=e^{j(2\pi k/N+\pi/N)}}, \qquad k = 0, 1, 2, \ldots, N-1.$$

Assume that N is even.

(a) The N-point MDFT of a sequence $x[n]$ corresponds to the N-point DFT of a sequence $x_M[n]$, which is easily constructed from $x[n]$. Determine $x_M[n]$ in terms of $x[n]$.

(b) If $x[n]$ is real, not all the points in the DFT are independent, since the DFT is conjugate symmetric; i.e., $X[k] = X^*[((-k))_N]$ for $0 \le k \le N-1$. Similarly, if $x[n]$ is real, not all the points in the MDFT are independent. Determine, for $x[n]$ real, the relationship between points in $X_M[k]$.

(c) (i) Let $R[k] = X_M[2k]$; that is, $R[k]$ contains the even-numbered points in $X_M[k]$. From your answer in part (b), show that $X_M[k]$ can be recovered from $R[k]$.

(ii) $R[k]$ can be considered to be the $N/2$-point MDFT of an $N/2$-point sequence $r[n]$. Determine a simple expression relating $r[n]$ directly to $x[n]$.

According to parts (b) and (c), the N-point MDFT of a real sequence $x[n]$ can be computed by forming $r[n]$ from $x[n]$ and then computing the $N/2$-point MDFT of $r[n]$. The next two parts are directed at showing that the MDFT can be used to implement a linear convolution.

(d) Consider three sequences $x_1[n]$, $x_2[n]$, and $x_3[n]$, all of length N. Let $X_{1M}[k]$, $X_{2M}[k]$, and $X_{3M}[k]$, respectively, denote the MDFTs of the three sequences. If

$$X_{3M}[k] = X_{1M}[k]X_{2M}[k],$$

express $x_3[n]$ in terms of $x_1[n]$ and $x_2[n]$. Your expression must be of the form of a single summation over a "combination" of $x_1[n]$ and $x_2[n]$ in the same style as (but not identical to) a circular convolution.

(e) It is convenient to refer to the result in part (d) as a modified circular convolution. If the sequences $x_1[n]$ and $x_2[n]$ are both zero for $n \ge N/2$, show that the modified circular convolution of $x_1[n]$ and $x_2[n]$ is identical to the linear convolution of $x_1[n]$ and $x_2[n]$.

8.65. In some applications in coding theory, it is necessary to compute a 63-point circular convolution of two 63-point sequences $x[n]$ and $h[n]$. Suppose that the only computational devices available are multipliers, adders, and processors that compute N-point DFTs, with N restricted to be a power of 2.

(a) It is possible to compute the 63-point circular convolution of $x[n]$ and $h[n]$ using a number of 64-point DFTs, inverse DFTs, and the overlap–add method. How many DFTs are needed? *Hint*: Consider each of the 63-point sequences as the sum of a 32-point sequence and 31-point sequence.

(b) Specify an algorithm that computes the 63-point circular convolution of $x[n]$ and $h[n]$ using two 128-point DFTs and one 128-point inverse DFT.

(c) We could also compute the 63-point circular convolution of $x[n]$ and $h[n]$ by computing their linear convolution in the time domain and then aliasing the results. In terms of multiplications, which of these three methods is most efficient? Which is least efficient? (Assume that one complex multiplication requires four real multiplications and that $x[n]$ and $h[n]$ are real.)

8.66. We want to filter a very long sequence with an FIR filter whose impulse response is 50 samples long. We wish to implement this filter with a DFT using the overlap–save technique. The procedure is as follows:

1. The input sections must be overlapped by V samples.
2. From the output of each section, we must extract M samples such that when these samples from each section are abutted, the resulting sequence is the desired filtered output.

Assume that the input segments are 100 samples long and that the size of the DFT is 128 ($= 2^7$) points. Assume further that the output sequence from the circular convolution is indexed from point 0 to point 127.

(a) Determine V.

(b) Determine M.

(c) Determine the index of the beginning and the end of the M points extracted; i.e., determine which of the 128 points from the circular convolution are extracted to be abutted with the result from the previous section.

8.67. A problem that often arises in practice is one in which a distorted signal $y[n]$ is the output that results when a desired signal $x[n]$ has been filtered by an LTI system. We wish to recover the original signal $x[n]$ by processing $y[n]$. In theory, $x[n]$ can be recovered from $y[n]$ by passing $y[n]$ through an inverse filter having a system function equal to the reciprocal of the system function of the distorting filter.

Suppose that the distortion is caused by an FIR filter with impulse response

$$h[n] = \delta[n] - 0.5\delta[n - n_0],$$

where n_0 is a positive integer, i.e., the distortion of $x[n]$ takes the form of an echo at delay n_0.

(a) Determine the z-transform $H(z)$ and the N-point DFT $H[k]$ of the impulse response $h[n]$. Assume that $N = 4n_0$.

(b) Let $H_i(z)$ denote the system function of the inverse filter, and let $h_i[n]$ be the corresponding impulse response. Determine $h_i[n]$. Is this an FIR or an IIR filter? What is the duration of $h_i[n]$?

(c) Suppose that we use an FIR filter of length N in an attempt to implement the inverse filter, and let the N-point DFT of the FIR filter be

$$G[k] = 1/H[k], \qquad k = 0, 1, \ldots, N-1.$$

What is the impulse response $g[n]$ of the FIR filter?

(d) It might appear that the FIR filter with DFT $G[k] = 1/H[k]$ implements the inverse filter perfectly. After all, one might argue that the FIR distorting filter has an N-point DFT $H[k]$ and the FIR filter in cascade has an N-point DFT $G[k] = 1/H[k]$, and since $G[k]H[k] = 1$ for all k, we have implemented an all-pass, nondistorting filter. Briefly explain the fallacy in this argument.

(e) Perform the convolution of $g[n]$ with $h[n]$, and thus determine how well the FIR filter with N-point DFT $G[k] = 1/H[k]$ implements the inverse filter.

8.68. A sequence $x[n]$ of length N has a discrete Hartley transform (DHT) defined as

$$X_H[k] = \sum_{n=0}^{N-1} x[n]H_N[nk], \qquad k = 0, 1, \ldots, N-1. \tag{P8.68-1}$$

where

$$H_N[a] = C_N[a] + S_N[a],$$

with

$$C_N[a] = \cos(2\pi a/N), \qquad S_N[a] = \sin(2\pi a/N).$$

Originally proposed by R.V.L. Hartley in 1942 for the continuous-time case, the Hartley transform has properties that make it useful and attractive in the discrete-time case as well (Bracewell, 1983, 1984). Specifically, from Eq. (P8.68-1), it is apparent that the DHT of a real sequence is also a real sequence. In addition, the DHT has a convolution property, and fast algorithms exist for its computation.

In complete analogy with the DFT, the DHT has an implicit periodicity that must be acknowledged in its use. That is, if we consider $x[n]$ to be a finite-length sequence such that $x[n] = 0$ for $n < 0$ and $n > N-1$, then we can form a periodic sequence

$$\tilde{x}[n] = \sum_{r=-\infty}^{\infty} x[n + rN]$$

such that $x[n]$ is simply one period of $\tilde{x}[n]$. The periodic sequence $\tilde{x}[n]$ can be represented by a discrete Hartley series (DHS), which in turn can be interpreted as the DHT by focusing attention on only one period of the periodic sequence.

(a) The DHS analysis equation is defined by

$$\tilde{X}_H[k] = \sum_{n=0}^{N-1} \tilde{x}[n]H_N[nk]. \tag{P8.68-2}$$

Show that the DHS coefficients form a sequence that is also periodic with period N; i.e.,

$$\tilde{X}_H[k] = \tilde{X}_H[k + N] \qquad \text{for all } k.$$

(b) It can also be shown that the sequences $H_N[nk]$ are orthogonal; i.e.,

$$\sum_{k=0}^{N-1} H_N[nk]H_N[mk] = \begin{cases} N, & ((n))_N = ((m))_N, \\ 0, & \text{otherwise.} \end{cases}$$

Using this property and the DHS analysis formula of Eq. (P8.68-2), show that the DHS synthesis formula is

$$\tilde{x}[n] = \frac{1}{N}\sum_{k=0}^{N-1} \tilde{X}_H[k]H_N[nk]. \tag{P8.68-3}$$

Note that the DHT is simply one period of the DHS coefficients, and likewise, the DHT synthesis (inverse) equation is identical to the DHS synthesis Eq. (P8.68-3), except that we simply extract one period of $\tilde{x}[n]$; i.e., the DHT synthesis expression is

$$x[n] = \frac{1}{N}\sum_{k=0}^{N-1} X_H[k]H_N[nk], \qquad n = 0, 1, \ldots, N-1. \tag{P8.68-4}$$

With Eqs. (P8.68-1) and (P8.68-4) as definitions of the analysis and synthesis relations, respectively, for the DHT, we may now proceed to derive the useful properties of this representation of a finite-length discrete-time signal.

(c) Verify that $H_N[a] = H_N[a + N]$, and verify the following useful property of $H_N[a]$:

$$\begin{aligned} H_N[a+b] &= H_N[a]C_N[b] + H_N[-a]S_N[b] \\ &= H_N[b]C_N[a] + H_N[-b]S_N[a]. \end{aligned}$$

(d) Consider a circularly shifted sequence

$$x_1[n] = \begin{cases} \tilde{x}[n-n_0] = x[((n-n_0))_N], & n = 0, 1, \ldots, N-1, \\ 0, & \text{otherwise.} \end{cases} \tag{P8.68-5}$$

In other words, $x_1[n]$ is the sequence that is obtained by extracting one period from the shifted periodic sequence $\tilde{x}[n - n_0]$. Using the identity verified in part (c), show that the DHS coefficients for the shifted periodic sequence are

$$\tilde{x}[n-n_0] \overset{\mathcal{DHS}}{\longleftrightarrow} \tilde{X}_H[k]C_N[n_0k] + \tilde{X}_H[-k]S_N[n_0k]. \tag{P8.68-6}$$

From this, we conclude that the DHT of the finite-length circularly shifted sequence $x[((n-n_0))_N]$ is

$$x[((n-n_0))_N] \overset{\mathcal{DHT}}{\longleftrightarrow} X_H[k]C_N[n_0k] + X_H[((-k))_N]S_N[n_0k]. \tag{P8.68-7}$$

(e) Suppose that $x_3[n]$ is the N-point circular convolution of two N-point sequences $x_1[n]$ and $x_2[n]$; i.e.,

$$\begin{aligned} x_3[n] &= x_1[n] \textcircled{N} x_2[n] \\ &= \sum_{m=0}^{N-1} x_1[m]x_2[((n-m))_N], \qquad n = 0, 1, \ldots, N-1. \end{aligned} \tag{P8.68-8}$$

By applying the DHT to both sides of Eq. (P8.68-8) and using Eq. (P8.68-7), show that

$$X_{H3}[k] = \tfrac{1}{2}X_{H1}[k](X_{H2}[k] + X_{H2}[((-k))_N]) + \tfrac{1}{2}X_{H1}[((-k))_N](X_{H2}[k] - X_{H2}[((-k))_N]) \quad \text{(P8.68-9)}$$

for $k = 0, 1, \ldots, N-1$. This is the desired convolution property.

Note that a linear convolution can be computed using the DHT in the same way that the DFT can be used to compute a linear convolution. While computing $X_{H3}[k]$ from $X_{H1}[k]$ and $X_{H2}[k]$ requires the same amount of computation as computing $X_3[k]$ from $X_1[k]$ and $X_2[k]$, the computation of the DHT requires only half the number of real multiplications required to compute the DFT.

(f) Suppose that we wish to compute the DHT of an N-point sequence $x[n]$ and we have available the means to compute the N-point DFT. Describe a technique for obtaining $X_H[k]$ from $X[k]$ for $k = 0, 1, \ldots, N-1$.

(g) Suppose that we wish to compute the DFT of an N-point sequence $x[n]$ and we have available the means to compute the N-point DHT. Describe a technique for obtaining $X[k]$ from $X_H[k]$ for $k = 0, 1, \ldots, N-1$.

8.69. Let $x[n]$ be an N-point sequence such that $x[n] = 0$ for $n < 0$ and for $n > N-1$. Let $\hat{x}[n]$ be the $2N$-point sequence obtained by repeating $x[n]$; i.e.,

$$\hat{x}[n] = \begin{cases} x[n], & 0 \le n \le N-1, \\ x[n-N], & N \le n \le 2N-1, \\ 0, & \text{otherwise.} \end{cases}$$

Consider the implementation of a discrete-time filter shown in Figure P8.69. This system has an impulse response $h[n]$ that is $2N$ points long; i.e., $h[n] = 0$ for $n < 0$ and for $n > 2N-1$.

(a) In Figure P8.69-1, what is $\hat{X}[k]$, the $2N$-point DFT of $\hat{x}[n]$, in terms of $X[k]$, the N-point DFT of $x[n]$?

(b) The system shown in Figure P8.69-1 can be implemented using only N-point DFTs as indicated in Figure P8.69-2 for appropriate choices for System A and System B. Specify System A and System B so that $\hat{y}[n]$ in Figure P8.69-1 and $y[n]$ in Figure P8.69-2 are equal for $0 \le n \le 2N-1$. Note that $h[n]$ and $y[n]$ in Figure P8.69-2 are $2N$-point sequences and $w[n]$ and $g[n]$ are N-point sequences.

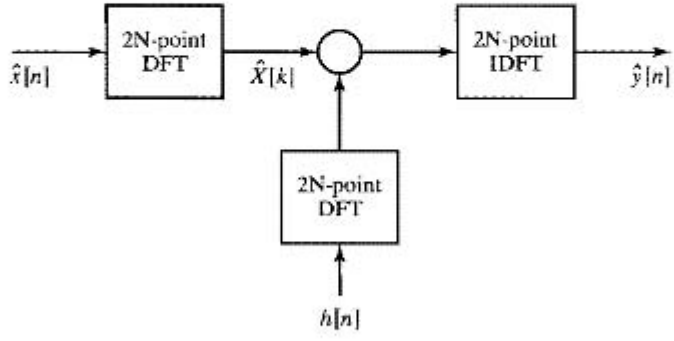

Figure P8.69-1

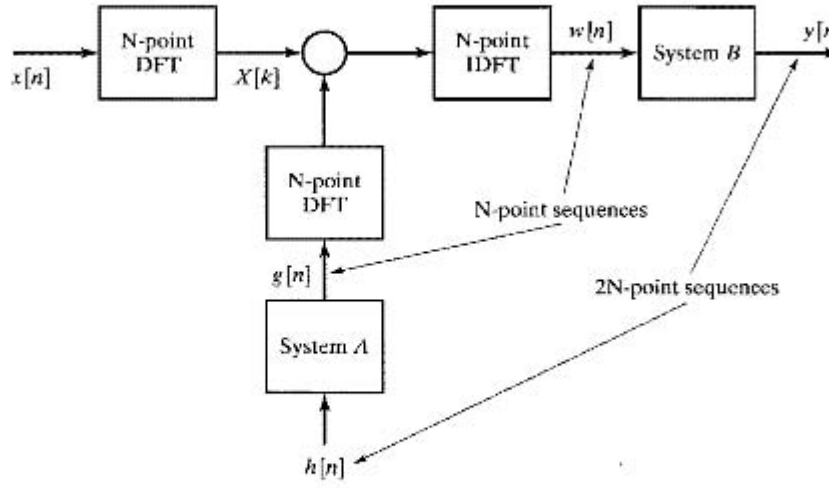

Figure P8.69-2

8.70. In this problem, you will examine the use of the DFT to implement the filtering necessary for the discrete-time interpolation, or upsampling, of a signal. Assume that the discrete-time signal $x[n]$ was obtained by sampling a continuous-time signal $x_c(t)$ with a sampling period T. Moreover, the continuous-time signal is appropriately bandlimited; i.e., $X_c(j\Omega) = 0$ for $|\Omega| \geq 2\pi/T$. For this problem, we will assume that $x[n]$ has length N; i.e., $x[n] = 0$ for $n < 0$ or $n > N - 1$, where N is even. It is not strictly possible to have a signal that is both perfectly bandlimited and of finite duration, but this is often assumed in practical systems processing finite-length signals which have very little energy outside the band $|\Omega| \leq 2\pi/T$.

We wish to implement a 1:4 interpolation, i.e., increase the sampling rate by a factor of 4. As seen in Figure 4.23, we can perform this sampling rate conversion using a sampling rate expander followed by an appropriate lowpass filter. In this chapter, we have seen that the lowpass filter could be implemented using the DFT if the filter is an FIR impulse response. For this problem, assume that this filter has an impulse response $h[n]$ that is $N + 1$ points long. Figure P8.70-1 depicts such a system, where $H[k]$ is the $4N$-point DFT of the impulse response of the lowpass filter. Note that both $v[n]$ and $y[n]$ are $4N$-point sequences.

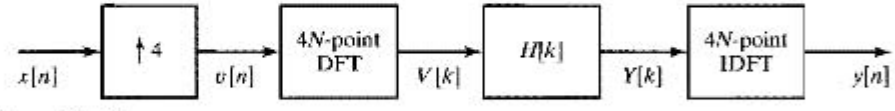

Figure P8.70-1

(a) Specify the DFT $H[k]$ such that the system in Figure P8.70-1 implements the desired upsampling system. Think carefully about the phase of the values of $H[k]$.

(b) It is also possible to upsample $x[n]$ using the system in Figure P8.70-2. Specify System A in the middle box so that the $4N$-point signal $y_2[n]$ in this figure is the same as $y[n]$ in Figure P8.70-2. Note that System A may consist of more than one operation.

(c) Is there a reason that the implementation in Figure P8.70-2 might be preferable to Figure P8.70-1?

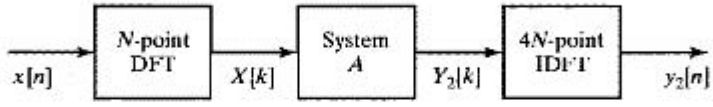

Figure P8.70-2

8.71. Derive Eq. (8.153) using Eqs. (8.164) and (8.165).

8.72. Consider the following procedure

(a) Form the sequence $v[n] = x_2[2n]$ where $x_2[n]$ is given by Eq. (8.166). This yields

$$v[n] = x[2n] \qquad n = 0, 1, \ldots, N/2 - 1$$
$$v[N-1-n] = x[2n+1], \quad n = 0, 1, \ldots, N/2 - 1.$$

(b) Compute $V[k]$, the N-point DFT of $v[n]$.
Demonstrate that the following is true:

$$X^{c2}[k] = 2\mathcal{R}e\{e^{-j2\pi k/(4N)}V[k]\}, \qquad k = 0, 1, \ldots, N-1,$$
$$= 2\sum_{n=0}^{N-1} v[n]\cos\left[\frac{\pi k(4n+1)}{2N}\right], \qquad k = 0, 1, \ldots, N-1,$$
$$= 2\sum_{n=0}^{N-1} x[n]\cos\left[\frac{\pi k(2n+1)}{2N}\right], \qquad k = 0, 1, \ldots, N-1.$$

Note that this algorithm uses N-point rather than $2N$-point DFTs as required in Eq. (8.167). In addition, since $v[n]$ is a real sequence, we can exploit even and odd symmetries to do the computation of $V[k]$ in one $N/4$-point complex DFT.

8.73. Derive Eq. (8.156) using Eqs. (8.174) and (8.157).

8.74. **(a)** Use Parseval's theorem for the DFT to derive a relationship between $\sum_k |X^{c1}[k]|^2$ and $\sum_n |x[n]|^2$.

(b) Use Parseval's theorem for the DFT to derive a relationship between $\sum_k |X^{c2}[k]|^2$ and $\sum_n |x[n]|^2$.